PHYSIOLOGICAL MECHANISMS DETERMINING YIELD IN OLIVE TREES: FROM PLOT TO GENES

Mecanismos fisiológicos que determinan la cosecha en olivares: de la parcela al gen

Adrián Pérez Arcoiza
Tesis Doctoral, 2023

Programa de Doctorado en Recursos Naturales y Medioambiente

IRNAS

UNIVERSIDAD DE SEVILLA

TESIS DOCTORAL

PHYSIOLOGICAL MECHANISMS DETERMINING YIELD IN OLIVE TREES:
FROM PLOT TO GENES

Memoria que presenta

D. Adrián Pérez Arcoiza

Para optar al título de Doctor por la

Universidad de Sevilla

Sevilla, abril de 2023

Universidad de Sevilla

Departamento de Cristalografía, Mineralogía y Química Agrícola

Programa de Doctorado Recursos Naturales y Medio Ambiente

Instituto de Recursos Naturales y Agrobiología de Sevilla (IRNAS, CSIC)

Instituto de la Grasa (IG, CSIC)

Universidad de Sevilla

Departamento de Cristalografía, Mineralogía y Química Agrícola

Programa de Doctorado Recursos Naturales y Medio Ambiente

Tesis Doctoral

PHYSIOLOGICAL MECHANISMS DETERMINING YIELD IN OLIVE TREES:

FROM PLOT TO GENES

Tesis Doctoral presentada por D. Adrián Pérez Arcoiza, en satisfacción de los requisitos necesarios para optar al grado de Doctor en Biología, dirigida por el Dr. Antonio Díaz Espejo y la Dra. Virginia Hernández Santana (Instituto de Recursos Naturales y Agrobiología de Sevilla. IRNAS, CSIC) y tutorada por el Dr. Isidoro Ángel Gómez Parrales (Dpto. Cristalografía Mineralogía y Química Agrícola, Universidad de Sevilla).

LOS DIRECTORES

Dr. Antonio Díaz Espejo   Dra. Virginia Hernández Santana

EL TUTOR   EL DOCTORANDO

Dr. Isidoro Ángel Gómez Parrales   D. Adrián Pérez Arcoiza

University of Seville

Department of Crystallography, Mineralogy and Agricultural Chemistry

Doctoral Program in Natural Resources and Environment

Ph.D. Dissertation

PHYSIOLOGICAL MECHANISMS DETERMINING YIELD IN OLIVE TREES:

FROM PLOT TO GENES

Ph.D. Dissertation presented by Adrián Pérez Arcoiza to fulfil the necessary requirements of the Doctor of Philosophy degree of Biology under the supervision of Dr. Antonio Díaz Espejo and Dr. Virginia Hernández Santana (Institute of Natural Resources and Agrobiology of Seville. IRNAS, CSIC), and being advised by Dr. Isidoro Ángel Gómez Parrales (Department of Crystallography, Mineralogy and Agricultural Chemistry, University of Seville).

THESIS SUPERVISORS

Dr. Antonio Díaz Espejo   Dr. Virginia Hernández Santana

THESIS ADVISOR   Ph.D. CANDIDATE

Dr. Isidoro Ángel Gómez Parrales   D. Adrián Pérez Arcoiza

FACULTAD DE QUÍMICA

Departamento de Cristalografía, Mineralogía y Química Agrícola

DR. ISIDORO ÁNGEL GÓMEZ PARRALES, COORDINADOR DEL PROGRAMA DE DOCTORADO EN RECURSOS NATURALES Y MEDIO AMBIENTE DE LA UNIVERSIDAD DE SEVILLA,

Certifica: que la presente memoria de Investigación titulada "PHYSIOLOGICAL MECHANISMS DETERMINING YIELD IN OLIVE TREES: FROM PLOT TO GENES", presentada por D. Adrián Pérez Arcoiza para optar al grado de Doctor por la Universidad de Sevilla, ha sido realizada en el marco del Programa de Doctorado en Recursos Naturales y Medio Ambiente del Departamento de Cristalografía, Mineralogía y Química Agrícola.

Sevilla, abril de 2023

DR. JOSÉ ENRIQUE FERNÁNDEZ LUQUE, DIRECTOR DEL INSTITUTO DE RECURSOS NATURALES Y AGROBIOLOGÍA DE SEVILLA, DEL CONSEJO SUPERIOR DE INVESTIGACIONES CIENTÍFICAS,

Certifica: que la presente Memoria de Investigación titulada "PHYSIOLOGICAL MECHANISMS DETERMINING YIELD IN OLIVE TREES: FROM PLOT TO GENES", presentada por D. Adrián Pérez Arcoiza para optar al grado de Doctor por la Universidad de Sevilla, ha sido realizada en el Instituto de Recursos Naturales y Agrobiología de Sevilla (IRNAS, CSIC), bajo la dirección de los Drs. Antonio Díaz Espejo y Virginia Hernández Santana, reuniendo todas las condiciones exigidas a los trabajos de Tesis Doctoral.

Sevilla, abril de 2023

NOTE: The entire Thesis is written in English. The summary and the conclusions are also written in Spanish to fulfill the requirements to obtain the "International Doctor" degree, under the Agreement 99/2011 (7.2/CG 17-6-11).

WORKS DERIVED FROM THIS Ph.D. THESIS

Perez-Arcoiza, A., Montesinos, S., Díaz-Delgado, R., Hernandez-Santana, V., Diaz-Espejo, A. *Canopy sixe quantified with digital surface models is the major direct and indirect determinant of olive fruit and oil yield*. Agric. Water Manag. (To be submitted) **(Chapter 2)**

Hernandez-Santana V., **Perez-Arcoiza A.,** Gomez-Jimenez MC., Diaz-Espejo A. (2021). *Disentangling the link between leaf photosynthesis and turgor in fruit growth*. Plant J 107: 1788–1801. **(Chapter 3)**

Perez-Arcoiza A, Diaz-Espejo A, Fernandez-Torres R, Perez-Romero LF, Hernandez-Santana V. (2023). *Dual effect of the presence of fruits on leaf gas exchange and water relations of olive trees*. Tree Physiol 43:277–287. **(Chapter 4)**

Perez-Arcoiza A., Hernández ML, Sicardo MD., Hernandez-Santana V., Diaz-Espejo A., Martinez-Rivas JM (2022). *Carbon supply and water status regulate fatty acid and triacylglycerol biosynthesis at transcriptional level in the olive mesocarp*. Plant Cell Environ 45:2366–2380. **(Chapter 5)**

OTHER WORKS PUBLISHED DURING THIS PhD THESIS

Fernández-Pascual E, **Pérez-Arcoiza A**, Alberto Prieto J, Díaz TE (2017) *Environmental filtering drives the shape and breadth of the seed germination niche in coastal plant communities*. Ann Bot 119: 1169–1177

Hernandez-Santana V, Fernandes RDM, **Perez-Arcoiza A**, Fernández JE, Garcia JM, Diaz-Espejo A (2018) *Relationships between fruit growth and oil accumulation with simulated seasonal dynamics of leaf gas exchange in the olive tree*. Agric For Meteorol 256–257: 458–469

A mi familia y amigos

En memoria de mamá

"Por si nun sabes ni tú ni otra xente,

nun hai barrera, pesllera ni candáu

que puedas impone-y a la llibertá de mio mente."

Virginia Woolf (1882-1941)

Muyeres - Humanes (2020)

"Al carro de la cultura española le falta la rueda de la ciencia"

Santiago Ramón y Cajal (1852-1934)

"El conocimiento obtenido gracias al método científico es un patrimonio de todas/os y como tal, debemos defenderlo frente a la amenaza de la ignorancia, el bulo y la desinformación."

#SinCienciaNoHayFuturo.

CONTENTS

II

SUMMARY

RESUMEN

x

Summary

In recent decades, population growth and increasing demand for water and food are putting the world's agri-food system to the test. In addition, the lack of water in agriculture due to climate change is presented as one of the main problems in food production. In this scenario of increasing food demand and water scarcity, the implementation of deficit irrigation management of super-high-density orchards could be an excellent alternative to traditional rainfed plantations, contributing to enhance production using water sustainably. The olive tree (*Olea europaea* L.), is one of the main crops in the Mediterranean area by its great economic and cultural importance in producing not only fruit yield but also well-valued virgin olive oil (VOO). Moreover, the olive tree has become a species model in studies on the water stress response, thanks to its wide "repertoire" of physiological mechanisms allowing this species to be productive in water deficit conditions. However, the success of applying a deficit irrigation strategy to enhance yield quality without severely penalizing quantity and enhancing water efficiency requires a multidisciplinary approach. Knowledge of fruit development and its oil production and the use of new techniques is not yet currently available.

This background justifies this PhD Thesis, whose main objective is unravelling the plant and fruit physiological mechanisms limiting fruit and virgin olive oil (VOO) yield in response to water stress from different approaches. Specifically, we had four objectives. i) To know which are the main biotic and abiotic factors involved in the final yield of the crop, ii) to assess the importance of water and photosynthesis in limiting fruit growth in response to water deficit, iii) to understand how fruits affect the tree water relations and, iv) to know the main carbon sources and how water stress affects the biosynthesis and quality of olive oil.

Four experiments were carried out in a twelve-year-old olive trees (*Olea europaea* L. cv Arbequina) in a commercial super-high-density olive orchard located in Utrera (Seville, southwest Spain) during the 2018 irrigation season from July to November. Two irrigation treatments were applied in all experiments; a well-watered (WW) treatment, whose trees were irrigated daily at full irrigation (FI) to replace irrigation needs (IN), and a water stressed (WS) treatment, whose trees were under a regulated deficit irrigation (RDI) regime receiving 45% of IN. An unmanned aerial vehicle (UAV) was flown over the orchard to obtain an estimation of the tree canopy, multispectral and thermal images like normalized difference vegetation index (NDVI) and canopy temperature. In addition, several plant-based sensors were installed: ZIM turgor sensors in leaves to monitor tree water status, fruit dendrometers to monitor fruit growth and sap flow sensors which along with portable infrared gas exchange (IRGA, LI-6400) measurements allowed to estimate and stomatal conductance (g_s) and photosynthesis rate (A_N). A molecular biology techniques were also used. Specifically,, RNA extraction and cDNA synthesis techniques were used to determine which main carbon source and genes are involved in VOO biosynthesis and quality.

The results at the plot scale showed that canopy size was the main determinant of fruit and VOO yield and the variability in canopy size within WW and WS treatments contributed to explaining the higher variability in WW compared to WS in both fruit yield and VOO. Morever, through physiological measurements at tree scale and the use of ZIM turgor sensors and fruit dendrometers, it was observed that photosynthesis and turgor did not affect growth limitation equally. Indeed, it was found that turgor loss was the main factor limiting growth under drought conditions, while photosynthesis was the dominant growth process in periods when cell division conditions are preponderant. It was also shown that leaf gas exchange (A_N and g_s) and leaf

XII

osmotic potential (Ψ_π) were increased by the presence of fruits, mainly observed in WW trees, highlighting the role of fruits as major water and carbon sinks. This enhancement of leaf gas exchange by the fruit presence in the trees was likely produced by lower concentrations of soluble sugars and starch in the leaves. Finally, the molecular biology measurements at the fruit scale revealed that carbon supply and water status affected VOO biosynthesis in the mesocarp, regulating the expression of *DGAT* and *PDAT* genes.

According to the findings in this PhD Thesis, it is concluded that UAVs allows the study of canopy size distribution, which is the major direct and indirect determinant of the variability of olive fruit and oil yield. It can be further concluded that reduction in the time of turgor-driven cell expansion is the greatest limitation of fruit growth, consistent with the sink limitation hypothesis. The sink strength of fruits for carbon and water is concluded to regulate leaf gas exchange, through the modification of leaf sugar accumulation, which in turn, changes leaf turgor. These changes in leaf turgor can be identified with ZIM turgor sensors, which together with the use of determining turgor-driven time to growth, makes them a promising tool for managing deficit irrigation.The last conclusion is that the main contribution of photoassimilates for oil biosynthesis in the mesocarp of olive fruit comes from the leaf, as compared to the fruit photosynthesis. This different source of carbon supply, together with the water status, affect oil synthesis and fatty acid composition by regulating the transcript levels of *DGAT*, *PDAT* and *FAD* genes.

Resumen

En las últimas décadas, el crecimiento de la población y la creciente demanda de agua y alimentos están poniendo a prueba el sistema agroalimentario mundial. Además, la falta de agua en la agricultura debido al cambio climático se presenta como uno de los principales problemas en la producción de alimentos. En este escenario de aumento de la demanda de alimentos y escasez de agua, la implementación de la gestión del riego deficitario en plantaciones superintensivas podría ser una excelente alternativa a los cultivos tradicionales de secano, contribuyendo a mejorar la producción utilizando el agua de manera sostenible. El olivo (*Olea europaea* L.) es uno de los principales cultivos en el área mediterránea por su gran importancia económica y cultural en la producción no solo de frutos, sino también de aceite de oliva virgen (AOV) de alta calidad. Además, el olivo se ha convertido en una especie modelo en estudios sobre la respuesta al estrés hídrico, gracias a su amplio "repertorio" de mecanismos fisiológicos que permiten a esta especie ser productiva en condiciones de déficit de agua. Sin embargo, el éxito de aplicar una estrategia de riego deficitario para mejorar la calidad de la cosecha sin penalizar severamente la cantidad y mejorar la eficiencia del agua, requiere un enfoque multidisciplinario. El uso de nuevas técnicas para comprender el desarrollo del fruto y la síntesis de aceite, aún no están del todo desarrolladas.

Este contexto justifica la tesis doctoral cuyo objetivo principal es desentrañar los mecanismos fisiológicos de la planta y el fruto que limitan la cosecha de aceitunas y la producción de aceite de oliva virgen (AOV) en respuesta al estrés hídrico desde diferentes enfoques. Específicamente, teníamos cuatro objetivos: i) conocer cuáles son los principales factores bióticos y abióticos implicados en la producción final del cultivo, ii) evaluar la importancia del agua y la fotosíntesis en la limitación del crecimiento del fruto en respuesta al déficit hídrico, iii) entender cómo los frutos afectan las

relaciones hídricas del árbol, y iv) conocer las principales fuentes de carbono y cómo el estrés hídrico afecta a la biosíntesis y calidad del aceite de oliva.

Se llevaron a cabo cuatro experimentos en olivos (*Olea europaea* L. cv Arbequina) de doce años en un olivar comercial superintensivo ubicado en Utrera (Sevilla, suroeste de España) durante la temporada de riego, entre julio y noviembre de 2018. En todos los experimentos se aplicaron dos tratamientos de riego: un tratamiento bien regado (WW), cuyos árboles fueron regados diariamente a plena capacidad para cubrir las necesidades de riego (NR), y un tratamiento de estrés hídrico (WS), cuyos árboles estaban bajo un régimen de riego deficitario regulado (RDR) recibiendo el 45% de NR. Se utilizó un vehículo aéreo no tripulado (UAV) para obtener una estimación de la copa de los árboles, imágenes multiespectrales y térmicas como el índice de vegetación de diferencia normalizada (NDVI) y la temperatura de la copa. Además, se instalaron varios sensores en la planta: sensores ZIM de turgencia de las hojas para monitorear el estado hídrico de los árboles, dendrómetros de fruto para monitorear el crecimiento de los mismos y sensores de flujo de savia que, junto con las mediciones de un sistemas de análisis infrarrojo de intercambio de gases portátil (IRGA, LI-6400), permitieron estimar la conductancia estomática (g_s) y la tasa neta fotosintética (A_N). También se utilizaron técnicas de biología molecular. Específicamente, se utilizaron técnicas de extracción de ARN y síntesis de cDNA para determinar qué fuente principal de carbono y genes están involucrados en la biosíntesis y calidad del AOV.

Los resultados a escala de la parcela mostraron que el tamaño de la copa era el principal determinante de la producción de frutos y de AOV y que la variabilidad en el tamaño de la copa dentro de los tratamientos WW y WS contribuyó a explicar la mayor variabilidad en la cosecha de frutos y de AOV en los árboles WW en comparación con WS. Además, a través de mediciones fisiológicas a escala del árbol y el uso de sensores ZIM de turgencia en hoja y

XVI

dendrómetros de frutos, se observó que la fotosíntesis y la turgencia no afectaron por igual a la limitación del crecimiento de los frutos. De hecho, se encontró que la pérdida de turgencia era el principal factor que limitaba el crecimiento en condiciones de sequía, mientras que la fotosíntesis era el proceso de crecimiento dominante en los períodos en los que las condiciones de división celular eran mayoritarias. También se demostró que el intercambio gaseoso (A_N y g_s) y el potencial osmótico de las hojas (Ψ_π) aumentaron por la presencia de frutos, observado principalmente en los árboles WW, destacando el papel de los frutos como principales sumideros de agua y carbono. Este aumento del intercambio gaseoso de las hojas por la presencia de frutos en los árboles probablemente se produjo por concentraciones más bajas de azúcares solubles y almidón en las hojas. Finalmente, las mediciones de biología molecular a escala de frutos revelaron que la fuente de carbono y el estado hídrico afectaron la biosíntesis de AOV en el mesocarpio, regulando la expresión de los genes *DGAT* y *PDAT*.

De acuerdo con los hallazgos de esta tesis doctoral, se concluye que los UAV permiten estudiar la distribución del tamaño de la copa, que es el principal determinante directo e indirecto de la variabilidad de la produccion de la aceituna y del aceite. También se concluye que la reducción en el tiempo de expansión celular impulsada por la turgencia es la mayor limitación del crecimiento de los frutos, lo que es consistente con la hipótesis de la limitación del sumidero. Se concluye que la fuerza de sumidero que tienen los frutos sobre el carbono y el agua regula el intercambio gaseoso de las hojas mediante la modificación de la acumulación de azúcares en las mismas, lo que a su vez hace modificar su turgencia. Estas modificaciones pueden ser identificadas mediante sensores ZIM en hoja, que junto con la determinación del tiempo necesario de turgencia para el crecimiento, los convierte en una herramienta prometedora para la gestión del riego deficitario. La última conclusión es que

la principal contribución de los fotoasimilados para la biosíntesis del aceite en el mesocarpio de la aceituna proviene de las hojas, en comparación con la fotosíntesis que realiza el fruto. Estas fuentes de carbono, junto con el estado hídrico, afectan la síntesis del aceite y la composición de ácidos grasos mediante la regulación de los niveles de transcripción de los genes *DGAT*, *PDAT* y *FAD*.

ACKNOWLEDGMENTS

AGRADECIMIENTOS

xx

ABBREVIATIONS

CHAPTER **1**:

INTRODUCTION

1. Introduction

1.1. The complex challenge of increasing productivity with scarce water resources

According to the United Nations (UN), the world's population is expected to increase by nearly 2 billion people in the next 30 years, more than 8 billion currently to 9.7 billion people in 2050 and could peak at nearly 11 billion around 2100. At the same time, the Food and Agricultural Organization (FAO) expects that the global demand for food will grow by 70-85% in the next 30 years (FAO, 2009). This growing global demand for food comes with an ever-increasing need to improve crop yields. Since the 1960s, the area of farmland has quadrupled to satisfy the global food demand. However, several recent studies indicate that the world has already passed 'peak agricultural land' (Fig. 1) (Goldewijk et al., 2017; Taylor and Rising, 2021). The lack of available land for agriculture makes it more necessary than ever to increase the crop productivity per surface unit to meet the growing demand for food.
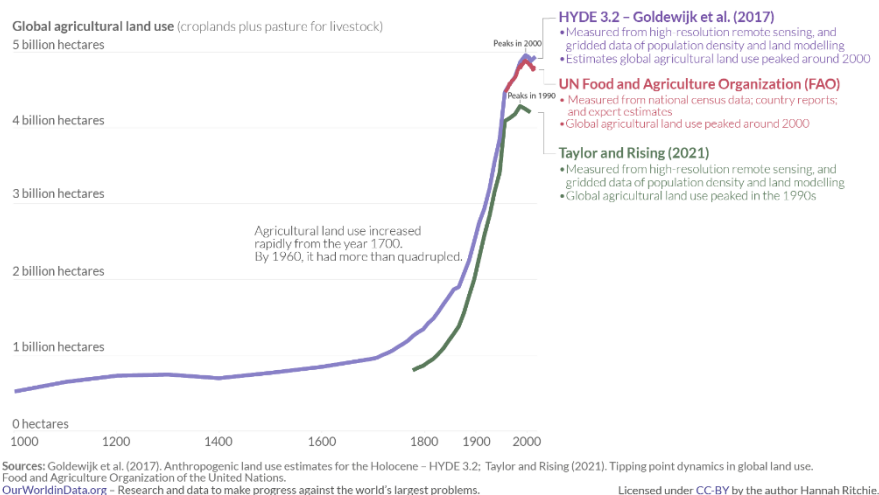
Fig. 1. Global agricultural land use (billion hectares) from the year 1000 to 2022. Source: OurWorldinData.org.

Inroduction

Moreover, productivity increment must be achieved under more constrained conditions than in the past because natural resources, such as water, are becoming increasingly scarce. Climate change has far-reaching implications for global food production due to the increased frequency of drought and intense precipitation events, which have already substantially impacted agricultural production worldwide through effects on plant growth and productivity, leading to significant economic losses. Thus, there is a need to apply new approaches to achieve more productive and sustainable agriculture (Dhankher and Foyer, 2018), in such a way that natural resources are used efficiently and sustainably. In this way, the aim is to increase the water productivity, that is, to increase the value of food benefits per drop of water used. In recent years, different approaches have been proposed to increase water productivity such as integrated aquaculture-agriculture (IAA) systems (Ahmed et al., 2014) and breeding practices that take advantage of the genetic variability of wild related species and different cultivars more tolerant to drought (Ruane et al., 2008; Trentacoste et al., 2018). This better adaptation to water deficit by some cultivars could be explained for example, by increasing the root system compared to leaf area in response to drought, as it has been observed in wild olive genotypes (Hernandez-Santana et al., 2019a).

Another approach to produce more food with less water consumption is through the implementation of deficit irrigation (DI) strategies.

DI strategies, consisting of irrigating at levels below 100% evapotranspiration, are attracting a lot of attention because water availability is arguably the most important environmental factor limiting crop growth and productivity but it must be used sustainably. Interestingly, in addition to the water-saving, DI scheduling also favours high-quality fruits, while minimizing yield losses (Moriana et al., 2003; Fernández et al., 2013; García et al., 2017). During the last years, great efforts have been made to save water through

deficit irrigation strategies (Fereres and Soriano, 2007; Ruiz-Sanchez et al., 2010; Fernández et al., 2013; Rosecrance et al., 2015). DI can be applied by the so called sustained deficit irrigation (SDI) approach, which consists of applying a certain amount of water demanded by the crop during the entire irrigation campaign (season) (Fereres and Soriano, 2007). An alternative is the application of a regulated deficit irrigation (RDI), which consists in reducing the amount of water applied at certain key phenological stages of the crop in which it is not so sensitive to drought, based on the tree physiology (Chalmers et al., 1981). Regardless of the method used, DI is frequently applied using crop coefficient methods, but new generation technological applications or Artificial intelligence are becoming increasingly used. However, neither method has provided yet a neat solution for DI succesfully, partly, due to their high level of empiriscim, which makes the extrapolation of automatic data processing and interpretation extremely difficult. Specifically, main declared shortcomings of crop coefficient methods are: empirical monthly coefficients, inaccurate potentical evapotranspiration estimation, poor valuation of total leaf area along time and absence of a rational method to determine the plant water stress intensity when not fulfilling plant water needs. Other methods based on plant monitoring (i.e. water status of vegetative organs) suppose a relevant improvement as they integrate both environmental and plant dynamics, but they have been used also greatly empirically (e.g. using reference trees to obtain thresholds or baselines), do not monitor any variable directly related to yield (plant water status not always reflect the fruit growth performance (Mills et al., 1996; Matthews and Shackel, 2005; Hernandez-Santana et al., 2018) and do not allow water needs calculations.

1.1.1. Are deficit irrigation strategies enough? The olive tree as a model

As mentioned, the implementation of a deficit irrigation strategy in commercial farms is not straightforward. To apply a RDI, the crop response to water stress and recovery must be well known. The success of a deficit irrigation management in semi-arid climates such as the Mediterranean, is determined by the study of those species adapted to water scarcity. In recent decades, this basic knowledge on typical species like olive (Fernández et al., 2013; Padilla-Díaz et al., 2016; Hernandez-Santana et al., 2017), almond (Goldhamer et al., 2006), citrus (Domingo et al., 1996; García-Tejero et al., 2010; Ballester et al., 2013a) and vines crops (Ruiz-Sanchez et al., 2010) could improved the optimization of yield under a RDI management. Among these species, olive tree has become a model to study the response to water stress due to its resistance to drought (Fernández, 2014; Diaz-Espejo et al., 2018), its capacity to keep a positive carbon balance (Angelopoulos et al., 1996; Giorio et al., 1999; Moriana et al., 2002; Hernandez-Santana et al., 2017) and its ability to be productive even under harsh environments (Angelopoulos et al., 1996; Giorio et al., 1999; Moriana et al., 2002; Hernandez-Santana et al., 2017). In the last years, several studies have identified in olive key mechanisms explaining its capacity to cope with soil water deficit and high vapor pressure deficit such as a high embolism resistance (Torres-Ruiz et al., 2017) and fine stomatal conductance regulation before cavitation occurs. Indeed, the mechanisms for this control of stomatal conductance are still being studied but up to now it has been identified that stomata closure respond to leaf turgor-mediated processes (Rodriguez-Dominguez et al., 2016), to ABA rapidly biosynthesized whose triggering factor is the reduction in leaf turgor (McAdam and Brodribb, 2016) and to losses in the hydraulic conductance of the distal organs, i.e. leaves (Torres-Ruiz et al., 2015; Hernandez-Santana et al., 2016b) and roots

(Rodriguez-Dominguez and Brodribb, 2020). The olive tree is a clear example of drought-resistant species, standing out for a good physiological response to the application of RDI (Fernández, 2014). In addition, despite the harsh environmental conditions to which it is subjected, it is capable of producing reasonably good fruit and virgin olive oil (VOO) yield results (Moriana et al., 2003; Gucci et al., 2007; Hernandez-Santana et al., 2017). One of the main physiological characteristics of this species is that it is capable of reaching severe levels of water stress due to its resistance to embolism formation in the xylem. This allows the olive tree to reduce its water potential to very low levels, as low as -4.0 and -5.5 MPa (Torres-Ruiz et al., 2013).

Although olive trees are traditionally cultivated in semiarid areas, in the last decades the traditional rainfed cultivation has been replaced by a super-high-density and irrigated orchards (Orgaz and Fereres, 2008) to improve productivity per unit of cultivated land. The irrigation management is designed based on the characteristics of the crop and the environmental conditions. In addition, in a super-high-density orchards, a RDI allows a better use of the supplied water. The excessive growth of the vegetative part can be controlled because under water stress conditions, the tree prioritizes fruit growth against the vegetative part (Fernández et al. 2013, Fernández 2014; Hernandez-Santana et al. 2017).

Although RDI seems to work for olive management, there are several problems that have been identified over the years, like estimation of full water requirements of the crop, range of water stress allowing for the maintenance of yield, or interpretation and use of plant sensors to manage the crop along the season. Additionally to these aspects, the following two will be specifically addressed in this PhD. Thesis: (i) there is an enormous variability among individual trees subjected to the same irrigation treatment, which usually gives confusing yield results comparing different levels of irrigation (Hernandez-

Santana et al., 2017; Padilla-Díaz et al., 2018; Fernández et al., 2020) and (ii) the success of the application of an RDI depends to a great extent on the knowledge of the whole tree physiology, but especially the fruit, which has not received as much as attention as the plant physiology. Difficulties in applying RDI also raise because we still do not have identified the key physiological variable which must be used as a target to manage irrigation and fertilization in fruit tree orchards. It is not well known either how to maintain the optimal conditions to enhance growth or increase the fruit quality in a changing environment. In this aspect, in recent years, there has been in-depth progress in the understanding of the physiological responses to water stress by the olive tree (i.e., stomatal conductance (g_s) (Diaz-Espejo et al., 2012), leaf, stem and fruit water potential (Ψ_{leaf}, $\Psi_{stem,}$ Ψ_{fruit}) (Girón et al., 2015; Fernandes et al., 2018), net photosynthesis (A_N) (Hernandez-Santana et al., 2017), etc., and several techniques have been developed allowing to monitor the physiological state of the crop to apply the correct irrigation management, i.e., trunk dendrometers (Fernández et al., 2011), sap flux density (J_s) (Hernandez-Santana et al., 2016a), ZIM turgor sensors (Padilla-Díaz et al., 2018; Rodriguez-Dominguez et al., 2019). In this way, even though the fruit is the main protagonist and the ultimate agronomical goal of all the advances made in recent years, the physiological knowledge of the fruit and its water-plant relations with the vegetative part of the tree, have been hardly studied.

For these reasons, the two mentioned main problems will be addressed throughout this PhD. Thesis from different scales and perspectives. Orchard productivity is determined by fruit yield, which in turn is defined by fruit size and number. Thus, fruit growth, quality (in olive it is VOO quality) and quantity are the central topics of this PhD. Thesis. The first problem, related to the tree-to-tree variability observed at harvest, will be evaluated from an agronomical point of view in a tree-plot scale study in **Chapter 2**. The second problem,

related to the physiology of the fruit, will be addressed in two leaf-fruit scale studies in **Chapter 3** and **Chapter 4,** and using molecular biology in a fruit-scale study in **Chapter 5**.

1.2. Tree-plot scale: What factors limit fruit and virgin olive oil yield?

The effect of an RDI management on super-high-density olive orchards has been studied for years to save water without penalizing fruit (Moriana et al., 2003; Dell'Amico et al., 2012; Fernández et al., 2013) and VOO yield and its quality (García et al., 2013; Caruso et al., 2014). However, several authors have noticed that despite applying the same amount of water, tree-to-tree variability in fruit and VOO yield is high (Alegre et al., 2002; Melgar et al., 2008; Iniesta et al., 2009; Gucci et al., 2019). This variability in yield seems to be affected by tree density and climate conditions (Fig. 2) (Fernández et al., 2020) but also because of other unknown factors not controlled.
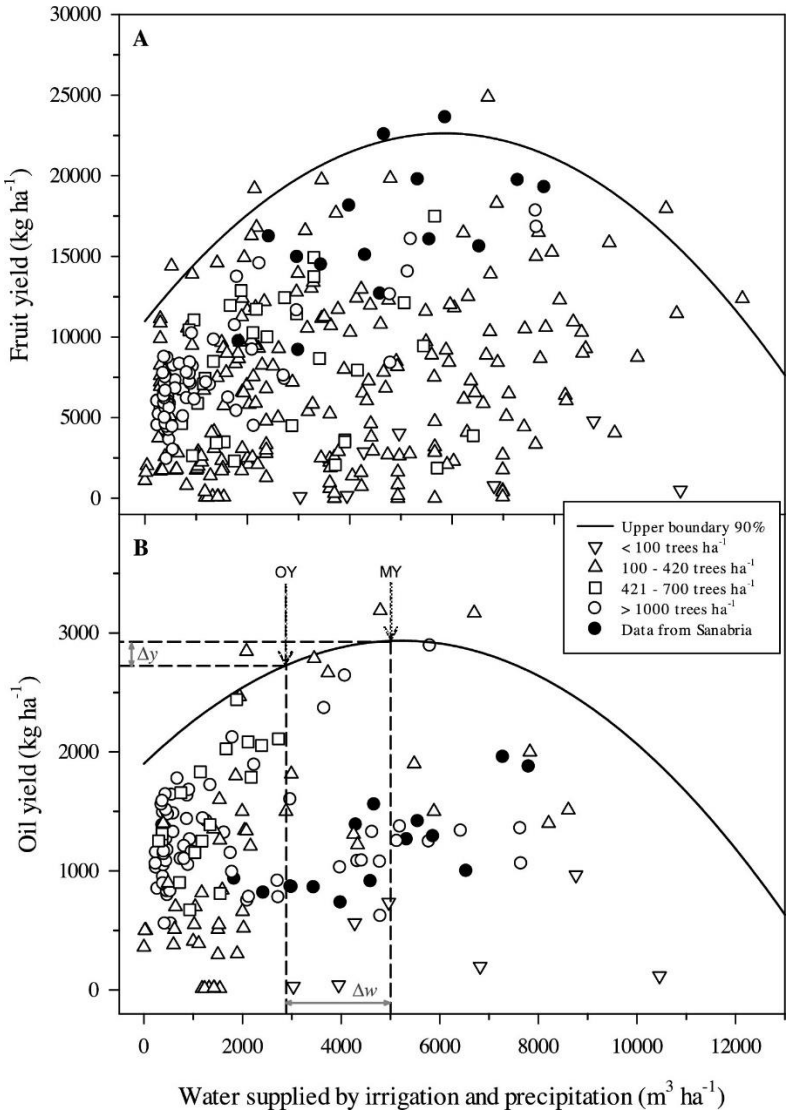
Fig. 2. Fruit yield **(A)** and oil yield **(B)** versus seasonal water supplied by irrigation and precipitation in olive orchards with different plant densities. Source: (Fernández et al., 2020).

Therefore, the application of an RDI is one of the main factors that affect fruit and VOO yield in a controlled way. However, there are several uncontrolled factors that could have relevant consequences on the results of

the RDI strategy. Some of these factors to consider are agronomic, such as tree size (canopy volume(V_{canopy}) and leaf area (LA)), or physiological (fruit load, fruit growth or oil accumulation).

In order to study the factors affecting yield, some of the main indicators that can be monitored are the V_{canopy}, the normalized difference vegetation index (Caruso et al., 2019; Caruso et al., 2022a), the canopy temperature (Caruso et al., 2021), the leaf nitrogen concentration, the number of shoots with fruits, the fruit fresh weight or oil accumulation per fruit. All these factors may be interacting with each other and may have a differential impact on fruit weight and VOO yield. Therefore, although the RDI strategy is showing promising results, there are still many unresolved questions, as irrigation might not be the only factor affecting fruit and VOO yield.

In this sense, in addition to water stress, fruit yield will be conditioned by several factors. In the first place, the tree size is an important factor that a priori is one of the main contributors to tree-to-tree variability. A tree with a larger leaf area have the potential to produce a greater number of fruits, since it poses a larger number of fruit-bearing shoots, and a large number of leaves is capable of producing a greater quantity of photoassimilates (Hernandez-Santana et al., 2017) and this is mainly conditioned by the pruning management (Albarracín et al., 2017). At the same time, a larger tree will have higher water requirements than a smaller tree. As we had to irrigate based on an average tree size, some will be over irrigated and other under irrigated. Secondly, fruit yield is directly conditioned by fruit growth, that is, the ability of the fruit to increase in size and gain fresh weight. On the other hand, VOO yield would be mainly conditioned by the oil accumulation capacity of the fruit. In either case, these mechanisms will be studied in this PhD Thesis in the main organ affecting production: the fruit.

1.3. The fruit: protagonist in agronomy, forgotten in physiology.

When applying RDI, the aim is to save water without severely affecting fruit yield (Moriana et al., 2003; Dell'Amico et al., 2012; Fernández et al., 2013) and increasing the quality of VOO yield (García et al., 2013; Caruso et al., 2014). Although the fruit has always been the main objective, advances in the development of a suitable irrigation strategy have been aimed at thoroughly understanding the plant physiology, leaving aside the physiology of the fruit. This approach assumes that the response of the parent plant and the fruit to water stress is similar. Contrary to the former, it has been shown a progressive decoupling of fruit water status from leaves in olive as water stress progressed (Fernandes et al., 2018).

Several works have pointed out to the fact that fruits are a priority for the plant (Génard et al., 2008; Hacket-Pain et al., 2017), and in recent years, it has been even demonstrated that olive fruits under water stress are both major carbon (Fig. 3) (Hernandez-Santana et al., 2018) and water sinks (Girón et al., 2015; Fernandes et al., 2018).
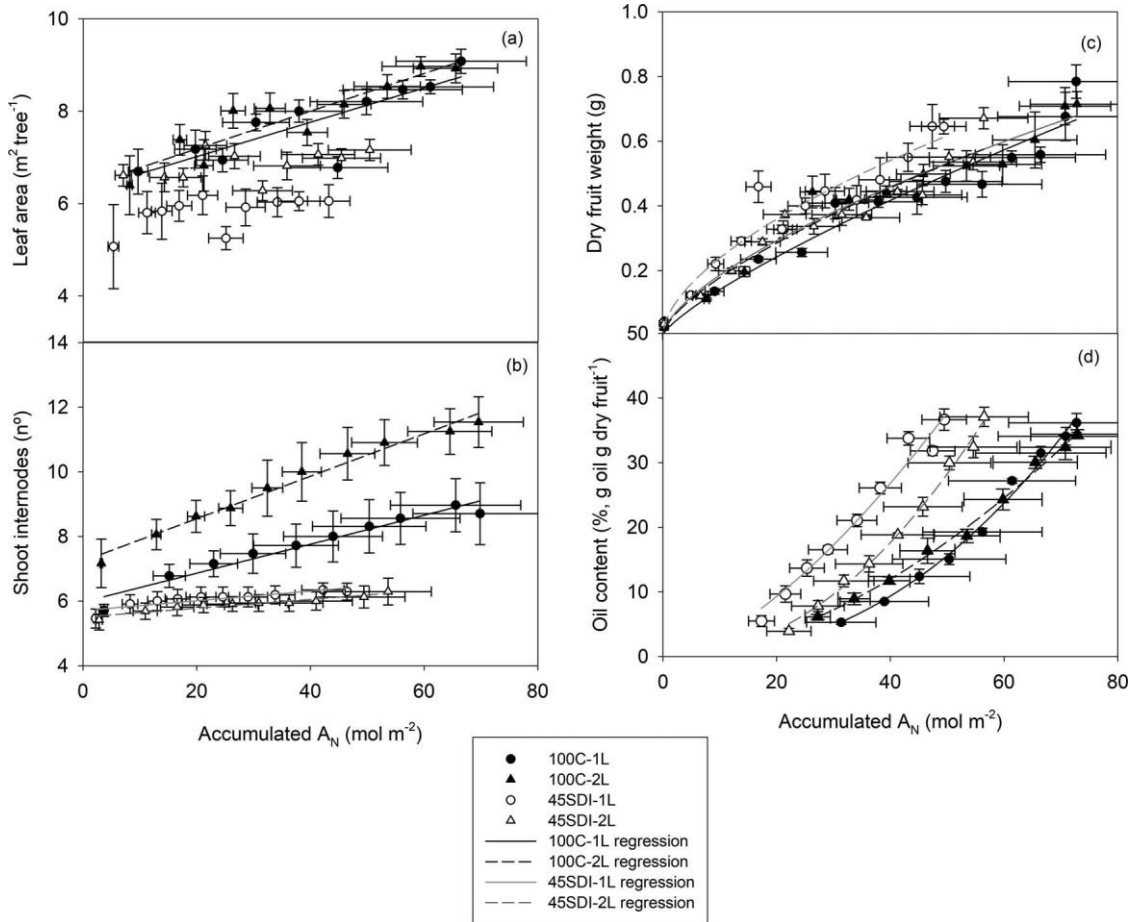
Fig. 3: Relationship between accumulated net photosynthesis (A_N) and (a) leaf area, (b) number of shoot internodes, (c) fruit dry weight and (d) oil content. Source: (Hernandez-Santana et al., 2018).

Besides water stress, in a very recent work studying several species, Rossi et al., (2022) showed that the fruit development stage also plays a major role in the different water and carbon relationship between the vegetative part of the plant and the fruit (Rossi et al., 2022). These recent works demonstrate how complex are fruit's carbon and water needs and their relations with the

whole plant, and that the assumption that the leaf physiology shows the water state of the fruit is not always correct. Thus, this PhD. Thesis is focused entirely on the fruit physiology at different scales, since it should be considered the main objective within future irrigation strategies.

1.3.1. What mechanisms are limiting fruit growth?

As mentioned before, fruit size, and hence fruit growth, is one of the main factors determining orchard yield. Plant growth has been widely explored (Hilty et al., 2021), but the reasons why growth is limited are not still fully understood. However, understanding how plant and fruit growth are limited is one of the most interesting but rather unknown topics because they will determine final fruit size, especially under water deficit conditions. In this sense, if we know the physiological mechanisms that regulate and limit the growth of plants and fruits, we will base our management decisions on that knowledge to minimize the growth limitation. However, optimizing growth in response to water stress remains a real challenge because the main processes that determine plant growth, and especially fruit growth, are related to the accumulation of both water and carbohydrates. To date, it is not known how each one affects growth under water stress conditions. For years, different hypotheses have been proposed about the effects of growth restrictions (Gifford and Evans, 1981). On the one hand, these restrictions would come from the source, that is, growth is limited because of carbohydrate assimilation reduction during photosynthesis. However, in the last years, a robust line of evidence suggests that growth restrictions would come from the sink effect mainly by tissues in expansion and with a greater demand of carbohydrates and water such as growing meristems and reproductive organs of the plant (Muller et al., 2011).

14
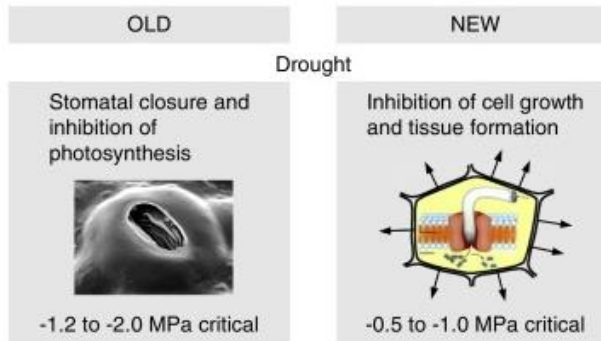
Fig. 4: A comparison of traditional and suggested novel priorities in plant growth control when water availability constrain plant growth (or productivity). Obtained and modified from Körner (2015).

Carbohydrates, produced by photosynthesis (A_N), play an important role in plant growth since a large part of the biomass for tissues and structural parts of plants comes from the carbon fixed during this process. Therefore, it is conceivable that part of the growth limitations is due to the availability of carbon. However, there is increasing evidence that plants not only limit their growth by the availability of carbon, but also by the availability of water (Fig. 4). Plant water relations are important in the elongation of tissues and the expansion of plant cells (Körner, 2003; Muller et al., 2011; Steppe et al., 2015) and, in fact, the elongation processes are more sensitive to turgor pressure than to photosynthetic assimilation (Hsiao et al., 1976). In recent years, all these facts suggest that the original model of plant growth focused only on source limitation is more complex and should be focused on a dual source-sink point of view (Fatichi et al., 2014; Fatichi et al., 2019). The issue is even more complicated because A_N under moderate water stress is mainly limited by stomatal conductance (g_s), which, in turn, is closely related with turgor pressure (Rodriguez-Dominguez et al., 2016). This shows that both photosynthesis and turgor maintain a close relationship that plays a

fundamental role. However, part of the problem in resolving this conflict is that it has not been possible to quantify the contribution of each of them.

These relevant knowledge gaps motivate the study of water and carbon limitation on fruit growth, which is a major objective of this PhD. Thesis.

1.3.2. The fruit load as major driver of tree water-carbon relations

One of the mechanisms that influence the optimization of fruit growth rates and, therefore, the final fruit yield, is the fruit load. However, fruit load not only defines yield but also may influence the water-carbon relations of the tree as fruits behave as strong sink organs. Indeed, fruit load effects have been studied in many fruit species, including olive trees, and it has been found that fruit load affects vegetative parameters (i.e. trunk growth, branch length and node numbers were reduced) (Martín-Vertedor et al., 2011a); g_s increased while Ψ_{stem} decreased (Naor et al., 2013) and specific water consumption (SPWC) increased (Fig. 5) (Bustan et al., 2016). Moreover, the effect of crop load on tree-water relationships has been reported to be variable, likely dependent on the level of tree water stress (Martín-Vertedor et al., 2011b; Naor et al., 2013).
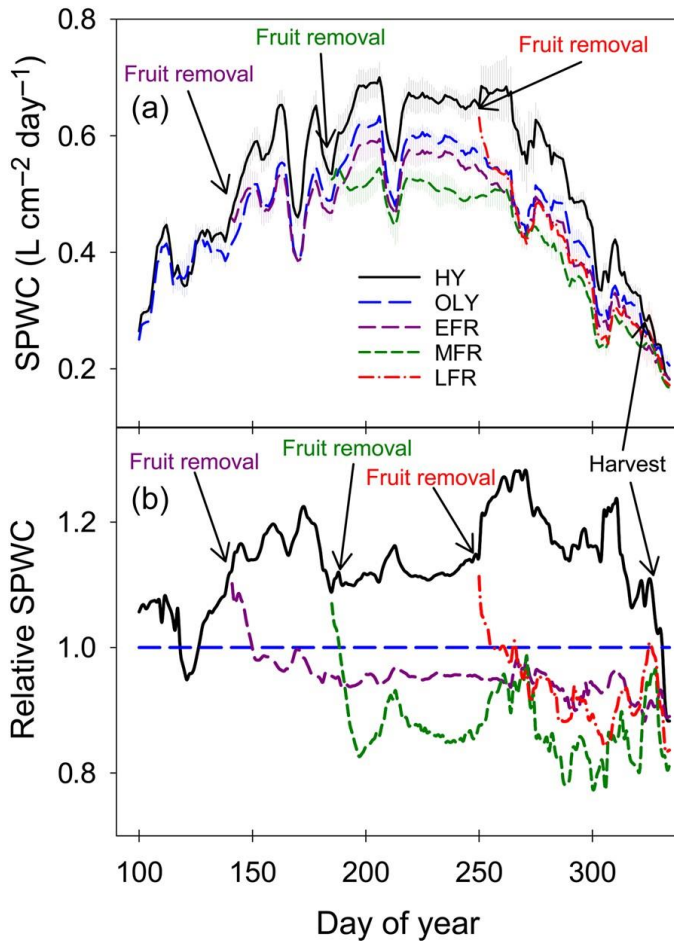
Fig. 5: Time course of specific water consumption (SPWC) for olive fruit season in 2011 **(a)**. Specific water consumption by HY (high yielding), OLY (originally low yielding), EFR (early fruit removal), MFR (mid fruit removal) and LFR (late fruit removal). Relative SPWC **(b)**—SPWC normalized to the OLY group. Error bars are standard errors. Source (Bustan et al., 2016).

It is known that high fruit loads affect tree water and carbon relationships.. However, there are still some unresolved questions regarding the mechanisms underlying this increase. Fruit growth requires a constant supply of water and carbon, and thus, the carbohydrates produced at the source (leaf) by photosynthesis are moved to sinks (fruits) at different moments of the day (Gersony et al., 2020). These carbohydrates or soluble

sugars, also known as non-structural carbohydrates (NSCs) are known to have osmoregulatory potential in plants (Fatichi et al., 2014; Martínez-Vilalta et al., 2016). The accumulation or decrease of NSCs and inorganic ions in the leaves as a function of the fruit load modifies Ψ_π but their effect has not been directly quantified.

1.4. Molecular scale: mechanisms involved in olive oil biosynthesis and quality during water stress.

As mentioned before, fruit quality is another key characteristic of fruit production. Interestingly, in olives, it has been shown that the amount of virgin olive oil content is less sensitive to water stress (Costagli et al., 2003) than other growth processes in the plant (Iniesta et al., 2009) and fruit (Hernandez-Santana et al., 2018). In addition, it has been observed that the fatty acid composition is only slightly changed under moderate water stress, and when it does, the quality of the oil is increased (Tovar et al., 2002; Gómez-Rico et al., 2007; Ahumada-Orellana et al., 2018; Hernández et al., 2018). However, the molecular mechanisms explaining why the oil accumulation is not affected and why the quality of virgin olive oil improves under water stress conditions are still not fully understood. Knowing all these mechanisms in depth could ensure a higher quality fruit and virgin olive oil yield with less resource consumption.

1.4.1. Olive fruit photosynthesis: Key as a carbon source to oil biosynthesis

Photosynthesis and its limitations by water deficit play a key role in fruit growth and oil biosynthesis processes (Lawlor and Cornic, 2002) because sugars and carbohydrates are the precursors to synthesize lipids in plant cells.

The olive fruit is a drupe consisting of an exocarp, a mesocarp, and a woody endocarp, which consists of a woody shell enclosing one or, rarely, two

seeds (Sanchez, 1994). The olive fruit mesocarp is where most of the TAG accumulates, along with the fact that it has active chloroplasts.

In this way, the fruit has two carbon sources for growth and oil biosynthesis; sugars imported from leaves via phloem, and sugars photosynthesised in the fruit mesocarp (Sánchez and Harwood, 2002). According to Sánchez and Harwood (2002), during the light period, fruit photosynthesis has an important role in re-fixing CO_2 produced by mitochondrial respiration. Measuring the relative contribution of each carbon source to fruit growth and oil biosynthesis is not easy. The measurements of gas exchange with an infrared gas analysis (IRGA) that occurs during fruit photosynthesis do not normally reach the compensation point, and thus, its contribution as a carbon source has always been thought to be modest (Blanke and Lenz, 1989). Sánchez (1995) and Sánchez and Harwood (2002), would show years later, using labelled ^{14}C, that fruit photosynthesis does have a positive contribution to fruit growth and oil biosynthesis. To understand the molecular mechanisms that regulate oil biosynthesis under different water conditions, it is necessary to evaluate the relative contribution of the different carbon sources (generated by leaf or by fruit photosynthesis) for triacylglycerol (TAG) biosynthesis in the olive mesocarp, and to study the expression levels of gene encoding TAG synthesizing enzymes (DGAT and PDAT) and fatty acid desaturases (FAD) which are involved on unsaturated fatty acid (UFA) composition. Thus, in this PhD. Thesis we studied the molecular and biochemical mechanisms that explain why oil accumulation is not affected by a RDI and why its quality is even improved.
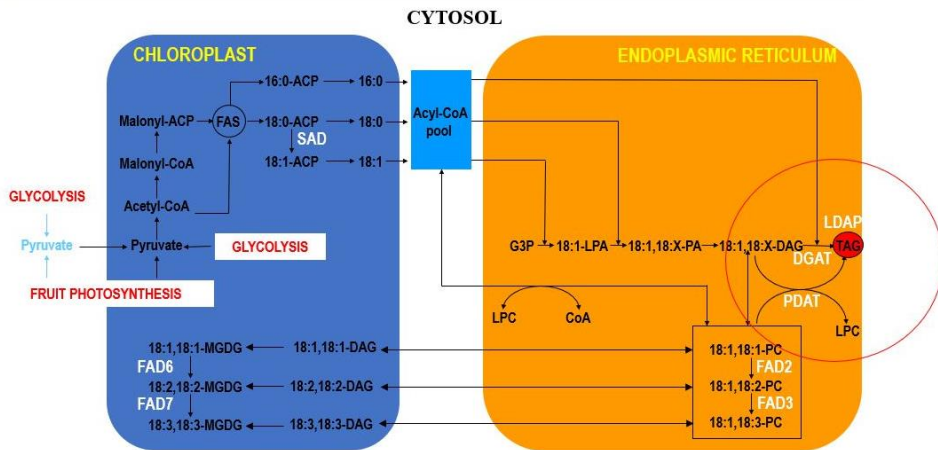
Fig. 6. Schematic representation of olive lipid biosynthesis pathway. Sugars are catabolized via glycolysis in the plastid to acyl-ACPs. They could be exported to the cytosol as acyl-CoAs. The latter are used by the Kennedy pathway (red circle and Fig. 8) for triacylglycerol (TAG) assembly on the endoplasmic reticulum. Oleic acid (18:1) could be desaturated by membrane-bound fatty acid desaturases (FAD) to linoleic and linolenic acids in the chloroplast and in the endoplasmic reticulum. Modified from Conde et al. (2008).

Sugars and carbohydrates come from the ultimate precursor of carbon for TAG biosynthesis, which is CO_2. The carbon fixation occurs by the photosynthesis process on olive fruit mesocarp (Sanchez, 1994; Sánchez and Harwood, 2002). The sugars from both carbon sources are catabolized in the fruit mesocarp via glycolysis. In this process, pyruvate is obtained, which is converted into acetyl-CoA, the precursor of de novo fatty acid biosynthesis (Fig. 6). Briefly, in higher plants, fatty acid biosynthesis begins in the plastids, with oleoyl-ACP (18:1-ACP) being the main product of plastidial fatty acid biosynthesis (Harwood, 2005). In the plastid, the synthesized acyl-ACPs can be used for glycerolipid assembly, for glycerolipid assembly and further desaturation, or cleaved by specific thioesterases to free fatty acids, activated

20

to acyl-CoAs, and exported to the cytosol. Thus, the acyl-ACP pool is now in the endoplasmic reticulum and available for incorporation into membrane glycerolipids and to allow de novo TAG formation via the Kennedy pathway (Fig. 7). This pathway involves the sequential acylation of glycerol 3-phosphate (G3P) to form diacylglycerol (DAG) and it is key because the synthesis of TAG is catalysed by the final acylation of diacylglycerol (DAG) by the enzyme diacylglycerol acyltransferase (DGAT). Additionally, an alternative acyl-CoA independent reaction catalysed by the phospholipid:diacylglycerol acyltransferase (PDAT) has been described for TAG synthesis (Dahlqvist et al., 2000), which transfers an acyl group from phosphatidylcholine (PC) to DAG, producing TAG.
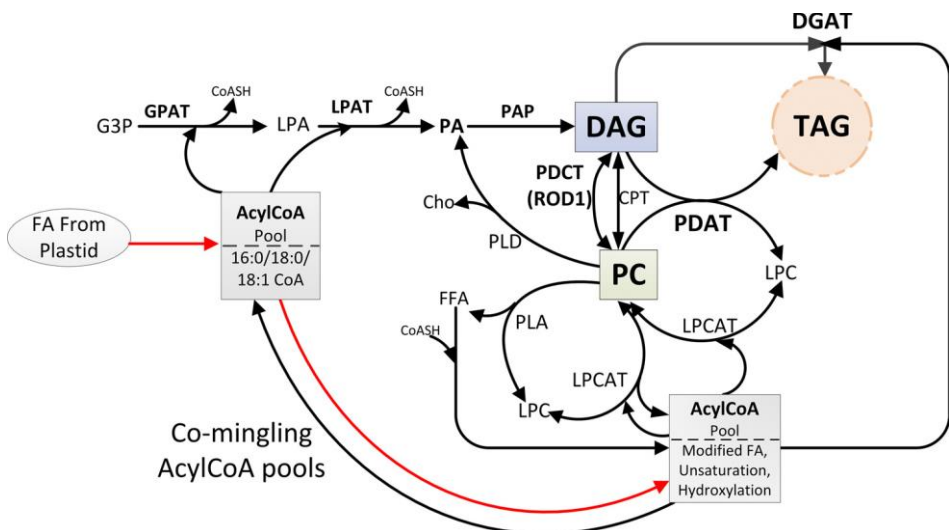
Fig. 7. The Kennedy pathway involving DGAT and PDAT enzymes in TAG assembly. Source: (Chapman and Ohlrogge, 2012).

On the one hand, two DGAT genes (*OeDGAT1-1* and *OeDGAT2*) have been isolated and characterized in olives, with different expression patterns but showing overlapping during olive mesocarp development (Banilas et al., 2011). In addition, two new DGAT1 genes (*OeDGAT1-2* and *OeDGAT1-3*) have

also been identified in the olive genome (Unver et al., 2017). Its importance is that DGAT1 enzymes have been mainly related to the accumulation of TAG in oilseeds, while DGAT2 is responsible for the incorporation of unusual fatty acids into TAG (Bates, 2016). On the other hand, three PDAT genes (*OePDAT1-1*, *OePDAT1-2*, and *OePDAT2*) have been recently cloned, characterized and investigated their contribution to oil synthesis in olive fruit (Hernández et al., 2021a).

1.4.2. The reason for determining virgin olive oil quality.

One of the advantages of applying a regulated deficit irrigation is that an improvement in the quality of virgin olive oil is appreciated (García et al., 2013; Caruso et al., 2014). Moreover, one of the main characteristics of virgin olive oil is that, during extraction, no harsh treatment is required to maintain the integrity of its water-soluble constituents as polyphenols and volatile compounds, which are responsible for its properties (Sánchez and Harwood, 2002; Rotondi et al., 2004; Aparicio and Harwood, 2013). The presence of those natural antioxidants that reduces lipid peroxidation, together with the high monounsaturated and low polyunsaturated fatty acid contents, means that olive oil maintains its benefits for human consumption (Harwood and Yaqoob, 2002).

In this way, virgin olive oil is composed of different fatty acids. Oleic acid is the one that is mainly present (55% - 83%), followed by palmitic acid (8% - 20%), linoleic acid (4% - 21%) and linolenic acid less than 1% (European Commission Regulation, 2003). In the fatty acid composition in olive oil, the activity of membrane-bound fatty acid desaturases (FAD) plays a fundamental role because oleic acid can be further desaturated to linoleic and linolenic acids by them. FAD2 and FAD3 are located in the endoplasmic reticulum, and FAD6 and FAD7/8 are in the chloroplast (Fig. 6). The difference between them is not

only their cellular locations but also their lipid substrate (Shanklin and Cahoon, 1998). To date, five genes encoding microsomal oleate desaturases (*OeFAD2-1* to *OeFAD2-5*) have been reported (Hernández et al., 2005; Hernández et al., 2020), and only one, *OeFAD6* gene has been identified (Banilas et al., 2005; Hernández et al., 2011). According to Hernández et al. (2009, 2020), there are two main genes determining the linoleic acid content in the virgin olive oil; *OeFAD2-2* and *OeFAD2-5.* Secondly, four members of the olive linoleate desaturase gene family have been isolated and characterized, two microsomal (*OeFAD3A*, Banilas et al., 2007; *OeFAD3B*, Hernández et al., 2016), and two plastidial (*OeFAD7-1*,Poghosyan et al., 1999; *OeFAD7-2*, Hernández et al., 2016), with *OeFAD7-1* and *OeFAD7-2* as the main genes that contribute to the linolenic acid present in the olive oil (Hernández et al., 2016).

1.5. Objectives

The described background motivates this Ph.D. Thesis, whose main objective is unravelling the plant and fruit physiological mechanisms limiting fruit and oil yield in response to water stress in olive trees from different approaches. In the next chapters, we will approach this from different perspectives and scales. Facing the problem from the plot scale, we intend to identify the annual variability that occurs in yield between trees and plots subjected to the same irrigation treatment (**Chapter 2**), continuing at a tree-fruit level, our objective was to understand the importance of photoassimilates (A_N) and the leaf turgor (P) in the fruit growth (**Chapter 3**), and how the presence or absence of fruits are able to modify plant water relations (**Chapter 4**), ending at a molecular scale, to understand why olives do not stop oil accumulation under water stress conditions (**Chapter 5**)

.

CHAPTER **2**:

CANOPY SIZE QUANTIFIED WITH DIGITAL SURFACE MODELS IS THE MAJOR DIRECT AND INDIRECT DETERMINANT OF OLIVE FRUIT AND OIL YIELD

Abstract

In this study, we explored the use of low-cost UAV imagery and automatic digital surface models for canopy size quantification and its further use to explain the fruit and oil yield in an olive orchard. The analysis was performed in well-watered plants (WW) and water-stressed plants (WS) subjected to deficit irrigation. Canopy size was hypothesised to be the main factor influencing yield directly or indirectly, and its relevance was compared with other factors related to canopy size, fruit growth and oil accumulation. The factors considered were: leaf nitrogen, fruit weight, fruit oil content, number of shoots with fruits per canopy volume, canopy temperature, and the normalised derived vegetation index (NDVI). Our results showed that canopy size was the major determinant of fruit and VOO yield. Moreover, the variability in canopy size within WW and WS treatments contributed to explaining the higher variability in WW compared to WS in both fruit yield and VOO. The factors that determined fruit yield and VOO yield were different, and the application of a deficit irrigation strategy modulated or changed the contribution of these factors. A detailed analysis of the contribution of each factor showed three general conclusions: 1) fewer factors were always necessary to explain the variability in WW than in WS with the factors considered; 2) more variance was explained in WW than in WS; 3) with the factors considered we were able to explain the more variance in VOO than fruit yield. This work illustrates the need to identify the essential variables driving yield, and to design the monitoring approach from the ground and remote sensing technologies.

Keywords: water stress; deficit irrigation; yield variability; low-cost UAV imagery; thermal images; NDVI

2.1. Introduction

Knowing in advance how much yield a certain plant, tree or crop will produce based on the environmental and physiological conditions of the plant, is becoming increasingly necessary in the current context of greater demand for water and food (Dhankher and Foyer, 2018). Specifically, in the Mediterranean region, one of the main crops whose yield management has been studied is the olive tree (*Olea europaea* L.). For several years, studies have been conducted to determine the effect of regulated deficit irrigation (RDI) strategies on fruit and virgin olive oil (VOO) yield. The objective was to save water without affecting fruit yield by applying a RDI (Moriana et al., 2003; Dell'Amico et al., 2012; Fernández et al., 2013), increasing VOO yield as well as its quality (García et al., 2013; Caruso et al., 2014). All these studies have been in the line of investing efforts in implementing irrigation based on plant physiology (Fernández, 2014; Diaz-Espejo et al., 2018; Hernandez-Santana et al., 2018).

However, irrigation affects fruit yield in the current (Iniesta et al., 2009) and the following years (Melgar et al., 2008; Gucci et al., 2019) varying from one year to another, even if the same strategy of irrigation is applied (Alegre et al., 2002). Moreover, even in the same experimental year, the high tree-to-tree variability in the same irrigation treatments may prevent significant differences from arising when comparing fruit and VOO yield between different irrigation treatments (e.g. Padilla-Díaz et al., 2018). Indeed, an extensive review using results from 24 olive orchards by Fernández et al. (2020) showed a remarkable fruit and VOO yield variability for the irrigation levels considered. Although in the results shown by Fernández et al. (2020), additional factors such as tree density or climate may play an important role, it seems that on-site variables must be affecting fruit and VOO yield in addition to irrigation amount. These uncontrolled factors can have relevant consequences on the RDI results. Thus,

although the RDI strategy is showing promising results, there are still some unknowns to be resolved, as irrigation is not the only factor affecting fruit and VOO yield.

This fruit and VOO yield variability observed for the same irrigation treatments could be partly explained by the canopy size because trees with greater leaf area should have higher yields (e.g. Hernandez-Santana et al. 2017). The dependence of yield on canopy size comes from two main aspects: a tree with a larger leaf area is capable of producing more photoassimilates (Hernandez-Santana et al., 2017) which is an important issue once the growing fruits become strong carbon sinks; and also a larger tree can carry larger crop load increasing the potential number of bearing-fruit shoots (previous year shoots). Canopy size can be affected by irrigation treatment in the long term because fruits become a priority for water-stressed trees, which results in reduced vegetative growth compared to well-watered trees (Iniesta et al., 2009; Dag et al., 2010; Hernandez-Santana et al., 2018).

Until now, there were no technologies to address the diversity of canopy sizes in large farms, but now they do exist, although we are not aware that they have been used to assess the effect of tree canopy size on yield. Indeed, recent studies carried out on olive orchards suggest that visible images obtained from unmanned aerial vehicles are useful for describing the canopy size distribution (Caruso et al., 2019; Caruso et al., 2022a; Caruso et al., 2022b). Several studies have shown that high-resolution images from unmanned aerial vehicles can be used to infer geometrical canopy characteristics, such as canopy volume or diameter and tree height (Zarco-Tejada et al., 2014; Caruso et al., 2019; de Castro et al., 2019; Jurado et al., 2020a). Some of these results have been used to evaluate the effect of deficit irrigation on canopy growth (Caruso et al., 2022b), which has a high impact on the estimation of water

needs and the potential crop load the trees can bear, but its effect on fruit or VOO yield has not been evaluated.

In addition to the valuable information given by visible images to estimate canopy size, other indicators also derived from images have proven useful to evaluate the water status of the plants and its relation with yield, such as the normalised difference vegetation index (NDVI) (Caruso et al., 2021) and canopy temperature (Egea et al., 2017). But although canopy size and plant water status are often used as the main determinants of crop performance, other factors related to the impact of canopy size (number of shoots with fruits) and its growth on yield (N, fruit and olive oil fresh weight) can be envisaged to be influencing fruit and VOO yield and will be evaluated in this work (Fig. 1).
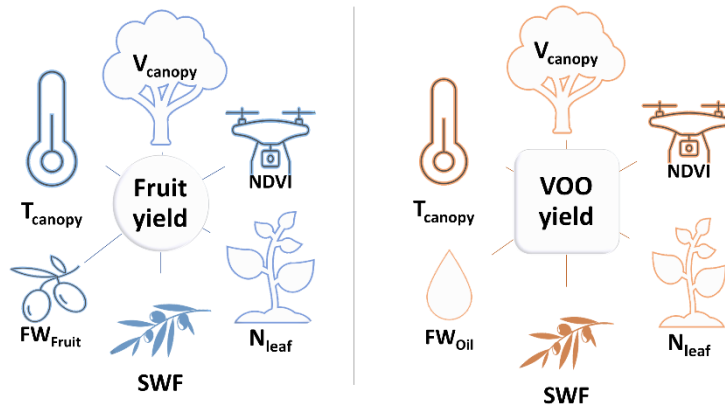
Fig. 1. Main factors affecting fruit yield (Kg tree^{-1}) (left) and virgin olive oil (VOO) yield (Kg tree^{-1}) (right). Canopy size (V_{canopy}) (m^3), NDVI, leaf nitrogen Kjeldahl (N_{leaf}) (g m^{-2}), shoots with fruits (SWF) (m^{-3}), fruit fresh weight (FW_{fruit}) (g fruit^{-1}), oil fresh weight per fruit (Fw_{oil}) (g fruit^{-1}) and canopy temperature (T_{canopy}) (°C).

This study aimed to identify the main factors influencing yield variability among trees in an olive orchard using current technologies that allow for rapid sampling over large field areas. We hypothesise that canopy size was the main factor influencing yield, given an irrigation treatment. We further hypothesize

that the relative contribution of this and other factors considered would depend on the plant water status produced by different irrigation treatments. Specifically, we expect that factors related to vegetative components, such as canopy volume and the number of shoots with fruits, would be the main determinants of yield in those plants with no limiting water resources. Meanwhile, other factors more directly related to the reproductive component, like fruit FW and the amount of oil accumulated per fruit, would be limiting in the case of trees subjected to deficit irrigation treatment. To achieve such a goal we i) use visible images from unmanned aerial vehicles to describe the plant size variability within the orchard and ii) applied a contribution analysis to quantify the relative role of canopy size and other factors influencing final fruit and VOO yield for a well-watered (WW) and watered stressed (WS) treatment. The identification of the driving factors of the yield in olive orchards and their nature will help to implement management practices to improve fruit and VOO yield and to make more realistic predictions.

2.2. Materials and methods

2.2.1. Description of the orchard and the experimental site

The experiment was conducted in a commercial super-high-density olive orchard (*Olea europaea* L. cv. Arbequina) near Utrera (Seville, southwest Spain) (37° 15' N, -5° 48' W) (Fig. 2.) from July to November of 2018. The study was carried out in 12-year-old olive trees planted in a 4 m × 1.5 m formation (1667 trees ha-1), in rows oriented north-northeast to south-southwest. In the orchard, the alternate bearing was not noticed in the last years (Fernández et al. 2013; Hernandez-Santana et al. 2017). The characteristic soil in the orchard had a sandy top and a bottom clay layer

(Arenic Albaquaf, USDA 2010). Further details on the orchard characteristics can be found in Fernández et al. (2013).

2.2.2. Climate conditions and meteorological measurements

In the area, the climate is Mediterranean, with mild, rainy winters and hot, dry summers, with hardly any rain during the months of the study. The annual rainfalls occur mainly between late September to May. Average evapotranspiration (ET_O) and precipitation are 1482 mm and 500 mm, respectively, for the 2002-2018 period (data recorded at the nearby of the study area, Los Molares station, 37° 10' 34'' N -5° 40' 22'' W belonging to the Regional Government of Andalusia). For the same period, the average maximum ($T_{a, max}$) and minimum ($T_{a, min}$) air temperatures were 24.8 °C and 10.6 °C, respectively. The hottest months are July and August, whose $T_{a, max}$ values over 40 °C. Also, at least once per year, between July and August, it is reached vapour pressure deficit (VPD) values over 7 KPa.

A weather station (Campbell Scientific Ltd., Shepshed, UK) in the experimental area monitored the main weather variables. Meteorological sensors were between 2 m and 3 m above the canopies. Values of wind speed (u), air temperature (T_a), air humidity (RH_a), global solar radiation (R_s), net radiation (R_n), photosynthetically active radiation (PPFD) and precipitation were recorded every 30 min.

2.2.3. Irrigation treatments

We applied two different irrigation treatments: a well-watered treatment (WW) with a full irrigated regime in which the trees were irrigated daily to replace their irrigation needs (IN) fully, and a watered stressed treatment (WS) whose trees received only 45% of IN. Each

irrigation treatment was applied in four 12 m × 16 m plots in a randomised design (n = 4) (Fig. 2).
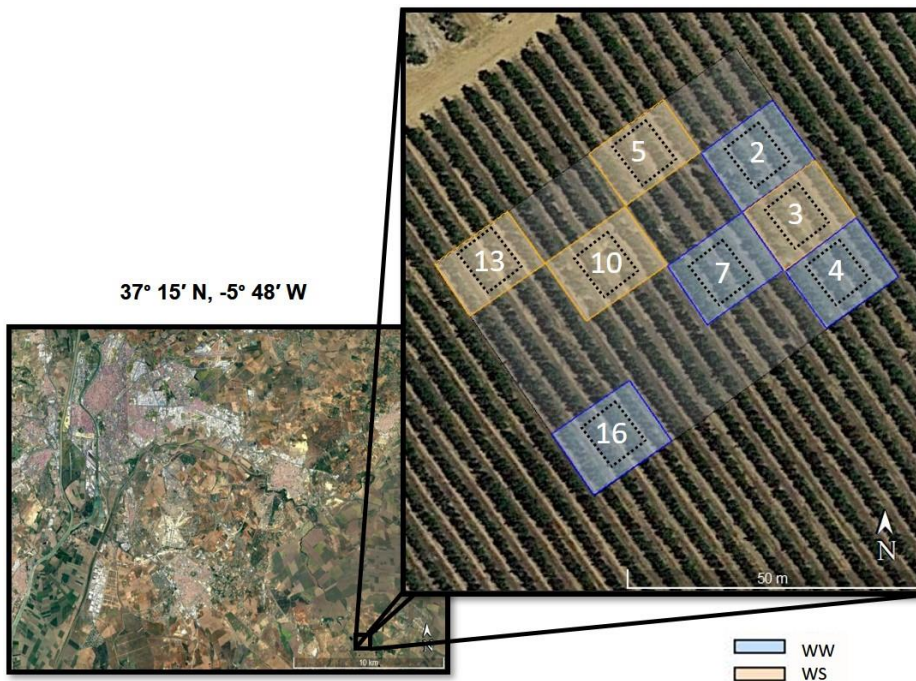
Fig. 2. Experimental orchard in Utrera (Seville, southwest Spain) (37° 15′ N, -5° 48′ W) in well-watered (WW) (blue) and water stressed (WS) (orange) trees in a randomised plots design. Numbers indicate the plot number, and dashed lines indicate the central trees of the plot where measurements were carried out.

There were 24 trees per plot, but measurements were made just in 4 central trees to avoid any border effect. The irrigation system consisted of a single pipe per tree row with three 2 L h^{-1} drippers per tree, 0.5 m apart. IN was calculated daily based on a simplified version of the stomatal conductance (g_s) model evaluated in this olive orchard by Diaz-Espejo et al. (2012) and described in greater detail in Fernandes et al. (2018). Briefly, the WW treatment was assumed to be at field capacity, i.e. a soil matric potential equal to 0. Following this model, g_s is described as a function of

34

air vapour pressure deficit (D), average radiation (R_s) and tree leaf area (LA), the latter estimated once every fifteen days for each plot during the irrigation season. The leaf area index (LAI) was measured at dawn with a LAI-2200 Plant Canopy Analyzer (Li-Cor, Inc., Lincoln, NE, USA), according to Diaz-Espejo et al. (2012). Assuming a perfect coupling between canopy and atmosphere, tree water consumption (E_p) was calculated as $E_p = D$ ($g_{s,sun}$ *LA$_{sun}$ + $g_{s,shade}$* LA$_{shade}$). The proportion of sunny to total leaf area was estimated to be 35%, according to Diaz-Espejo et al. (2002) and Fernández et al. (2008). Soil evaporation (E_s) was estimated according to Orgaz et al. (2006). Finally, IN was estimated as $E_p + E_s$.

For the WS treatment, we applied the regulated deficit irrigation (RDI) strategy recommended by Fernández et al. (2013) and improved by Fernández et al. (2018). This strategy considers three periods in the growing cycle at which the crop is highly sensitive to water stress. During these periods, irrigation replaced the crop water needs. Period 1 extended from the final stages of floral development to full bloom (second fortnight of April); period 2 was in the 6 to 10 weeks after bloom, during active pit hardening (June); and period 3 was at a period of approximately three weeks prior to ripening, after the midsummer period of high atmospheric demand (from late August to mid-September). Between periods 2 and 3 (late June to late August), the olive tree is considered to be resistant to drought and thus, it was irrigated less, only twice per week, amounting to a total of ca. 20% IN for the whole period. From the end of period 3 to harvesting (mid-November) ca. 40% of IN was supplied. Further details on regulated deficit irrigation can be found in Fernández et al. (2013) and Hernandez-Santana et al. (2017). The RDI period occurred from DOY 196 to 243, and the irrigation recovery started for WS trees afterwards.

2.2.4. Fruit and virgin olive oil (VOO) yield measurements

The harvest was carried out on November 13th of 2018. All the fruits of each of the four central trees of each plot were manually collected. Fruit yield (Kg tree^{-1}) was measured by taking the fresh weight of all the fruits of each tree. From the fruit yield sample of each tree, we randomly took two replicates of 1Kg. Olive oil was physically extracted the next day of harvest using an Abencor system small-quantity mill (MC2 Ingeniería Sistemas, Seville, Spain) according to Martínez et al. (1975), Ben-David et al. (2010) and Morales-Sillero et al. (2017). Finally, to obtain VOO yield (Kg tree^{-1}), we applied oil percentage to fruit yield per tree.

2.2.5. Measurements of factors affecting fruit and VOO yield

2.2.5.1. Estimation of canopy volumes from UAV

We carried out pre-irrigation unmanned aerial vehicle (UAV) flight campaigns on June 27th, August 30th, and October 24th of 2018 (Fig. 2). Only the images from the flight of August 30th were used as that day the water stress produced by the treatments was the most severe of the three dates. Flights were always performed between 11h and 13h UTC. We used a Phantom 4 Pro+ multirotor UAV (DJI Innovations, Shenzhen, China) equipped with a visible camera 4K 20 Mpix resolution. Two flight heights were applied; one at 120 m providing a Ground Sampling Distance (GSD) of 1.37 cm, and a low one at 50 m, providing a GSD of 0.59 cm. We used an identical methodology as used in previous works in olive orchards (Zarco-Tejada et al., 2014; Caruso et al., 2019). Briefly, geometric and radiometric processing was implemented with Pix4D© software, producing orthomosaics, point clouds and digital surface (DSM) and terrain (DTM) models (Fig. 3 and 4). DSM and DTM from the low flight during the third campaign were used to retrieve a Canopy Height Model (CHM).

36
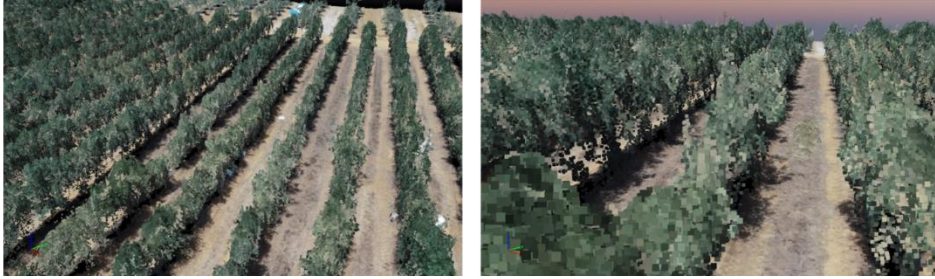
Fig. 3. 3-D reconstruction of olive tree canopies from the unmanned aerial vehicle (UAV) using the Pix4D software. Original pixel resolution was 0.59 cm, although it was increased for the representation.
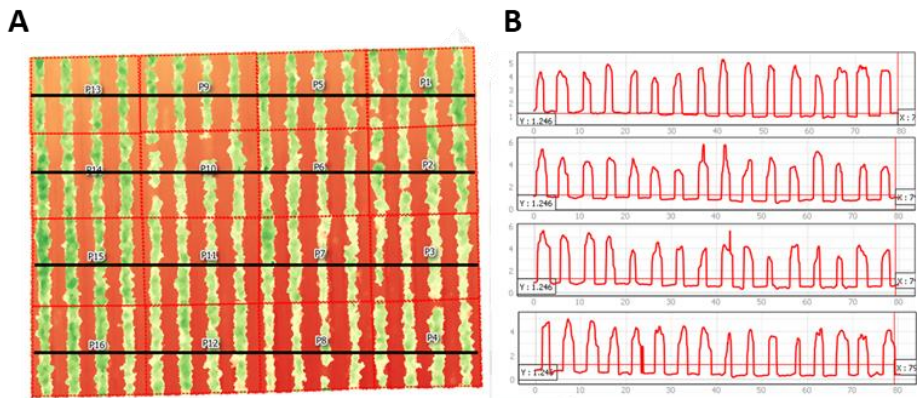
Fig. 4. A) Spatial distribution of canopy heights in the experimental orchard. Black lines represent transects as an example to show the estimation of digital surface model (DSM) and digital terrain model (DTM) **B)** used to calculate the volume of trees.

Plant crowns were visually digitised over CHM to estimate maximum heights and plant volumes. A DSM is a numeric matrix in which each element (pixel) represents the height above the sea level. Both ortho-pictures and DSM files were incorporated into a Geographic Information System (QGIS), together with the location of our plots, to extract the study area. DSM data contains the level value every 0.059 x 0.059 m, which allowed us to estimate the elevation of the different parts of the tree in a

detailed way. From the skeletonisation of the hedgerows and their position in the plots, we quantified the volume of the tree crowns, discounting the trunk height.

To determine the tree height, we randomly sampled 5% of the trees in the study area and obtained the average trunk height, which was 1.04 m. The volume of the hedgerow was the result of summing up the height of all pixels multiplied by its resolution (0.0034 m^2). This quantification includes the height from the soil surface to the base of the crown, so the average trunk height was discounted. Furthermore, the exact location of each trunk in the hedgerow was determined, and the volume of each tree was estimated, assuming that all trees occupy the same space in the direction of row (i.e. the difference among trees was determined by differences in row width and tree height).

2.2.5.2. Multispectral and thermal images

On the same dates as previous flights in the visible band, it was acquired as well images from a multispectral camera and a thermal camera (Fig. 5). A Sensefly eBee fixed-wing equipped with a multispectral Parrot Sequoia camera was used to calculate NDVI. The sensor has four bands: Green (550 nm), Red (660 nm), Red Edge (735 nm) and Near-infrared (790 nm). Flight height was at 53 m providing a GSD ~ pixel size of 5.02 cm. The Sensefly eBee fixed wing was then equipped with a thermal camera ThermoMap (7.5-13.5 μm). In the second flight, height was 53 m providing a GSD of 9.27 cm.
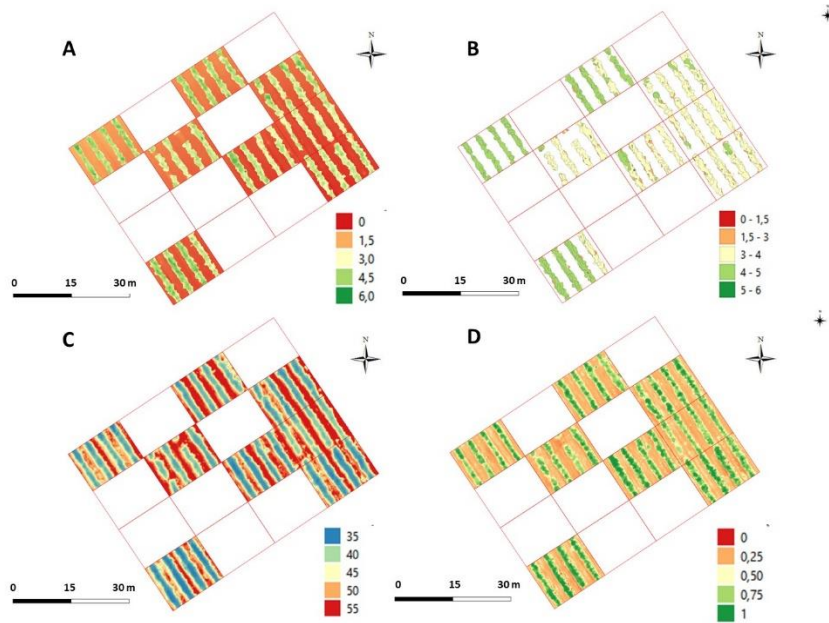
Fig. 5. Representation of tree heights (m) in the studied plots obtained from the estimation of **A)** digital surface model (DSM), **B)** digital terrain model (DTM), **C)** Thermal image (°C) obtained from an unmanned aerial vehicle (UAV) equipped with the thermal camera Thermomap and **D)** normalized difference vegetation index (NDVI) image obtained from an UAV equipped with a multispectral camera Parrot Sequoia.

2.2.5.3. Leaf nitrogen Kjeldahl (N_{leaf}) concentration

Leaf samples were taken in July for nutrient analysis. Enough current-year leaves were sampled from the middle portion of shoots around the canopy to have at least 0.4 g of dry weight to analyse Nleaf. Samples were washed in distilled water, dried at 70 °C until constant weight, grounded and passed through a 500 mm stainless-steel sieve. N_{leaf} concentration was determined by Kjeldahl method*.*

2.2.5.4. Average number of shoots with fruits (SWF)

Two days before the harvest, on November 11, 2018, 8 canopy area sections were sampled (4 on the east and 4 on the west side of the tree) in each of the 4 trees in each plot. To do the sampling, a 30 x 30 x 15 cm

39

sampling frame was used, and photographs were taken. Later, in the laboratory, the images were analysed manually by counting the number of shoots with fruits and calculating SWF per m3 of the canopy. The value obtained for each tree is the average of the 8 samplings*.*

2.5.5. Fruit and oil FW per fruit (FW$_{fruit}$ and FW$_{oil}$)

On the day of harvest, FW$_{fruit}$ was obtained from 100 fruits from each tree using an accurate electronic balance (Balance XS105, Mettler Toledo, Columbus OH, USA). FW$_{oil}$ was calculated by applying oil percentage of each tree (obtained as is described in Section 2.4) to FW$_{fruit}$.

2.2.6. Statistical analyses

To compare fruit and VOO yield between the irrigation treatments WW and WS we used a one-way ANOVA ($p < 0.05$). To study the factors affecting fruit and VOO yield, we applied a multiple regression model to analyse the relative contribution of each studied factor (V$_{canopy}$, NDVI, N$_{leaf}$, SWF, FW$_{fruit}$, FW$_{oil}$ per fruit and T$_{canopy}$) considered as a regressor to fruit and VOO yield. We calculated the relative importance metrics of each regressor using the R-package relaimpo (Grömping, 2006). Using this package, the regressors of the models can be correlated, and each regressor's contribution is not just the R^2 from univariate regression as it would happen if the regressors would not be correlated. We calculated relative importance in linear regression using the "lmg" method in the "calc.relimp" function, as suggested by Grömping (2006). The former analyses were conducted using the statistical software R (R Core Team, R version 4.1.0, 2021).

2.3. Results

2.3.1. Canopy size distribution

The mean canopy size was higher in WW, 7.02 m^3, than in WS, 5.95 m^3 (Fig. 6). The value of the median with respect to the mean indicates that in the case of WW the canopy sizes were biased toward bigger trees than in the case of WS. On the other hand, WS trees were biased toward smaller trees. The standard deviation (SD) was slightly higher in WW than in WS (6m^3 vs 4m^3). Overall, the distribution of canopy sizes showed the expected pattern according to the water supplied by the irrigation treatments.
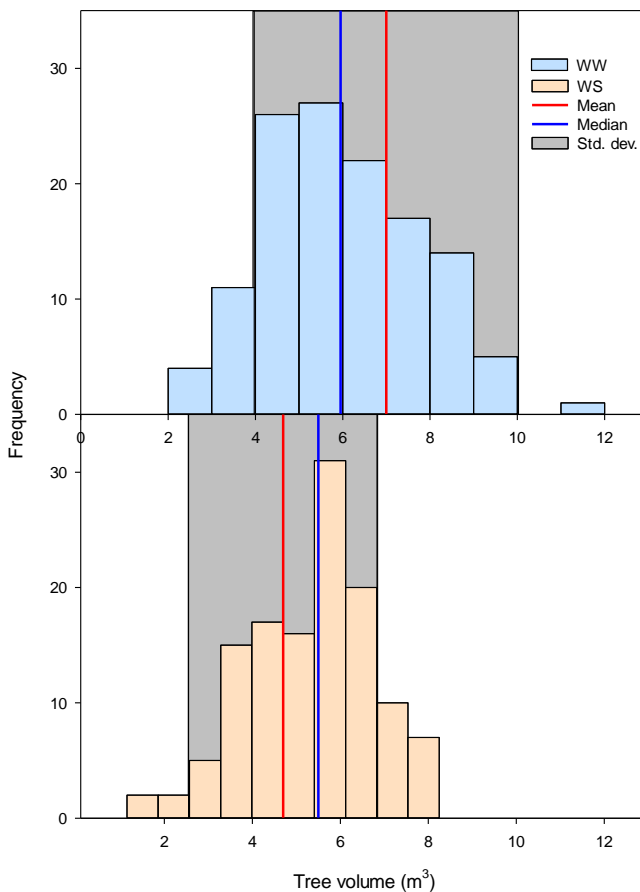
Fig. 6. Canopy volume (m^3) distribution in **A)** well-watered (WW) (blue) (n=127) and **B)** water stressed (WS) (orange) trees (n=125). Red and blue lines represent mean and median respectively. For WW, mean and median values are 7.02 and 5.95 respectively. For WS, mean and median values are 5.31 and 4.50 respectively.

2.3.2. Fruit and VOO yield

Both fruit and VOO yield showed a similar trend: WW trees presented higher variability than WS ones (Fig. 7). In WW trees, the mean fruit yield observed was significantly higher than in WS trees (15.16 Kg tree^{-1} and 12.61 Kg tree^{-1}, respectively) (Table1 and Fig. 7A). The mean of VOO yield per tree obtained was also significantly higher in WW than in WS trees (0.91 Kg tree^{-1} and 0.61 Kg tree^{-1}, respectively) (Table1 and Fig. 7B).
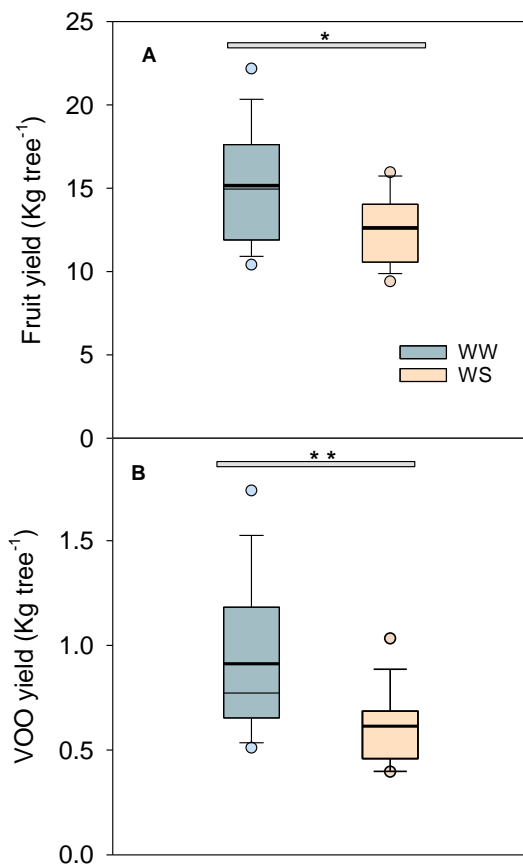
Fig. 7. Box-plot of the **A)** fruit yield (Kg tree^{-1}) and **B)** virgin olive oil (VOO) yield (Kg tree^{-1}) obtained in the campaign of 2018 according to well-watered (WW) (blue) (n=15) and water stressed (WS) (orange) trees (n=16). Lower and upper box boundaries 25th and 75th percentiles, respectively, line inside box median, bold line inside box mean, lower and upper error lines 10th and 90th percentiles, respectively, circles data falling outside 10th and 90th percentiles. Asterisks showed significant differences (p < 0.05) between WW and WS trees to one-way ANOVA.

2.3.3. Effect of irrigation and canopy volume on fruit and VOO yield.

We observed a linear relationship between V_{canopy} and fruit yield (Fig. 8A) and VOO yield (Fig. 8B). In both water treatments, the linear model based on V_{canopy} explained more variability in VOO yield ($R^2 = 0.55$, $p < 0.05$ and $R^2 = 0.40$, $p < 0.05$ for WW and WS, respectively) than fruit yield ($R^2 = 0.50$, $p < 0.05$ and $R^2 = 0.33$, $p < 0.05$ for WW and WS, respectively). Still, $V_{canopy,}$ on its own, was not able to explain most of the variability, suggesting that other factors are playing a role. It is noteworthy that fruit yield was affected by canopy volume in a similar fashion in both water treatments, as the similar slope in the relationship between both variables suggests it. WS trees produced proportionally less fruit yield at any given canopy volume. However, VOO yield did not follow this trend, and VOO yield in WS trees was less impacted by the increase in canopy volume than in WW trees.

2.3.4. Irrigation effect on V_{canopy}, NDVI, N_{leaf}, SWF, FW_{fruit}, FW_{oil} per fruit and T_{canopy}.

Not all factors showed the same response to the water treatments (Fig. 9 and Table 1). The V_{canopy} mean between WW and WS trees were similar (5.40 m^3 and 5.04 m^3, respectively) (Fig. 9A). The mean between WW and WS trees was also similar (1.59 g m^{-2} and 1.53 g m^{-2}, respectively) (Fig. 9C).

In the case of FW_{fruit} and FW_{oil} per fruit, both showed significant differences. For FW_{fruit}, WW trees showed higher values than WS trees ($1 \cdot 10^{-3}$ Kg fruit^{-1} and $6.4 \cdot 10^{-4}$ Kg fruit^{-1}, respectively) (Fig. 9E). A similar trend was found on FW_{oil} whose mean was significantly higher on WW than WS trees ($5.86 \cdot 10^{-5}$ Kg fruit $^{-1}$ and $3.14 \cdot 10^{-5}$ Kg fruit^{-1}, respectively) (Fig. 9F).

This was not the case with SWF, where differences in means were not found between WW and WS trees. The average number of shoots with fruits was 877.78 m^{-3} and 924.77 m^{-3}, respectively (Fig. 9D).

Finally, two indicators of plant activity and water stress, like NDVI and T$_{canopy}$, showed a significant difference between treatments in both factors in WW compared to WS trees. NDVI presented significantly higher values on WW than WS trees (0.62 and 0.57, respectively) (Fig. 9B). In the case of T$_{canopy}$, it was significantly lower on WW than WS trees (37.9 °C and 39.9 °C, respectively) (Fig. 9G).
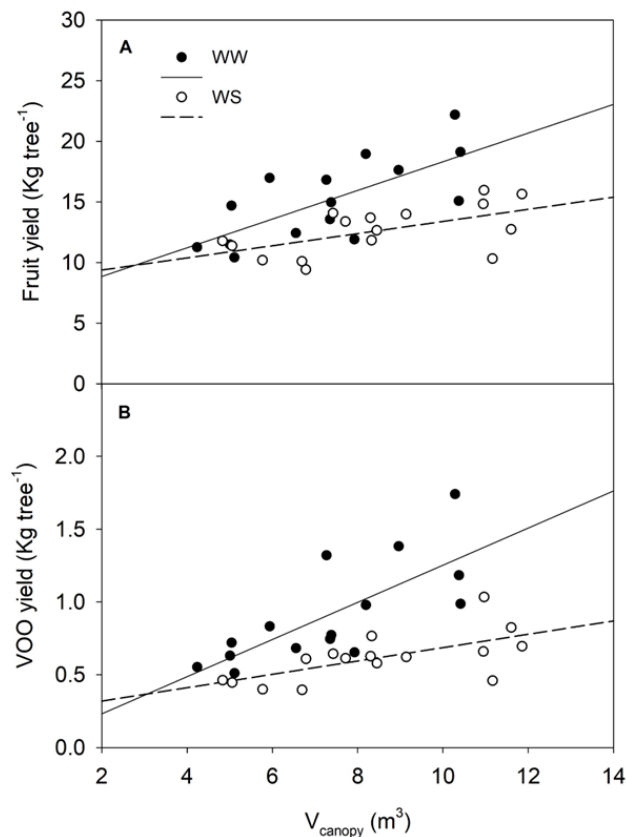
Fig. 8. Scatter plot between A) canopy volume (m^3) and fruit yield (Kg tree^{-1}) and B) canopy volume (m^3) and VOO yield (Kg tree^{-1}) in well-watered (WW) (n=15) and water stressed (WS) trees (n=16). Every dot represents a tree. Linear regression lines ($y = a + bx$) were fitted to each irrigation treatment. Solid and dashed line are the correlation in WW and WS R^2 = 0.50 (p < 0.05) / R^2 = 0.33 (p < 0.05), respectively for A) and R^2 = 0.55 (p < 0.05) / R^2 = 0.40 (p < 0.05) respectively for B).
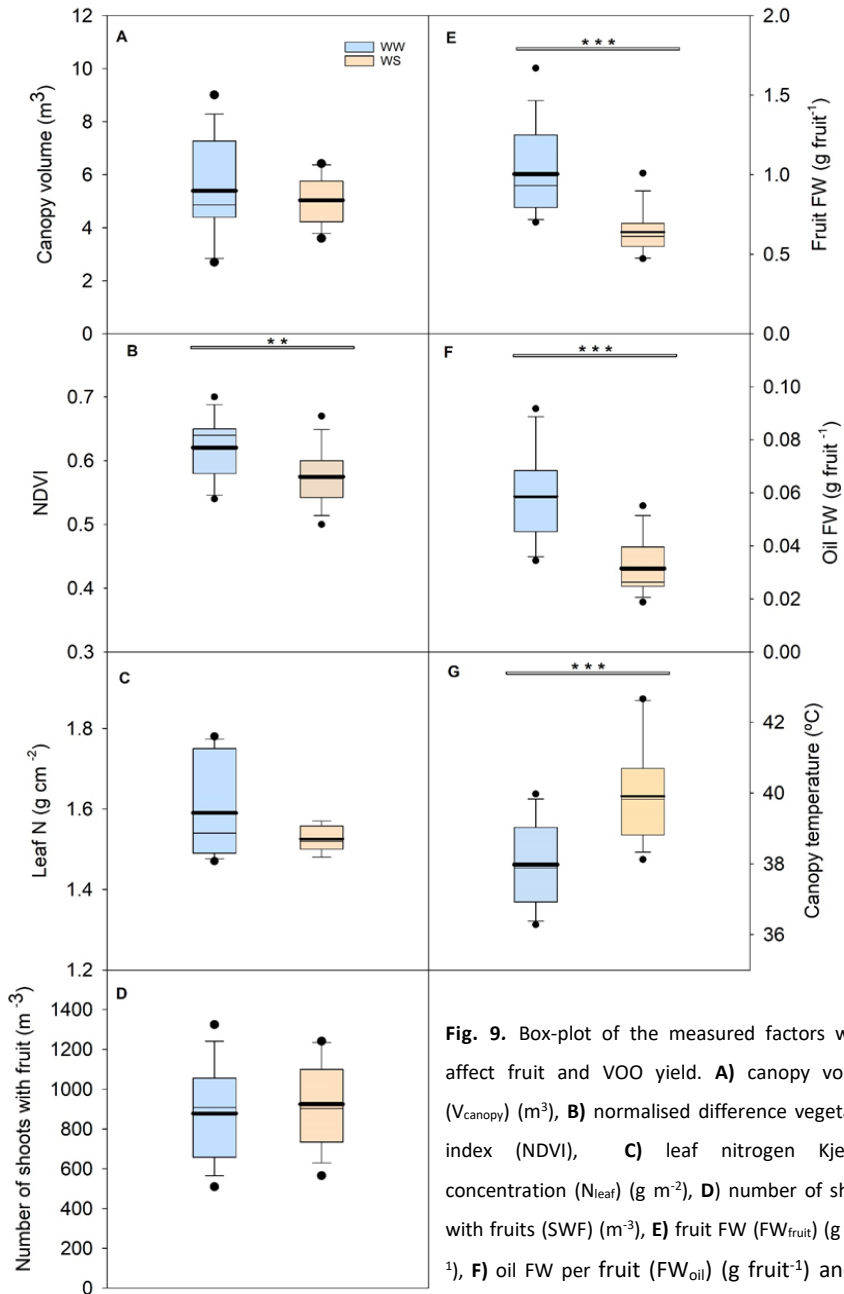
Fig. 9. Box-plot of the measured factors which affect fruit and VOO yield. **A)** canopy volume (V_{canopy}) (m^3), **B)** normalised difference vegetation index (NDVI), **C)** leaf nitrogen Kjeldahl concentration (N_{leaf}) (g m^{-2}), **D)** number of shoots with fruits (SWF) (m^{-3}), **E)** fruit FW (FW_{fruit}) (g $fruit^{-1}$), **F)** oil FW per fruit (FW_{oil}) (g $fruit^{-1}$) and **G)** canopy temperature (T_{canopy}) (°C) in well-watered (WW) (n=15) and water stressed (WS) trees (n=16). Lower and upper box boundaries 25th and 75th percentiles, respectively, line inside box median, bold line inside box mean, lower and upper error lines 10th and 90th percentiles, respectively, circles data falling outside 10th and 90th percentiles. Asterisks showed significant differences (p < 0.05) between WW and WS trees according to one-way ANOVA.

45

Table 1. Mean ± SE and coefficient of variation (CV) values of fruit and VOO yield (Kg tree^{-1}) and canopy volume (V$_{canopy}$) (m^3), NDVI, leaf N Kjeldahl (N$_{leaf}$) (g m^{-2}), shoots with fruits (SWF) (m^{-3}), fruit FW (FW$_{fruit}$) (Kg fruit^{-1}), oil FW per fruit (FW$_{oil}$) (Kg fruit^{-1}) and canopy temperature (T$_{canopy}$) (°C) on well-watered (WW) and water stressed (WS) trees.

	WW		WS	
	Mean ± SE	CV (%)	Mean ± SE	CV (%)
Fruit yield (Kg tree^{-1})	15.16 ± 0.88	22.54	12.61 ± 0.51	16.06
VOO yield (Kg tree^{-1})	0.91 ± 0.09	38.59	0.61 ± 0.04	27.32
V$_{canopy}$ (m^3)	5.40 ± 0.48	34.27	5.04 ± 0.23	17.91
NDVI	0.62 ± 0.01	7.69	0.57 ± 0.01	7.82
N$_{leaf}$ (g m^{-2})	1.59 ± 0.03	7.26	1.53 ± 0.01	2.14
SWF (m^{-3})	877.78 ± 62.42	27.54	924.77 ± 51.62	22.32
FW$_{fruit}$ (Kg fruit^{-1})	$1 \cdot 10^{-03} \pm 7 \cdot 10^{-05}$	27.14	$6.4 \cdot 10^{-04} \pm .3.52 \cdot 10^{-05}$	22
FW$_{oil}$ (Kg fruit^{-1})	$5.86 \cdot 10^{-05} \pm 4.43 \cdot 10^{-06}$	29.3	$3.14 \cdot 10^{-05} \pm 2.73 \cdot 10^{-06}$	34.79
T$_{canopy}$ (°C)	37.98 ± 0.30	3.12	39.91 ± 0.34	3.38

2.3.5. Relative importance of each factor on fruit and VOO yield variability

We analysed the relative contribution of each factor to fruit and VOO yield variability for WW and WS trees (Fig. 10 and Table 2). The variability explained by the model for WW trees on fruit and VOO yield were 78% and 95%, respectively. Meanwhile, the variability explained for WS trees on fruit, and VOO yield was 68% and 86%, respectively. V$_{canopy}$ explained variability in most cases significantly. Its contribution explains 21.80% of the fruit yield on WW trees, 22.41% of the fruit yield on WS trees, 32.45% of VOO yield on WW trees and 8.80% of the VOO yield on WS trees. The SWF only played a role in WW trees models, contributing to fruit and VOO yield variability in 9.94% and 7.53%, respectively, despite not being significant. Attending indicators of plant activity like NDVI and T$_{canopy}$, are both considered to explain variability on WS trees. NDVI was statistically significant, influencing 14.25% on fruit yield in WS trees but

46

was not significant for VOO yield in WS trees, explaining only 2.53% of its variability. T_{canopy} was significant in all cases except in VOO yield on WW trees because it is not included in the model. Remarkably, its major influence (32.42%) was observed on fruit yield for WW trees. In the case of N_{leaf}, it is significant in all cases except for fruit yield in WW trees, which is not included in the model. Its major contribution is to explain fruit VOO on WW and WS trees (41.73% and 13.67%, respectively). FW_{fruit} was significant and contributed to fruit yield similarly in WW and WS trees, with 12.34% and 12.95%, respectively. On the other hand, FW_{oil} contributed much more to VOO yield in WS than in WW trees (50.38% and 13.38%, respectively).

Table 2. Results of the linear models relating fruit and VOO yield in WW and WS trees. They are explained by using multiple linear models. It is shown the intercept and each column values are the slopes for each variable which explains fruit and VOO yield on WW and WS trees. Statistical significance levels: ·, P < 0.1; *, P < 0.05; **, P < 0.01; ***, P < 0.001, ns, not significant; NI, not included variable after model selection.

		Intercept	V_{canopy}	NDVI	N_{leaf}	SWF	FW_{fruit}	Fw_{oil}	T_{canopy}	R^2
Fruit yield	**WW**	83.2 *	0.26 ns	NI	NI	$3.36 \cdot 10^{-4}$ ns	8524 *	NI	-2.16 *	0.78
	WS	167.49 *	1.15 *	19.09 ·	-84.66 *	NI	18429.84 **	NI	-1.56 *	0.68
VOO yield	**WW**	-2.71 ***	0.05 ·	NI	1.74 ***	$1.89 \cdot 10^{-5}$ ·	NI	5925 *	NI	0.95
	WS	7.74 *	0.06 *	0.73 ns	-3.31 *	NI	NI	14470 ***	-0.09 *	0.86
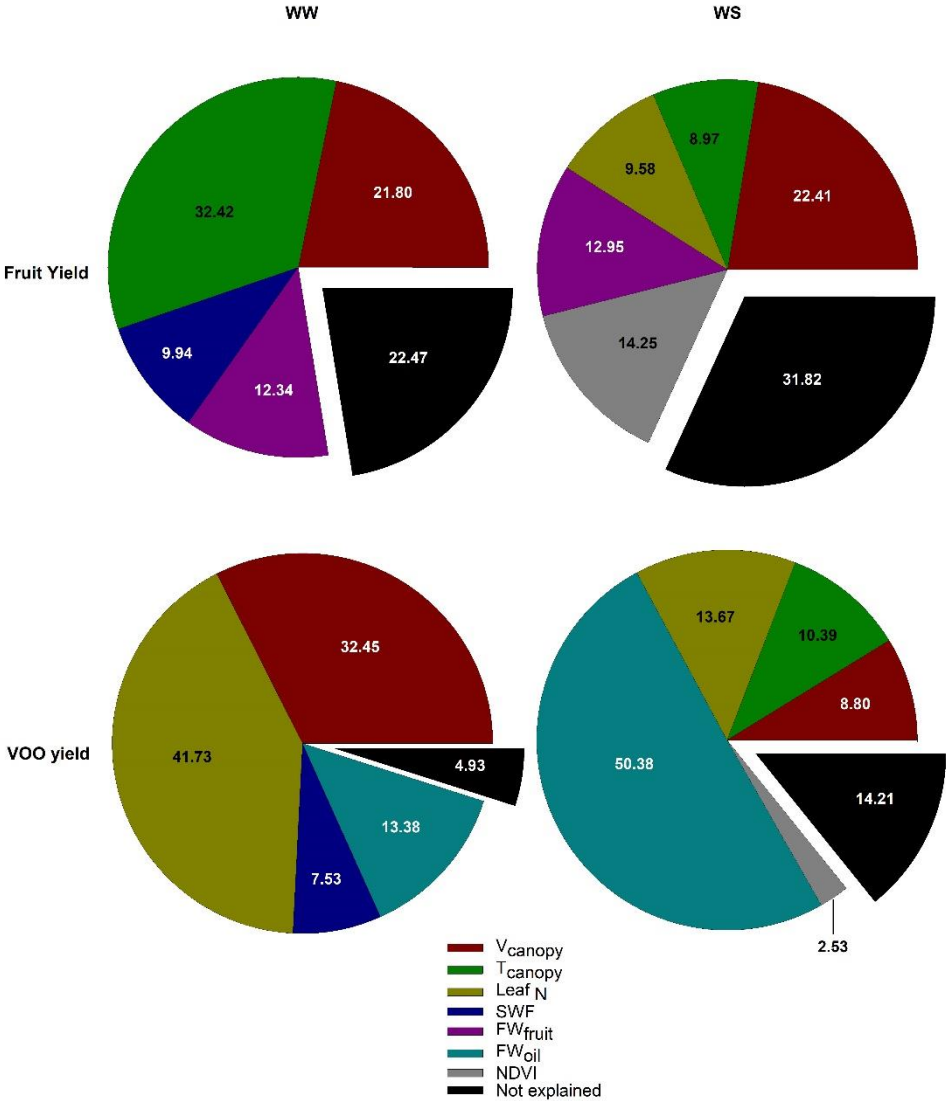
Fig. 10. Relative contribution (%) for fruit yield (above) and VOO yield (below) increment models explained by canopy volume (V_{canopy}), NDVI, leaf N Kjeldahl (N_{leaf}), shoots with fruits (SWF), fruit FW (FW_{fruit}), oil FW per fruit (FW_{oil}) and canopy temperature (T_{canopy}) for well-watered (WW) (left) and water stressed (WS) (right) trees. The analysis was conducted using sixteen trees per treatment. Total variance explained by model in fruit yield WW, fruit yield WS, VOO yield WW and VOO yield WS were $R^2=0.78$ $R^2=0.68$, $R^2=0.95$, $R^2=0.86$, respectively.

2.4. Discussion

Precision agriculture will unavoidably take a major role in the management of agriculture and particularly in fruit tree orchards, in the context of climate change. Technology is increasingly involved in supporting farmers' decisions, and the use of remote sensing from satellites and drones or plant sensors is becoming common (Singh et al., 2020). The incorporation of remote sensing in agriculture will serve, among other applications, to describe farm heterogeneity, not only with the aim of identifying homogeneous management units, but also to detect locations in the farm where the crop is underperforming (Bellvert et al., 2016; Longchamps et al., 2022). However, we still do not know which measurable variable is the most informative for farmers' purposes. Different irrigation strategies or final farm goals (fruit yield for table olives or VOO in the case of olive trees) might require the monitoring of different variables. What is the most informative to describe the yield variability? Is it more useful for factors affecting the yield the acquisition of NDVI or thermal images? Or, how is the canopy size distribution in the orchard, and what is its impact on yield variability?

Answers to these questions are not straightforward, but in this study, we have started to understand that setting the optimal use of the technology requires a multidisciplinary approach. To describe the variability of fruit yield and VOO, our study combined traditional agronomical analysis of yield in olive orchards with remote sensing data. Data acquisition was oriented to the plant's response to water stress and the distribution of canopy sizes in the orchard. As it was hypothesized, our results show that canopy size is a major factor determining fruit and VOO yield, given an irrigation treatment. Moreover, our results show that both fruit yield and VOO showed higher variability in WW than in WS (Fig. 7) and that the factors that determined fruit yield and VOO

yield were different, and deficit irrigation modulated or changed the contribution of these factors (Fig. 10).

2.4.1. Canopy volume as a major determinant of yield

Our results demonstrated a major role of the canopy volume in determining fruit and VOO yield (Fig. 8) as well as being the factor explaining the variability of fruit and VOO yield more consistently in WW and WS treatments (Fig. 10). This effect is produced both directly and indirectly. The direct impact is obvious, as a larger canopy will contain more reproductive shoots. The indirect effect is related to differential water consumption by different canopy volumes, i.e., a bigger canopy with more leaves demands more soil water content than a small one. In turn, this differential water consumption produces different levels of water stress, provided these trees with different canopy sizes are irrigated with the same amount of water in each treatment. Since currently, it is not possible to irrigate each individual tree "à la carte" on a farm, we must do it based on an average canopy size which will over-irrigate some trees and under-irrigate others. In the case of small trees, it is unlikely that we are inducing hypoxia or flooding by over-irrigation with a localised irrigation system. However, in trees which are bigger than the average, we might be inducing different water stress levels by supplying less water than demanded by trees. Yield variability measured in WW in both fruit and VOO yield was always larger than in WS, mirroring the higher variability found in canopy sizes between WW and WS (Fig. 6). Up to now, the differential distribution of tree sizes within a treatment is hardly considered due to its complexity despite the reported impact on yield (e.g. Fernández et al., 2013; Hernandez-Santana et al., 2017). Thus, the proposed approach can provide useful information despite some methodological issues that must be considered. The resolution achieved in our remote sensing measurements with a drone was high (0.1 m) and allowed us to isolate the signal of the plant from

that of the soil, which is a remarkable advantage over satellite (Mengmeng et al., 2017). Still, images from the drone can only capture the top part of the plant, and that surface represents only a percentage of the canopy volume where fruits develop. Therefore, we might not be considering some factors that affect olive production by applying a deficit irrigation strategy.

2.4.2. Differential variability in fruit and VOO yield in WW and WS treatments

The analysis of the studied factors that putatively affect yield (Figs. 9, 10) showed three general conclusions: 1) fewer factors were always necessary to explain the variability in WW than in WS; 2) more variance was explained in WW than in WS; 3) it was easier to explain the variance in VOO than fruit yield. The two first points suggest that water stress involves more factors than the ones considered in this study. Or just that the variables chosen do not adequately represent the consequences of deficit irrigation. Thereby, the activity of the plant inferred from NDVI measurements or the stress intensity estimated from thermal images might not represent the relevant processes behind the differences observed. NDVI is probably the most used remote index. It has been used successfully in forestry and in agronomy to measure the tree vigour (Jurado et al., 2020b), it correlates well with LAI and foliar chlorophyll (Caruso et al., 2019) and gross primary production (Maselli et al., 2012). It has the drawback that it integrates two aspects of the plant: its photosynthetic activity and the amount of the vegetation component in the image (i.e. the total leaf area). In our study, both components play a role since there are changes in the photosynthetic activity of the plant (seasonal adjustments and irrigation treatments), and differences in the vegetation component since a range of canopy sizes has been found. Therefore, similar NDVIs values could

mean slightly different things. If we are comparing the two irrigation treatments, NDVI is a valid index and can discriminate them (Fig. 9B). However, discerning the subtle differences induced by canopy size within an irrigation treatment is more complicated and requires more precision than when comparing different levels of irrigation.

In the case of thermal images, they have been successfully used as a stress index, especially in agronomy, to detect diseases (Calderón et al., 2013) or to monitor the transpiration status of the canopy (Blonquist et al., 2009; Ballester et al., 2013b). Canopy temperature increases with stomatal closure as an unavoidable consequence of the leaf energy balance (Grant et al., 2006). Their use in this study was particularly sound since one of the main responses to water stress reported in olive is the reduction of stomatal conductance (Perez-Martin et al., 2014). As expected, WS showed a significantly higher canopy temperature than WW (Fig. 9G). However, despite canopy temperature being a good indicator of water stress, the contribution analysis showed that canopy temperature explained more variability in WW than in WS for fruit yield (Fig. 10). The reason for this result makes sense for two reasons: 1) the canopy size distribution was larger in WW than in WS (Fig. 7) with smaller and bigger trees in WW than in WS. As commented before, irrigation is calculated for an average canopy size (i.e. leaf area), and thus, there will be over-irrigated trees (the smallest ones) and under-irrigated trees (the biggest ones). Therefore, the probability of inducing a wider range of water stress in WW is higher than in WS due to different tree water demands. 2) Canopy temperature reflects changes in stomatal conductance, which matches well with the assumption that different canopy sizes induce different water stress levels. However, when we consider the irrigation treatments, we are in different regions of this stress induced by the plant size. One of the earlier responses to water stress is stomatal closure (Rodriguez-Dominguez and Brodribb, 2020), especially strong

in an isohydric species like the olive tree (Rodriguez-Dominguez et al., 2016; Diaz-Espejo et al., 2018). This means that the expected range in stomatal conductance and its consequence in the limitation of CO_2 assimilation rate, and hence in yield (Hernandez-Santana et al., 2018), will be expressed more likely in WW than in WS. WS trees are not expected to show a high variability in stomatal conductance induced by the variability in canopy sizes, as it was the case in WW. The level of water stress imposed by the 45% deficit irrigation in this study is enough to reduce the stomatal conductance of the smaller trees to minimum (Fernández et al., 2013; Hernandez-Santana et al., 2017; Padilla-Díaz et al., 2018; Fernandes et al., 2021). Therefore, as in the case of NDVI, thermal images are complex to interpret, and our results show that depending on the irrigation strategy we are applying, it might have a bigger or smaller impact on explaining yield variability.

2.4.3. Fruit vs. VOO yield variability

The hypothesis for the fact that we have been able to explain a higher percentage of the variability in VOO than in fruit yield with the factors studied is most likely because the nature of the processes that determine oil accumulation and fruit growth is also different. Fruit yield depends significantly on the water content of the fruits, both during the growing period, when the fruit determines its potential size (Gucci et al., 2009), and in the last weeks before the harvest, when fruits can gain or lose water depending on the weather conditions or soil water availability. On the contrary, the synthesis of oil is a process that integrates a longer period of time, and it is more modulated by water stress and carbon source provided by photosynthesis (Hernandez-Santana et al., 2018; Perez-Arcoiza et al., 2022), as well as affected by the sink strength of different crop loads (Naor et al., 2013). A close inspection of the factors that influenced VOO shows that most of the variability was explained

by factors related to the activity of the plant and not to structural aspects like the number of shoots with fruits or canopy size, which had a major role in explaining the variability in fruit yield. The amount of oil per fruit in the case of WS, or the leaf nitrogen in the case of WW, contributed significantly to explaining the variability in VOO. As previously mentioned, the canopy size distribution induces a factor of variability in each treatment by its indirect effect on the impact of other factors like soil water availability and different crop loads. These factors could have been better reflected in the variables measured, resulting in a better prediction of the variability in VOO than fruit yield.

2.5 Conclusions

Digital agriculture of the future requires the implementation of new and advanced technology. Revisiting old concepts of precision agriculture, like intra-field variability in crops, can now be approached with current methodologies and their consequences analysed to understand the key factors that govern the yield in farms. Our work focuses on the distribution of canopy sizes in an olive tree orchard, which plays a major role in generating, both directly and indirectly, the yield variability that it is usually found on the farm. The case of the olive tree with two different market products, fruits and oil, shows that the factors contributing to yield vary depending on the process studied and the irrigation treatment applied. If confirmed in following studies under other growing conditions, this result suggests that we must focus our monitoring efforts on different variables depending on the irrigation strategy we are implementing or the final product we are interested in. Moreover, this work illustrates well the need for basic physiological knowledge that explains the differences found, which can describe the processes of fruit growth correctly. The processes of fruit growth and oil synthesis will be approached in

the following chapters of this PhD thesis to contribute to the establishment of a robust basis for the management of olive orchards in the future.

CHAPTER **3**

DISENTANGLING THE LINK BETWEEN LEAF

PHOTOSYNTHESIS AND TURGOR ON FRUIT GROWTH

Published as:

Abstract

Despite the importance of understanding plant growth, the mechanisms underlying how plant and fruit growth declines during drought remain poorly understood. Specifically, it remains unresolved whether car- bon or water factors are responsible for limiting growth as drought progresses. We examine questions regarding the relative importance of water and carbon to fruit growth depending on the water deficit level and the fruit growth stage by measuring fruit diameter, leaf photosynthesis, and a proxy of cell turgor in olive (*Olea europaea* L.). Flow cytometry was also applied to determine the fruit cell division stage. We found that photosynthesis and turgor were related to fruit growth; specifically, the relative importance of photosynthesis was higher during periods of more intense cell division, while turgor had higher relative importance in periods where cell division comes close to ceasing and fruit growth is dependent mainly on cell expansion. This pattern was found regardless of the water deficit level, although turgor and growth ceased at more similar values of leaf water potential than photosynthesis. Cell division occurred even when fruit growth seemed to stop under water deficit conditions, which likely helped fruits to grow disproportionately when trees were hydrated again, compensating for periods with low turgor. As a result, the final fruit size was not severely penalized. We conclude that carbon and water processes are able to explain fruit growth, with importance placed on the combination of cell division and expansion. However, the major limitation to growth is turgor, which adds evidence to the sink limitation hypothesis.

3.1. Introduction

Understanding plant growth will be relevant to solving some of the various challenges currently facing humanity, from mitigating climate change (as woody tissues constitute the main terrestrial biotic pools for long-term sequestration of atmospheric CO_2) to achieving food security in a time of unprecedented population growth. However, several questions remain unanswered regarding the physiological basis that limits plant growth (Körner, 2015). Indeed, despite its relevance to improving productivity, the optimization of fruit growth in response to water stress remains a challenge. Importantly, water deficit conditions are expected to limit the productivity of more than half of all cultivated land within the next 50 years (Dhankher and Foyer, 2018).

The main processes that determine plant growth in general, and fruit in particular, are related to the accumulation of water and carbohydrates. To what degree each of these fluxes impacts plant growth under conditions of water deficit and, thus, affects crop yield, is still intensely debated. The two main hypotheses about the effects of these limitations on growth (Gifford and Evans, 1981) are limitation by source (impact of carbohydrate assimilation–photosynthesis) and limitation by the sink (tissue expansion, meristematic activity, and carbohydrate demand from new vegetative or reproductive growth). Although there is no doubt about the role of net photosynthesis (A_N) in plant growth (approximately half of plant biomass is C), there are justified reasons to question the general assumption that A_N is the main limiting factor of plant growth under drought conditions (Körner, 2015). Indeed, there is increasing evidence that tree growth is limited not only by the availability of carbon, but also by environmental water factors that limit elongation and cell development in growing tissues (Körner, 2003; Muller et al., 2011; Steppe et al., 2015). After cell division, cells in tissues expand; however, cell elongation is

limited by cell turgor above a minimum threshold (Lockhart, 1965). Moreover, growth would stop under less severe levels of water deficit due to the greater sensitivity of growth to turgor pressure (Hsiao et al., 1976) than to photosynthetic assimilation. Thus, it has been suggested that plant growth should change from a source-driven plant growth model to a combined source-sink-driven one (Fatichi et al., 2014; 2019). The reason why the hypothesis stating that growth is limited by carbon has functioned adequately may be related to many of these described processes being strongly related and optimized for production, making it difficult to separate the effects of each individual process (Fatichi et al., 2014). Indeed, A_N is mainly limited by stomatal conductance under moderate water stress, which in turn, is closely related to turgor (Rodriguez-Dominguez et al., 2016). Despite its importance, the role of turgor, conditioned by water and osmotic potential, is not yet completely known. A very early study (Lockhart, 1965) recognized that turgor pressure may need to exceed a certain minimum value before irreversible expansion occurs (i.e., both processes would not be linearly related). However, the variation in zero growth thresholds among a broad range of woody species remains to be evaluated beyond the few species that have currently been studied (Mitchell et al., 2014).

All these questions become even more complicated to answer when regarding fruit growth in crop trees since, in general, plants prioritize fruits with respect to the distribution of their carbon resources (Génard et al., 2008) and this trait has been selected for in crop species (Sinclair, 1998; Morison et al., 2008). Thus, in fruit trees, there is a very strong competition between reproductive flux and wood growth (Ryan et al., 2018) which could be significantly modified by agrotechnical treatments (Fishman and Génard, 1998). Fruit growth also shows different behaviors when compared to other organs, likely due to fleshy fruits containing high concentrations of sugar that

help to lower the osmotic potential, thus maintaining turgor under more severe water stress conditions than possible in other organs (Muller et al., 2011). Compared to other plant tis- sues, another special characteristic of fruits is their ability to store other substances (e.g., oil in olive [*Olea europaea*] fruits) that make the water component less important than in other species in which water fluxes are major determinants of fruit growth (e.g., grape [*Vitis vinifera*], Greenspan et al., 1996; peach [*Prunus persica*], Morandi et al., 2007 and pear [*Pyrus communis*], Morandi et al., 2014). In a prior study following this rationale, we successfully explained the accumulated dry matter of fruits over periods of 2 weeks in olive trees using the hypothesis of carbon limitation (Hernandez-Santana et al., 2018). Moreover, in that work we compared different sink organs (shoot, leaf area, and fruit) and demonstrated that under water stress conditions trees prioritized fruit growth over vegetative growth, suggesting that fruits had the highest sink strength. Here we intend to advance this knowledge, providing a different view on the disentanglement of source or sink as major limitations of growth thanks to a synchronous estimation of A_N, a proxy of cell turgor, and fruit diameter increment, besides flow cytometry measurements to determine the fruit cell division stage.

Thus, our main objective is to assess the leaf water and carbon relationships on the daily and sub-daily dynamics of olive fruit growth, including how water deficit and the fruit growth stage affect these relationships. Our central hypothesis is that both leaf A_N and turgor will help to explain fruit diameter increment, as they are strongly related and each plays a major role depending on the level of water deficit and the growth stage (cell division/expansion). We further hypothesize that A_N is a major driver of growth during fruit formation, when cell division processes are more dominant than cell expansion processes, with turgor becoming the major variable limiting growth in the latter stage. Thus, we have the following objectives: (i) to

describe the sub-daily and daily dynamics of fruit equatorial diameter increment in terms of photosynthesis and turgor-related values, (ii) to assess the dependence of fruit equatorial diameter increment on carbon assimilation and turgor pressure thresholds, (iii) to evaluate how the former relationships are differentially affected by water deficit, and (iv) to analyze if the fruit growth stage (cell division/expansion) is a determinant of the driving variable of fruit growth. We used olive trees because the olive tree is considered a plant model that is very resistant to drought and its physiology has been comprehensively studied in the last decade (Fernández, 2014; Diaz-Espejo et al., 2018).

Understanding the underlying basis for changes in leaf carbon supply (studied here as a proxy of source), leaf turgor, and fruit growth relationships (sinks) under two levels of soil water content and fruit growth stage may help to clarify the somewhat conflicting underlying hypothesis explaining growth dynamics reported in drought studies on woody species. To this end, in this work we aim at adding evidence to the sink, source, or combined source-sink limited hypothesis. In a more application-based sense, achieving our objectives will help improve resilience of agricultural crops to drought. In particular, through breeding and agronomic practices, the basis for future methods managing productivity based on water consumption and the relationships of water and carbon with fruit growth pat- terns can be established. Surprisingly, although fruit growth is the final target in fruit tree orchards, most of the methodologies applied currently to manage irrigation, even in precision agriculture, are based on the vegetative organs (Ortuño et al., 2006; Ben-Gal et al., 2010; Padilla-Díaz et al., 2016).

3.2. Materials and methods

3.2.1. Experimental site description and treatments

The study was conducted in a commercial super-high-density olive orchard (*Olea europaea* L. cv. Arbequina) located in Utrera (Seville, southwest Spain) (37° 15' N, -5° 48' W) during the months of July, August, and September of 2018. The study was conducted in 12-year-old trees, planted in a 4 m × 1.5 m formation (1667 trees ha^{-1}), in rows oriented North-Northeast to South-Southwest. The soil in the orchard, had a sandy top and a bottom clay layer (Arenic Albaquaf, USDA 2010). Further details on the orchard characteristics can be found in Fernández et al. (2013).

The climate of the area is Mediterranean with mild, rainy winters and hot, dry summers, with hardly any rain during the months of the study. Average potential evapotranspiration (ET$_o$) and precipitation are 1482 and 500 mm, respectively (Los Molares, Regional Government of Andalusia, 2002–2018).

We had two different treatments: a WW treatment in which the trees were irrigated daily to replace their irrigation needs (IN) fully and a WS treatment produced by the water deficit of adding only 45% of the water applied in WW. Each irrigation treatment was applied in three 12 m × 96 m plots in a randomized design (*n* = 3). There were 24 trees per plot, but measurements were made just in two central trees to avoid any border effect.

IN was calculated daily based on a simplified version of the stomatal conductance (g_s) model evaluated in this olive orchard by Diaz-Espejo et al. (2012) and described in greater detail in Fernandes et al. (2018). Briefly, the WW treatment was assumed to be at field capacity, i.e., a soil matric potential equal to 0. Following this model, g_s is described as a function of air vapor pressure deficit (*D*), average radiation (*Rs*) and tree leaf area (A), the latter of which was estimated each fortnight for each plot during the irrigation season. The leaf area index (LAI) was measured at dawn with a LAI-2200 Plant Canopy

Analyzer (Li-Cor, Inc., Lincoln, NE, USA) according to Diaz-Espejo et al. (2012). Assuming a perfect coupling between canopy and atmosphere, tree water consumption (Ep) was calculated as $Ep = D \cdot (g_{s,sun} \cdot A_{sun} + g_{s,shade} \cdot A_{shade})$, with A_{sun} being the sunnyleaf area percentage (35%, according to Diaz-Espejo et al. 2002 and Fernández et al. 2008) and A_{shade} being the shaded leaf area. Soil evaporation (Es) was estimated according to Orgaz et al. (2006). Finally, IN was estimated as $Ep + Es$.

For the WS treatment we applied the regulated deficit irrigation strategy recommended by Fernández et al. (2013) and Hernandez-Santana et al. (2017) and improved by Fernández et al. (2018). In our study, the regulated deficit irrigation period occurred from DOY 196 to 243, after which the irrigation post-water stress started. The measurements included in this work began on DOY 185 (4th of July) and ended on DOY 273 (30th of September), thereby including three different periods for WS trees: an initial period of pre-water stress (DOY 185-196), a water stress period (DOY 196-243), and a post-water stress period (DOY 244-273). As mentioned before, WW trees were irrigated daily for the whole experimental period.

3.2.2. Meteorological variables

Meteorological variables were recorded using a weather station (Campbell Scientific Ltd., Shepshed, UK) located in the middle of the experimental area, with the meteorological sensors located above the canopy. The station recorded 30 min averages of air temperature (T_{air}) and relative humidity (R_H), thus allowing the calculation of D. R_s was also measured in the same station.

3.2.3. Predawn leaf water potential ($\Psi_{leaf,\ pd}$)

Predawn leaf water potential ($\Psi_{leaf,\ pd}$) was measured every 2 weeks for the study period (DOY 182-273) with a Scholander-type pressure chamber (PMS Instrument Company, Albany, Oregon, USA). We sampled two leaves from current-year shoots of two central trees of the three plots per treatment.

3.2.4. Leaf and fruit osmotic potential

Four leaves and fruits were sampled at midday from one central tree of the three plots per treatment to assess the relationship between fruits and leaves (Fig. S1). After samples were collected, the leaves and fruits were cleaned with a damp paper towel, packed in aluminium foil, immediately frozen in liquid nitro- gen, and stored at -80°C until analysis. Leaf and fruit osmotic potential were determined with a thermocouple psychrometer with six standard C-52 sample chambers (Wescor Inc., Logan, UT, USA) connected to a datalogger (PSYPRO; Wescor Inc.).

3.2.5. Fruit equatorial diameter measured manually and fruit dry weight

Six fruits of two trees each from four plots and treatments (n = 48) were collected every 2 weeks. Fruit equatorial diameter and DW were measured for each fruit with an electronic calliper and a precision electronic balance (Balance XS105; Mettler Toledo, Columbus OH, USA), respectively.

3.2.5. Fruit equatorial diameter

We installed gauges in one fruit of two central representative trees per plot for the two treatments (n = 6 per treatment). Due to mal- function, one fruit tracked in WS trees was not used, having a total of five fruits monitored.

The fruit dendrometers were adapted using a linear potentiometer (model MM(R)10-11) with internal spring return (Megatron Elektronik GmbH and Co., Munich, Ger- many) coupled to a sensor holder. The sensors were connected to a datalogger (CR1000; Campbell Scientific Ltd, Shepshed, UK) which recorded data of fruit equatorial diameter every 5 min. These data were validated using manually measured equatorial diameters of six fruits per plot every 15 days for the whole study; we obtained good agreement between both datasets ($R^2 = 0.99$).

The data registered by these gauges include growth as well as swelling and shrinkage produced by water moving in and out of the fruit. Thus, sub-daily data were only used for a synchrony / asynchrony study among variables while to minimize the former effect and focus on the fruit equatorial diameter increment, daily values were used for the analyses with Ψ_{pd}. Moreover, these daily values were accumulated for 3 days to establish the relationships between the increment of fruit equatorial diameter with A_N and turgor as DW accumulation may be negligible on a daily scale, as observed in Hernandez-Santana et al. (2018). Moreover, to understand the robustness of these relationships we also considered shorter temporal aggregations (1 and 2 days) as well as one longer temporal aggregation of 4 days. The same relationship trends were found as when aggregating 3 days but their R^2 values were weaker. Ideally, longer periods should have also been tested for the relationship between the increment of fruit equatorial diameter with A_N and turgor, but this was not possible because then there were too few points for the relationships.

3.2.6. Modeled net photosynthesis

Sap flow sensors were used to obtain an automatic and continuous estimation of g_s and A_N. To derive A_N from sap flow-related measurements, we used the approach explained in full detail in Hernandez-Santana et al. (2016a)

68

and extended in Hernandez-Santana et al. (2018). Briefly, we established relationships between sap flux density (J_s), normalized by D and g_s, to simulate g_s continuously. The J_s/D versus g_s calibration equations were established using 20–21 data points from each instrumented tree (Fig. S2). Using the simulated g_s every 30 min, we modeled A_N (Fig. S3) applying a biochemical model (Farquhar et al., 1980). This modeling is possible because in olive the main limitation of A_N is produced by stomatal closure (Díaz-Espejo et al., 2006; 2007). Details on the modeling and measurements needed to apply the Farquhar model in this olive orchard can be found in Hernandez-Santana et al. (2018). Accumulated A_N was calculated by summing up the quantity of simulated A_N every 30 min.

To obtain J_s (mm h^{-1}), we monitored four trees per treatment using the compensation heat pulse (CHP) method (Tranzflo NZ Ltd., Palmerston North, New Zealand; Green et al., 2003). Details on installation can be found in Hernandez-Santana et al. (2016a; 2018). Briefly, probe sets were installed on the East-facing side of the trunk and J_s was measured at 5 mm with heat pulses released every 30 min during the experimental period controlled by a CR1000 datalogger connected to an AM25T multiplexer (Campbell; Campbell Scientific Ltd, Shepshed, UK).

Values of gs and A_N were measured on four clear days from May to August, every 30–60 min from dawn to noon, in three sun-exposed current-year leaves per instrumented tree. Two portable photosynthesis systems (Li-cor 6400-XT; Li-Cor, Lincoln NE, USA) were used, equipped with a 2 × 3 cm standard chamber, at ambient light and CO_2 conditions.

3.2.7. Leaf turgor pressure-related values

Relative changes in leaf turgor pressure were recorded *in situ* with a non-invasive online- monitoring leaf patch clamp pressure probe (ZIM turgor

sensors; YARA-ZIM Plant Technology GmbH, Hennigsdorf, Germany). The ZIM turgor sensor records the output pressure (P_p), a variable inversely correlated with the leaf turgor pressure (Zimmermann et al., 2008) in several species (Rüger et al., 2010a; Ehrenberger et al., 2012), including olive leaves (Ehrenberger et al., 2012). We installed four ZIM turgor sensors per treatment (one ZIM turgor sensor per tree and plot in three plots per treatment plus an extra one in one tree of the plots). The probes were clamped on the Eastern leaves of the canopy approximately 1.5 m above the ground. P_p was recorded every 5 min for the whole study period. Although P_p values are closely related to leaf turgor, their absolute values depend on the particular clamping for a given leaf. To enable outputs to be averaged and compared between probes, P_p was normalized (Rodriguez-Dominguez et al., 2019). Values were transformed into turgor pressure (P) to ease understanding of the diurnal and seasonal dynamics. We used the specific equations relating P_p to P measured with turgor pressure probes in olive leaves reported by Ehrenberger et al. (2012b) and the osmotic potential (Table S1) measured. ZIM turgor sensors are only able to measure P values of > 50 kPa; below this value leaves are in a nearly turgorless state and measurements become unreliable (Ehrenberger et al., 2012).

We were interested in knowing how many hours these values are above a certain threshold that determines if tissue cells are growing. Several wall-yielding threshold pressures have been reported for various tissues; however, we used 0.9 MPa as our growth threshold following (Génard et al., 2001). Thus, we calculated how many hours per day the P value of the leaves is above the threshold (P_{hours}) and compared this value to fruit growth, with a similar approach to Coussement et al. (2021).

3.2.8. Flow cytometry analysis

Flow cytometry was used to precisely determine the period of cell division via nuclei ploidy profiles from pericarp tissues (epicarp and mesocarp) of developing fruits using the method of Loureiro (2009). The pericarp tissues (0.1– 0.2 g fresh weight) were chopped with a razor blade in 0.5 ml of ice-cold buffer (0.2 M Tris-HCl, 4 mM MgCl$_2$, 2 mM EDTA, 86 mM NaCl, 10 mM metabisulfite, pH 7.5, and 1% Triton X-100), filtered over a 30-µm nylon mesh and stained with 4,6-diamidino-2-phenylindole (DAPI). The nuclear DNA content distribution was then analyzed with a FACS CantoII flow cytometer and the data obtained were processed using FACSDiva 6.1.2 software (BD Biosciences, Franklin Lakes, NJ, USA). Four biological replicates, including 10000 nuclei each, were performed per treatment. DNA content (C value) of fruit pericarp tissues was determined by flow cytometry using internal calibration standards (Loureiro, 2009). C values were calculated according to Doležel et al. (2007), as follows: 2C DNA (pg) = (mean of the problem sample G1 peak × 2C DNA content of the standard [pg])/mean of the standard G1 peak. At least three biological replicates were measured per sample.

3.2.9. Flow cytometry analysis

We performed regression modeling to determine the relationship between the leaf variables analyzed (A_N or P$_{hours}$) and the fruit equatorial diameter increment, as well as the relationships of A_N, P, and the increment of fruit equatorial diameter with leaf water potential (Ψ_{pd}). The collinearity between P$_{hours}$ and A_N was assessed using the variance inflation factor (VIF). Differences between the flow cytometry data, DW, and fruit equatorial diameter measured manually for WW and WS were analyzed with *t*-tests for independent measurements. When several samples were collected from the same tree, they were averaged per tree for the statistical analyses. SigmaPlot

software (version 12.0; Systat Software, Inc., San Jose, CA, USA) was used to conduct these univariate regression analyses and provide best-fit curves to the relationships as well as for the *t*-tests, while R software (R version 4.0.3 [2021-06-16]) was used for the VIF analyses. In addition, we used the CCF to study the sub-daily and daily kinetics of A_N, P, and the increment of fruit equatorial diameter. This analysis allowed to describe the relationship between two time series (A_N or P with the increment of fruit growth) identifying lags to obtain the most dominant correlations and better describe the synchrony and asynchrony between the variables. When the CCF pattern was affected by the underlying time series structures and trends of the variables (basically sub-daily time series) making the determination of lags difficult, we used the transformed variables. For the independent variables (A_N or P) we used the residuals resulting from ARIMA structures and for the dependent variable (increment of fruit equatorial diameter) we used the filtered variable series using the previous ARIMA model. These analyses were conducted with R software using the packages 'forecast' (Hyndman et al., 2020) and 'tseries' (Trapletti and Hornik, 2020).

3.3. Results

As the water stress treatment progressed, pre-dawn leaf water potential (Ψ_{pd}) in water stressed (WS) trees decreased from -0.7 MPa to below -3 MPa (Fig. 1a). The slight recovery observed on day of the year (DOY) 221 was due to an irrigation event produced by a malfunction of the irrigation system. The lowest Ψ_{pd} in well-watered (WW) trees, across the whole study period, was approximately -1 MPa, which coincided with moments when the air vapor pressure deficit (D) was at maximal values, around 3 kPa on daily average (Fig. 1b), with instantaneous values of 7.5 kPa. Accumulated daily average solar

72

radiation (R_s) decreased notably from the beginning to the end of the study period (Fig. 1c).

The fruit equatorial diameter measured manually every 2 weeks was higher in WW trees than in WS trees because the former maintained a constant increase throughout the entire study period (Fig. 2a). On the contrary, in WS fruits there was hardly any increment of equatorial diameter during the water stress period. However, the greater increase in equatorial diameter of WS fruits compared to WW fruits during the post-water stress period made the differences between the two treatments less important. Similar trends were observed in the fruit dry weight (DW) measurements (Fig. 2b).

Regarding the sub-daily data of fruit growth and physiological variables, the minima and maxima were achieved in different moments of the day for the three variables analyzed. Fruit equatorial diameter achieved its minimum in the afternoon and started to increase at night until early in the morning (Fig. 3a,d,g). Similarly, the calculated turgor pressure (P) (Fig. 3c,f,i) achieved maximum values in the night-time study periods and minima during the daytime. However, the sub-daily A_N dynamics were different, increasing just after dawn, achieving a maximum in the morning (Fig. 3e), and staying stable or decreasing afterwards. The effect of water stress was remarkable during the so-called water stress period when the fruit diameter increment stopped and the fluctuations observed at the day-scale increased, reflecting the irrigation events. The diameter increment resumed during the post-water stress period. An important reduction was shown by A_N in WS trees during the water stress period, being almost half of the maximum A_N of WW trees, even though, in that period, the A_N of WW trees was also lower than in the other two periods (Fig. 3e) as a consequence of the stomatal limitation imposed by the highest D values of the whole study period (Fig. 1b).
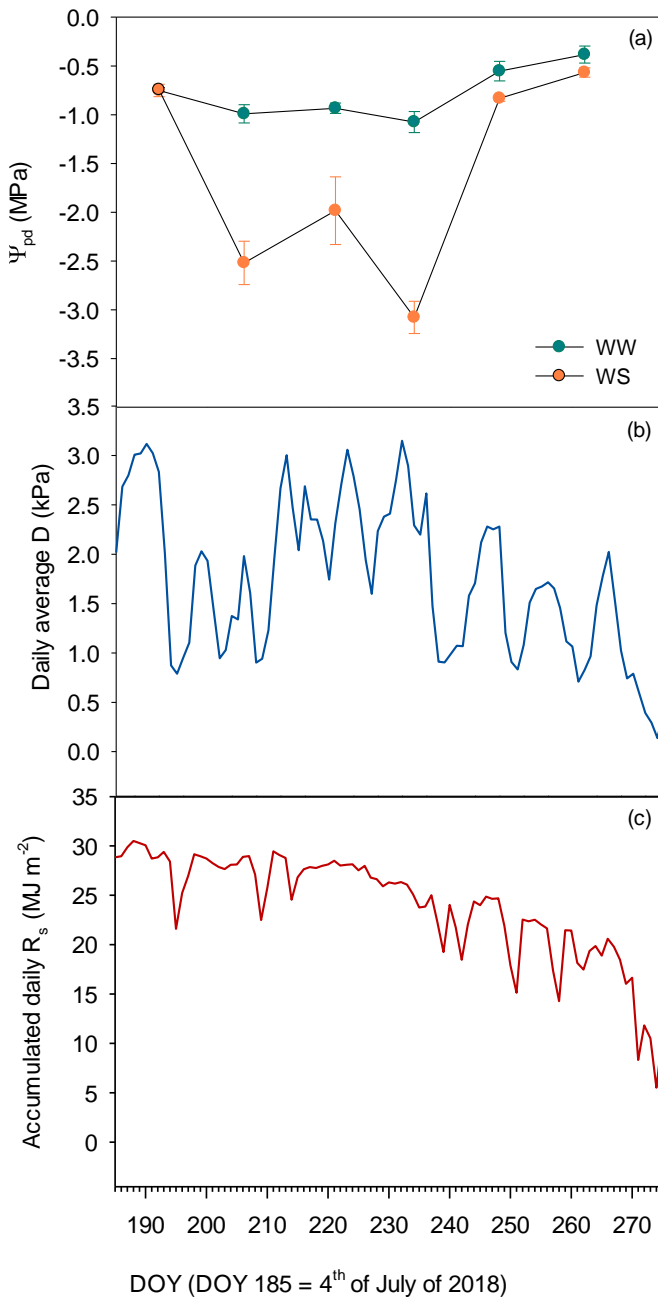
Fig. 1. (a) Pre-dawn leaf water potential (Ψ_{pd}), **(b)** daily average vapor pressure deficit (D), and **(c)** total daily solar radiation (Rs) measured in well-watered (WW) and water stressed (WS) trees during the whole study period. The gray rectangle denotes the water stress period applied to WS trees, which is preceded by the pre-water stress period and followed by the post- water stress period. Each point in (a) is the average of 12 leaves and the bars indicate ±SE

74
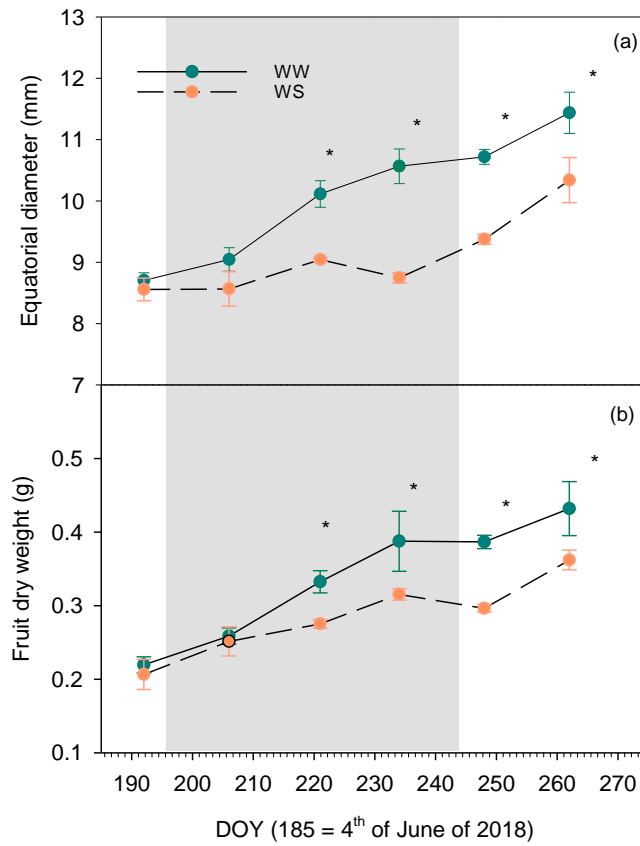
Fig. 2. Temporal variation of (a) equatorial diameter and (b) fruit dry weight for well-watered (WW) and water stressed (WS) trees. Each point is the average of eight fruits collected from eight trees per treatment. Asterisks denote significant differences (P < 0.05) and bars are ±SE
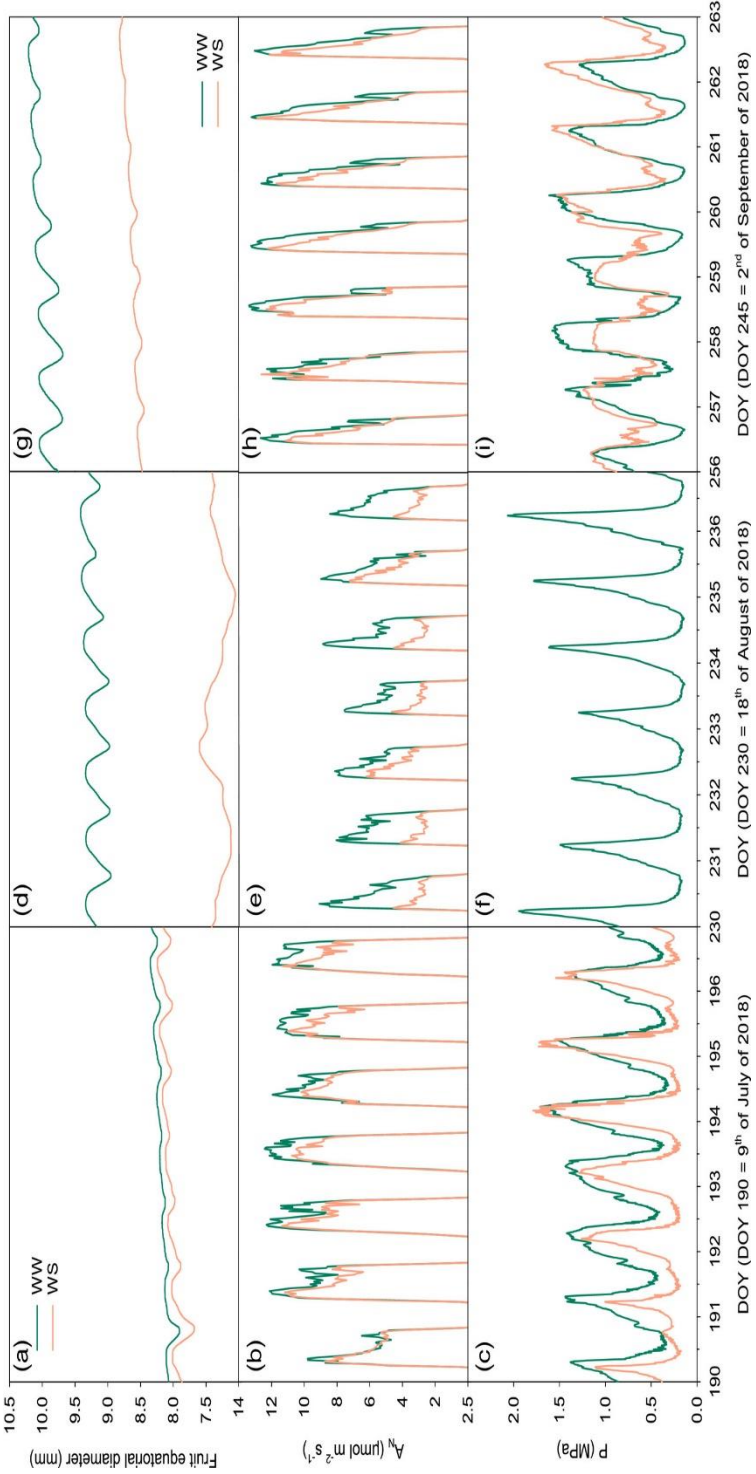
Fig. 3. Sub-daily temporal variation of (a, d, g) fruit equatorial diameter, (b, e, h) net photosynthesis (AN), and (c, f, i) turgor pressure (P) for the well-watered (WW) and water stressed (WS) trees for three contrasting periods: before water stress was applied to WS trees (left), during water stress (center), and post- water stress (right). Each line is the average of the outputs of six and five sensors to track WW and WS fruit diameters, respectively, four sap flow sensors to model A_N, and four ZIM turgor sensors used to simulate P. The fluctuations correspond to day/night variation. No SE bars are shown for clarity purposes.

These trends were in accordance with the temporal shifts revealed by the cross-correlation function (CCF) analysis (Table 1). The shorter lags obtained for the most dominant correlations between the time series of P and fruit diameter than for A_N indicated closer synchrony between P and the increment of fruit diameter than between A_N and the increment of fruit diameter.

Table 1. Time in hours identified for the best lagged relationship of photosynthesis (A_N) and turgor pressure (P) with fruit diameter increment for sub-daily data. The relationships have been evaluated using the average of six and five fruits for well-watered (WW) and water stressed (WS) treatments and four trees for A_N and P for both treatments.

		Pre-water stress	Water stress	Post-water stress
A_N- fruit diameter	WW	6	10	10.5
	WS	7.5	6.5	10.5
P-fruit diameter	WW	-0.5	2	1.5
	WS	-3		6.5

The normalized variation of daily fruit equatorial diameter (%) in WW trees was less variable in WW than in WS trees, which were affected by the irrigation frequency in July and August, resulting in pronounced cycles of fruit shrinkage and swelling (Fig. 4a). After irrigation post- water stress, the normalized daily variation of fruit equatorial diameter in WS trees was always positive and more constant than in the previous period and than for WW. Normalized A_N (%) under WW conditions showed maximum values at the beginning of the experiment and minimum values during August (Fig. 4b), when D was the highest. Similar to the results for the fruit, total daily normalized A_N in WS, which was similar to WW in the pre- water stress period, showed a steeper decline than WW in July and August (Fig. 3b), recovering after irrigation

frequency was increased again. Normalized P (%) for WW trees was at a medium value at the beginning of the study, with small oscillations, and increased in August, decreasing again in September. Daily oscillations were also found in P (%) of WS, the maximum values being lower at the beginning than at the end of the study period (Fig. 4c).
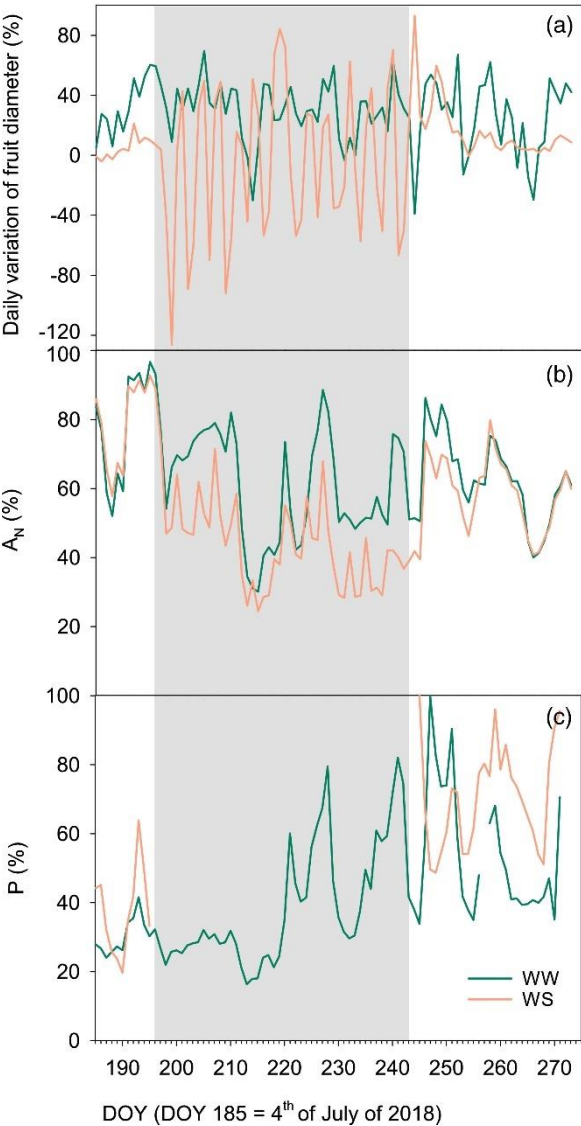
Fig. 4. Temporal patterns of normalized daily variation of **(a)** fruit equatorial diameter, **(b)** total daily net photosynthesis (A_N), and **(c)** daily maximum turgor (P).

Once these kinetics were described, we analyzed daily normalized variables to determine the sensitivity of each variable to water deficit. An analysis of the response of the normalized variables to Ψ_{pd} showed that the reduction of normalized daily increment of fruit equatorial diameter was steeper than that of daily A_N in response to water deficit (Fig. 5). Both relations were linear, negative, and significant ($p < 0.01$ in both cases with $R^2 = 0.61$ and 0.76 for A_N and the daily variation of fruit equatorial diameter, respectively).
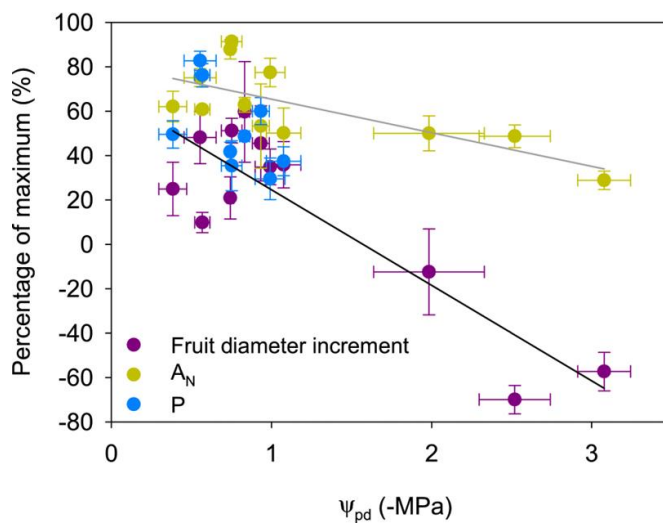
Fig. 5. Relationships between pre-dawn leaf water potential (Ψ_{pd}) and the percentage of the maxima of the daily increment of fruit equatorial diameter, total daily net photosynthesis rate (A_N), and daily maximum turgor (P) for the 6 days when Ψ_{pd} was measured in well-watered (WW) and water stressed (WS) trees.
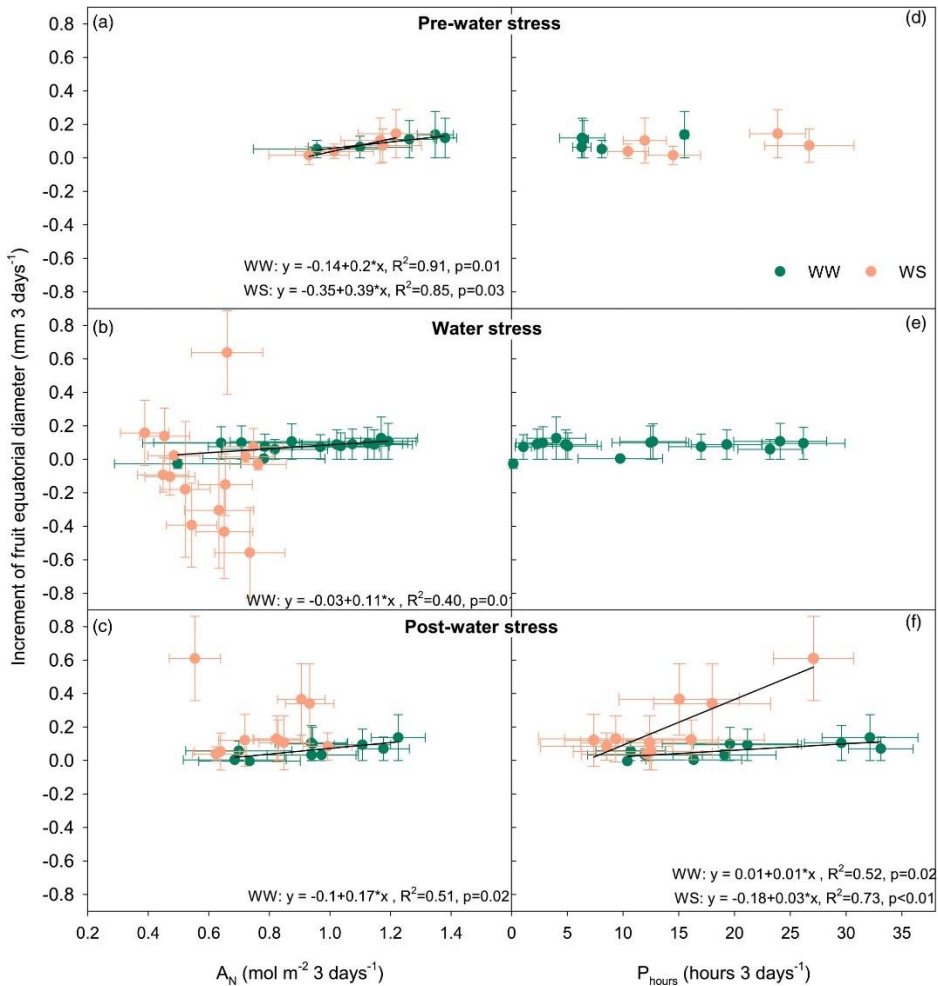
Fig. 6. Relationship between fruit equatorial diameter increment and **(a–c)** accumulated net photosynthesis (A_N) and **(d–f)** the hours that turgor is above a threshold (P_{hours}) in well-watered (WW) and water stressed (WS) trees for three consecutive days during the pre-water stress (a, d), water stress (b, e), and post-water stress (c, f) periods. Only statistically significant relationships are shown. Each point represents the average of the data collected in all trees instrumented, six and five fruits for WW and WS trees, and four trees for A_N and P modeling. The bars indicate ± SE.

During the water stress period, the maximum turgor decreased to values not measurable with the ZIM turgor sensors; thus, we could not adjust any significant curve because we do not have data beyond -1.1 MPa. However, it can be considered that most of the turgor beyond that value was below the threshold allowing for growth. The dynamics of P were more in accordance with the pronounced decrease in fruit equatorial diameter variation observed beyond -1.1 MPa than with the dynamics of A_N, which was only marginally reduced until reaching lower values than -2.5 MPa.

To analyze which variable better accounted for fruit equatorial increment, a further data analysis was con- ducted to search for significant regression between turgor and photosynthesis with fruit equatorial diameter. Specifically, to analyze the putative role of turgor in fruit diameter increment we computed the hours (P_{hours}) above a certain level of P, at which conditions for growth are supposed to occur, as described in 3.2. section. For this purpose, we used the three periods (pre- water stress, water stress, and post-water stress) for the two irrigation treatments. In each period the data were pooled together for three consecutive days from the beginning of the experiment to the end. Collinearity analyses resulted in VIF values between 1.1 and 1.6 in all cases except in the period after water stress, where VIF was 2.5 for WW trees. Thus, no correlation or just moderate correlation was found, which is considered not severe enough to conduct corrective measurements. The relationships between the variables analyzed showed different patterns for the different periods and the two treatments. We found significant and positive linear relationships between accumulated A_N and the fruit equatorial diameter increment for WW for every period analyzed ($p < 0.05$; Fig. 6a–c). Before the water stress treatment was applied, WS trees also showed a strong, positive, and significant relationship between A_N and fruit equatorial diameter (Fig. 6a). On the contrary, a plot of P_{hours} against the fruit equatorial diameter increment

(Fig. 6d–f) showed significant and positive relationships for both treatments but only in the post-water stress period (Fig. 6f). Especially robust was the P_{hours}-fruit equatorial diameter increment relationship for WS in the post-water stress period, showing a much more pronounced slope than WW. Indeed, the total increment of the fruit equatorial diameter for WS was 0.57 while it was only 0.14 for WW. Moreover, this higher increment in WS than in WW was only explained by P_{hours}, as A_N was not significantly related with the diameter increment. For the analysis, we could not consider P_{hours} for the water stress period (DOY 197–243); however, it was assumed that P was below levels at which no growth occurs.

Cell division activity during olive fruit development for the two treatments (WW and WS) was characterized by flow cytometric analysis of the nuclear DNA contents in olive fruit pericarps (Fig. 7). The analyses of cell division activity showed that for WW there was an increment of 2C cells and a decrease of 4C cells up to DOY 245, when a plateau was reached. This plateau was also achieved in WS for the same dates, but the increase and decrease in 2C and 4C cells, respectively, were delayed and more pronounced. The higher proportion of 4C cells in comparison to 2C indicated that fruits underwent intensive cell division at the beginning of the study period. Important levels of cell division were still found afterwards, during the water stress period in both treatments, being more intense in WS than in WW as the proportion of 4C cells was higher in WS (41.4% on average for the whole water stress period) than in WW (30.5%) trees. Notably, at the end of the water stress period, and especially in the post-water stress period, the proportion of 2C cells increased while the proportion of 4C cells decreased remarkably in fruits of both treatment groups (Fig. 7a,b). This indicates that cell division activity was almost completely stopped. The 8C cells represented 1.5 and 7.2% of the cells in fruits of WW and WS trees, respectively (Fig. 7c).
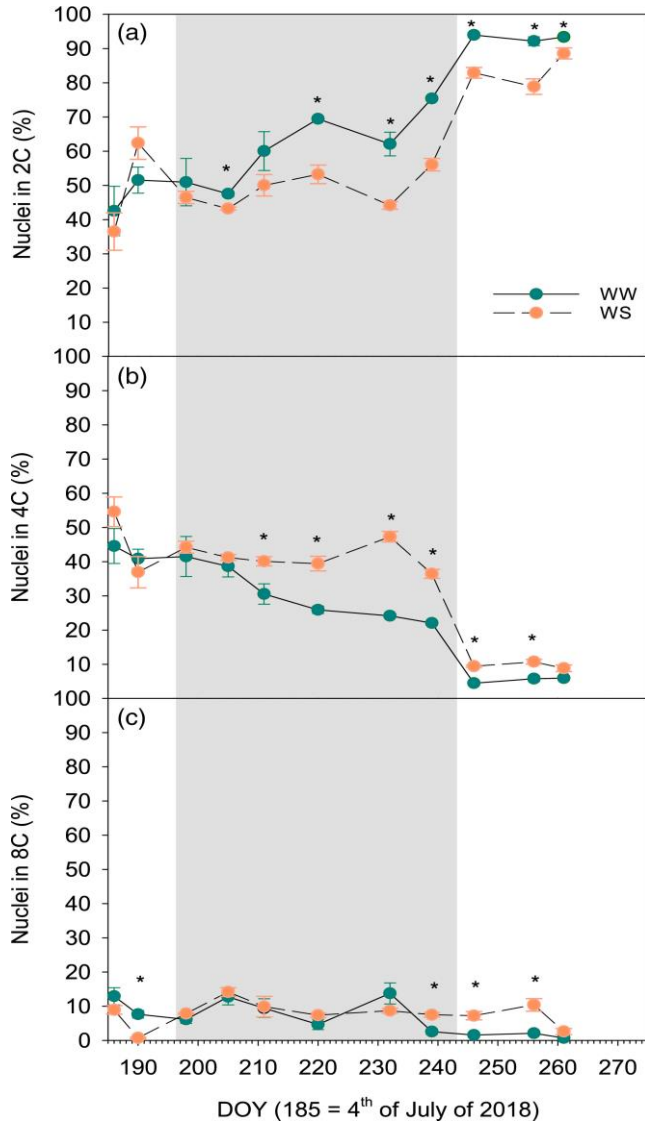
Fig. 7. Nuclear ploidy levels from fruit pericarps following well-watered (WW) and water stressed (WS) treatment during olive fruit development. Each point is the average of four samples. The gray rectangle denotes the water stress treatment period applied to WS trees, which is preceded by the pre-water stress period and followed by the post-water stress period. Asterisks denote significant differences between WW and WS trees (P < 0.05) and bars are ± SE.

3.4. Discussion

3.4.1. Synchronous determination of leaf photosynthesis, turgor, and fruit growth to disentangle their relation

The open debate concerning the main process limiting growth is far from declining, although there is increasing evidence of a larger role of sink limitation than of source limitation. However, both limitations play different roles at different time points, as shown in this work. To study these processes, we studied net CO_2 assimilation as the source limitation and a proxy of leaf turgor for the sink, because sink limitation is understood to represent tissue expansion mainly.

Some authors have explained the current perception of source as the main limiting factor as a consequence of leaf gas exchange measurements being more accessible to scientists than turgor-related technology (Körner, 2015). In this work, we attempted to overcome these technological limitations by fully evaluating, on a fine time scale, the effects of proxies of turgor, photosynthesis, and growth. Studies like this one, tracking physiological variables simultaneously, continuously, and during long periods (Flexas et al., 2018), are not frequent. We modeled A_N through sap flow measurements, as this method has successfully been performed in olive trees (Hernandez-Santana et al., 2016a; 2018). Additionally, we used ZIM turgor sensors, whose output is accepted as a good proxy of turgor (Ehrenberger et al., 2012; Rodriguez-Dominguez et al., 2019), and thus, they have been used in growth studies with a similar purpose to this work (Hilty et al., 2019).

Simultaneously, we continuously measured the equatorial diameter to have a related measurement of fruit growth. Measuring data every 30 min for 90 days allowed us to show how the increment of fruit diameter, net photosynthesis (A_N), and leaf turgor are related at a fine temporal scale over a long period.

84

3.4.2. Higher sensitivity of turgor than of photosynthesis to drought limits fruit growth

In accordance with the current growing body of evidence pointing to growth being more sensitive to water status than to photosynthesis, our results showed that the fruit diameter increment ceased at similar leaf water potential values that caused turgor to be significantly reduced (Fig. 5). In contrast, the decrease of A_N was not as severe as for the other two variables for the same range of leaf water potential values. In addition, the increment of fruit growth at sub-daily time steps showed stronger synchrony with P than with A_N (Fig. 3, Table 1). However, we still observed a strong relationship (Fig. 6) between A_N and growth. There are various hypotheses to explain these apparently contradictory results, the most obvious being that carbon and water flow in the plant are so strongly related that it is difficult to separate them (although, see Tardieu et al., 2011 for a non-coordination perspective of these processes). This would mean that A_N is not necessarily linked with fruit diameter increments. Instead, it is merely statistically correlated such that, with decreasing turgor, A_N would also decrease. However, according to the analysis of collinearity, the correlation of A_N with fruit diameter increment is low or not direct, meaning that there could also be other correlated processes that lead to more growth when A_N is large. The link between water and photosynthesis in leaves may exist at several different levels (as is very well described in Xiong and Nadal, 2020). This relation begins in the stoma (water loss and CO_2 capture) and progresses inside the leaf (shared pathways for water and CO_2 conditioning leaf hydraulic conductance and photosynthesis); moreover, a pathway linking cell and tissue structure with CO_2 assimilation and the bulk modulus of elasticity (ε), possibly through internal CO_2 diffusion, was more recently described. The strong correlation found between photosynthesis and growth can also be explained by internal source–sink regulation ending in growth-limiting

photosynthesis (Körner, 2013), which could have been responsible for the wrongly established hierarchy of restraints in the literature (Fatichi et al., 2014). The differential sensitivity of carbon source and sink activities to water stress could lead to an imbalance between carbon supplied by photosynthesis and carbon used for tissue growth and respiratory costs. A mismatch between these two quantities would be sub-optimal and create a long-term surplus of assimilated carbon. Under normal conditions, this situation is avoided via various mechanisms that lead to a downregulation of photosynthesis. Also, the photosynthesis–growth relation could be produced by the different growth-related processes to which assimilated carbon can be dedicated besides structural functions, specifically, the supply of energy to meristematic tissues, turgor generation in expanding cells accumulating osmotically active carbon compounds, and growth-related processes via carbon signaling (Muller et al., 2011).

3.4.3. Turgor time as key variable to limit fruit growth especially in periods of low cell division activity

The main finding of our study contributing to the source-sink debate is that the time the plant was above a zero growth threshold, described as P_{hours}, was strongly related to the fruit diameter increment (Fig. 6), although a relation between A_N and fruit diameter was also found. Moreover, P_{hours} became more important for explaining fruit diameter increment than A_N (Fig. 6) towards the end of the fruit development period. This relation arose in both WW and WS treatment groups, suggesting that the mechanism explaining this relationship was independent of the irrigation treatment. During the last period of fruit development, there was an outstanding decrease in cells in division (Fig. 7) despite the fact that fruit diameter increased substantially in the same period, especially in WS trees (Fig. 4). Thus, during the final period, growth would be mainly driven by cell expansion with cell division processes becoming much less

important. Considering that turgor is more critical for cell expansion than for cell division, these results would help to explain why P_{hours} was strongly related to fruit diameter increment during this period. Indeed, in olive fruits, cell division and expansion have been described to occur concomitantly during the first period of mesocarp growth (from fertilization – in May – to 6–8 weeks after full bloom), according to Rallo and Rapoport (2001). After that period and until fruit maturation, growth of the mesocarp is solely due to cell expansion. However, our results regarding cell division potentially extend this process to 8–10 weeks. An even more outstanding result is that WS plants maintained a higher proportion of cells in division compared to WW. This suggests two things: that water stress slowed down the cell division process, although not enough to stop it, and that the cell division rate was limited by the water status of the plant, a limitation that was released after the unexpected irrigation event on DOY 220. The growth of the mesocarp is the dominant process in olive fruit growth due to its high growth potential compared to the endocarp, which also stops growing 2 months after flower fertilization (Rapoport, 2008). The fact that there was no A_N–fruit diameter relationship in WS trees during the post-water stress period, as there was for WW trees, or in the pre- water stress period may be explained by the fact that, under WW conditions, tight relationships linking carbon availability and growth illustrate the source limitation of growth in sink organs (fruits here). These relationships probably reflect the different uses of carbon compounds mentioned previously (structural and non-structural growth-related processes). Under water deficit conditions, these relationships can be modified, suggesting that other mechanisms, possibly involving cell wall rheology or water fluxes to growing cells, override the role of carbon and take the lead in growth limitation (Muller et al., 2011). A complementary effect that cannot be entirely ruled out and may help to explain the more dominant role of turgor towards the end of the study

period is that the night hours, when turgor is at its highest and most growth occurs, are longer for this period in our latitude (Fig. 1c).

Even though current models propose that cell expansion is driven by turgor pressure acting on the wall, this process has presented several challenges for researchers besides the technical ones, as mentioned before. Given that irreversible extension is not a linear function of turgor pressure, it may have to exceed a minimum value before irreversible expansion occurs (Lockhart, 1965), which makes it difficult to establish a zero growth threshold for different plant organs (Génard et al., 2001) and species (Mitchell et al., 2014). In this work, we prove the utility of the turgor threshold of 0.9 MPa (Génard et al., 2001) in growth studies because it allowed us to calculate the cumulative sum of turgor time enabling growth and compare normalized growth expression of two different treatments of water availability, as has been done in a very recent work (Coussement et al., 2021). This threshold, together with typical olive osmotic values (Table S1), resulted in a leaf water potential of -1.5 MPa for WW, which was very similar to the result published (-1.4 MPa) by Mitchell et al. (2014) and only a little bit more negative than the value for which turgor and fruit growth decreased more markedly (Fig. 5). Aside from extensibility and the threshold turgor, growth adjustment during stress can occur through osmoregulation, thus maintaining turgor pressure while leaf water potential is reduced. This process could help to permit the resumption of growth when water stress is recovered (Hsiao et al., 1976), which could help to explain the outstanding increment of fruit equatorial diameter in WS compared to WW.

3.4.4. Methodological considerations

We are aware of some shortcomings of our study, but overall they do not invalidate our conclusions. All carbon assimilated was assumed to be eventually available for growth and metabolism, which is not consistent with

recent results on the dynamics of non-structural carbohydrates (NSC). NSC play an important role as carbohydrate storage, which would buffer any mismatch between supply and demand (Muller et al., 2011; Fatichi et al., 2014). Considering our 90-day study period, the storage could have buffered the mismatch between carbon supply and demand, such that the assimilated carbon could be used when turgor is above the zero growth threshold. This would mean that the relation between A_N and fruit diameter increment could have been affected by some carbon coming from reserves. However, the fraction of carbon allocated to storage relative to structural growth and metabolic maintenance may be small over long periods, and most process-based models of forest and tree productivity have traditionally considered this in a similar manner (Sala et al., 2012). Additionally, it has been shown in olive trees that the carbohydrate reserves are not as important for fruit growth as they are for the olive's survival strategy (Bustan et al., 2011). Another limitation of our study is that fruit dendrometers measure not just growth but also water flow in and out of the olive fruit (Fernandes et al., 2018). However, stem radial growth increment has been considered as a suitable proxy for expansive growth in above- ground tissues (Mitchell et al., 2014). Variations in the size of organs result from changes in hydration, temperature, and growth (Génard et al., 2001). At a daily scale, the recurrent shrinking and swelling that are a function of the changing levels of hydration may significantly exceed those resulting from daily growth of tissues or direct temperature variations (Kozlowski, 1972). However, on a long- term basis, diameter variation also depends on growth (Génard et al., 2001). Therefore, although we used sub-daily and daily values for the more descriptive trends, we used values of the totals of three consecutive days for the analyses (Fig. 7) in an attempt to minimize the swelling and shrinkage effect (Zweifel et al., 2016; Hilty et al., 2019) as well as include the time it takes to reshuffle carbon stores and change

transport rates to the sinks (Muller et al., 2011). Ideally, growth would have been measured in other organs also acting as sinks, preferentially in the leaves, where A_N and turgor was estimated. However, the existing technology to do this, basically, leaf clips, is not suitable for field measurements as wind causes noisy recordings. Although interesting and promising technological approaches have started to be tested recently (Hilty et al., 2019), their utility still needs to be tested in long field studies such as this one. However, despite the special relevance of fruits from a physiological and agronomical point of view, leaf area index (LAI) and the number of fruits per tree could also be relevant attributes for understanding source–sink relationships. They were not studied together with fruit growth here because LAI showed a constant increment rate for WW and no increase for WS. In addition, LAI was not measured continuously as the rest of the variables in this study and thus, we think it does not add relevant information. The number of fruits were not considered either because no significant differences were found between the two treatments (WW: 9223 ± 1447, WS: 9863 ± 407). These results are in accordance with previous works conducted in the same orchard for different years (Fernández et al., 2013; Hernandez-Santana et al., 2018). Fruits are a good target to study the growth limitation processes because they are a priority in agronomical species. Ideally, turgor should have been measured in fruit instead of using leaf turgor as its proxy. Nevertheless, the use of leaf turgor is based on the strong relationship found between fruits and leaves from a hydraulic perspective (Fig. S1). This is in accordance with previously published results on a strong relationship between fruit and leaf water potential and the turgor loss point in olive (Fernandes et al., 2018) (Fernandes et al., 2018) and other species (McFadyen et al., 1996; Galindo et al., 2016). However, we must recognize that the temporal dynamics and extent of the relationships between fruit and leaf

turgor are not fully known. Therefore, our results, despite being promising, must be evaluated in the future when there is technology available to do so.

3.4.5. *Implications for improving agriculture resilience to drought*

Our study opens possibilities to determine the thresholds of water stress levels in deficit irrigation strategies, which are usually determined based on the water status of the plant or other agronomical indices other than fruit growth, which should be the main target as it is directly related to yield. We have demonstrated that under water stress, even though fruit growth seems to stop, there is cell division, and the final size of the fruit is not severely penalized when the trees are hydrated again during the cell expansion period (Fig. 2), similar to results shown in Hernandez-Santana et al. (2018). This shows that temporary sink limitations might be recovered later in the season, thus making turgor-driven sink limitations that occur seasonally much less important at an annual scale. This last result is of outstanding relevance for regulated deficit irrigation approaches because it explains the physiological mechanism driving the disproportionate growth of fruits of WS trees compared to WW ones.

3.5. Conclusions

Our results are consistent with the sink limitation hypothesis suggesting that under water stress, reductions in turgor-driven cell expansion have a greater and more immediate impact on fruit growth than smaller reductions in photosynthesis. Besides a photosynthesis-fruit diameter relation, we found a strong relation between a turgor related variable and fruit diameter increment towards the end of the experimental period, when most of the cell division activity stopped. Therefore, we conclude that growth declines do not necessarily indicate C limitation, as traditionally assumed, but when taken together all our results provide strong support for the hypothesis that fruit

growth is co-limited by both A_N and turgor depending on cell division stage of the fruit development and regardless the tree water status. Specifically, photosynthesis, as the origin of carbon skeletons required by plants to build up all their structures for both maintenance and growth and other related-growth measurements, would be important during cell division but during cell expansion turgor is more dominant, specially in water-stressed trees.

3.6. Supplementary material
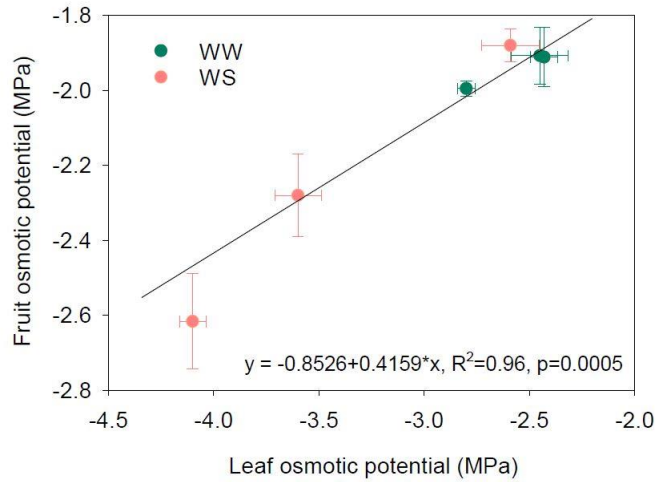
Fig. S1. Relationship between fruit and leaf osmotic potential for well-watered (WW) and water stressed (WS) trees.
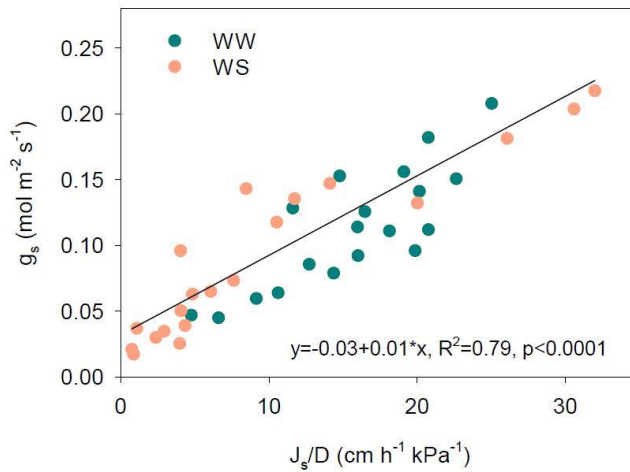
Fig. S2. Relationship used to simulate stomatal conductance (g_s) from the ratio between sap flux density (J_s) and vapor pressure deficit (D) for two trees, one well watered (WW) and another water stressed (WS)
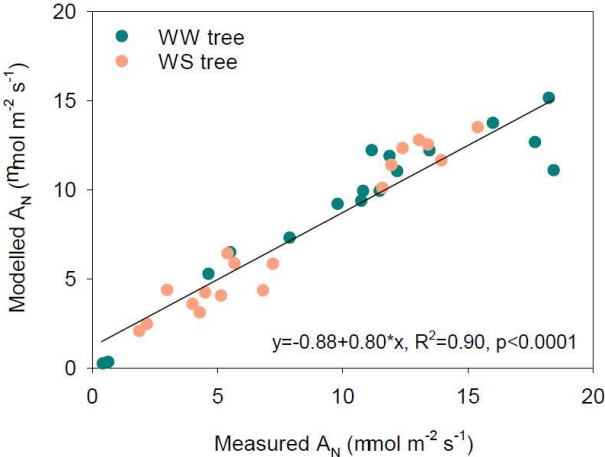
Fig. S3. Comparison of net photosynthesis (A_N) measured with an IRGA and calculated using the Farquhar model for two trees, one well watered (WW) and another water stressed (WS).

CHAPTER **4**:

DUAL EFFECT OF THE PRESENCE OF FRUITS ON LEAF GAS EXCHANGE AND WATER RELATIONS OF OLIVE TREES

Abstract

The presence of fruits provokes significant modifications in plant water relations and leaf gas exchange. The underlying processes driving these modifications are still uncertain and likely depend on the water deficit level. Our objective was to explain and track the modification of leaf-water relations by the presence of fruits and water deficit. With this aim, net photosynthesis rate (A_N), stomatal conductance (g_s), leaf osmotic potential (Ψ_π), leaf soluble sugars and daily changes in a variable related to leaf turgor (leaf patch pressure) were measured in olive trees with and without fruits at the same time, under well-watered (WW) and water stress (WS) conditions. Leaf gas exchange was increased by the presence of fruits, this effect being observed mainly in WW trees, likely because under severe water stress, the dominant process is the response of the plant to the water stress and the presence of fruits has less impact on the leaf gas exchange. Ψ_π was also higher for WW trees with fruits than for WW trees without fruits. Moreover, leaves from trees without fruits presented higher concentrations of soluble sugars and starch than leaves from trees with fruits for both WW and WS, these differences matching those found in Ψ_π. Thus, the sugar accumulation would have had a dual effect because on one hand, it decreased Ψ_π, and on the other hand, it would have downregulated A_N, and finally g_s in WW trees. Interestingly, the modification of Ψ_π by the presence of fruits affected turgor in WW trees, the change in which can be identified with leaf turgor sensors. We conclude that plant water relationships and leaf gas exchange are modified by the presence of fruits through their effect on the export of sugars from leaves to fruits. The possibility of automatically identifying the onset of sugar demand by the fruit through the use of sensors, in addition to the water stress produced by soil water deficit and atmosphere drought, could be of great help for fruit orchard management in the future.

4.1. Introduction

The olive tree is traditionally grown in the Mediterranean basin, and although it has been historically cultivated under rain-fed conditions, its positive productivity response to irrigation has increased the surface of irrigated trees (Orgaz and Fereres, 2008). Water scarcity in the regions where olive grows demands to develop a specific strategy to apply deficit irrigation (Moriana et al., 2003; Dell'Amico et al., 2012; Fernández et al., 2013) and to study the response of the olive tree to water stress (Connor and Fereres, 2005; Fernández, 2014). Although the response of olive trees to soil water deficit has been extensively studied (Lavee, 1996; Connor and Fereres, 2005; Fernández, 2014), the effect that the fruit, specifically the fruit load, may have on this response has been neither as widely examined nor included in deficit irrigation strategies. However, studying the effect of fruit load on the response of olive to water stress is relevant because previous studies have found that fruit load plays a relevant role in modifying tree water consumption (Bustan et al., 2016), plant water relations (Martín-Vertedor et al., 2011a; Naor et al., 2013; Bustan et al., 2016), fruit size (Trentacoste et al., 2010), and yield and oil accumulation (Naor et al., 2013). However, the importance of the effect of crop load on tree–water relationships has been reported to be variable, likely dependent on the level of tree water stress (Martín-Vertedor et al., 2011a; Naor et al., 2013). Moreover, other studies have confirmed that fruit growth has a preference over vegetative growth (stem or leaves) especially under water stress (Iniesta et al., 2009; Dag et al., 2011; Hernandez-Santana et al., 2018; Rosati et al., 2018), fruits being major water (Girón et al., 2015; Fernandes et al., 2018) and carbon (C) sinks (Hernandez-Santana et al., 2018).

Despite these findings on the importance of fruit load for modifying plant carbon and water relations, the mechanisms explaining the modification

of leaf gas exchange by fruit load have not been explored thoughtfully. Indeed the higher demand in fruit-bearing plants compared with plants with a low crop load or without fruits have been reported to increase leaf photosynthesis and stomatal conductance (Naor et al., 2013; Bustan et al., 2016). The modification of stomatal conductance produced by different fruit loads and water availability could be mediated by a photosynthesis reduction generated by the accumulation of soluble sugars in the leaf provoked by a decrease of C sinks (i.e., fruits) in trees with low fruit load compared with trees with great fruit loads. The inhibition of photosynthesis by end-product is a well-tested effect (Kelly et al., 2013) which has been already shown to occur in a large number of crop species (Goldschmidt and Huber, 1992). The sugar accumulation in the leaves and consequent reduction of photosynthesis can be produced by the decrease of sink strength of the plant (Herold, 1980; Paul and Foyer, 2001) produced, for example, by a low fruit load. Indeed, in Bustan et al. (2011), stored non-structural carbohydrates in olives decreased in summer, under maximum carbohydrate demand for fruit growth and oil production. However, despite the known function of some soluble sugars on osmotic potential (Martínez-Vilalta et al., 2016), they have been rarely used to explain the observed effects of different levels of fruit loads on plant water relations (Dell'Amico et al., 2012; Girón et al., 2015; Fernandes et al., 2018). Changes on leaf osmotic potential, as a consequence of soluble sugar dynamics, together with concomitant fluctuations of leaf–water potential (Naor et al., 2013; Bustan et al., 2016) due to the presence of fruit, could have an impact on leaf turgor pressure, which can be monitored by a sensor in field-grown olives trees (Hernandez-Santana et al., 2021). Thus, as the fruit load could have an effect on leaf turgor pressure through its effect on the leaf osmotic potential, this variable could be used to identify the sink effect of fruits on tree water relations. Moreover, because stomatal behavior and leaf turgor pressure are

100

closely interrelated (Buckley, 2019), the measurement of this variable allows the estimation of stomatal conductance (Rodriguez-Dominguez et al., 2019).

Hence, this work aims to explain and track the modification of leaf–water relations and leaf gas exchange by the presence of fruits and water deficit in olive trees. Specifically, we aim to (i) study the leaf sugar effects and water deficit on leaf-water relations and (ii) explore a method to identify the effect of fruit-sink effect on leaf-water relations. We hypothesize that photosynthetic regulation would be affected by the sink demand of fruits, and thus the leaf gas exchange would be lower in trees without fruits than in trees with fruits, with water deficit modulating this response. Sugar accumulation in the leaf under low sink demand would also decrease the osmotic potential of leaves, and hence decrease the turgor loss point. We hypothesize further that we would be able to detect these changes with a leaf turgor sensor. Thus, we would be able to have a method to identify the effect of fruit sink demand on tree water relations. If successful, the monitoring of turgor could be used to identify the onset of fruit sugar demand in commercial orchards.

4.2. Materials and methods

4.2.1. Orchard and climate conditions

The experiment was conducted in 2018 (from July to November) in a super-high-density olive orchard (Olea europaea L. cv. Arbequina) near Utrera (Seville, southwest Spain) (37° 15' N, −5° 48' W). The olive trees used were 12 years old and planted in rows N-NE to S-SW oriented, in a 4 m × 1.5 m spacings (1667 trees ha −1). The soil of the orchard had a sandy top layer and a bottom clay layer (Arenic Albaquaf, USDA 2010, https://www.nrcs.usda.gov/Internet/FSE_DOCUMENTS/nrcs142p2_050915.pdf). Further details on the orchard characteristics can be found in Fernández et al. (2013).

In the area, the climate is Mediterranean with mild, rainy winters and hot, dry summers. During the months of the experiment, there were rarely rain events because annual rainfall occurs mainly between late September and May. The only rainfall events (5 days with >10 mm) occurred after day of the year (DOY) 283 (10 October), but they did not affect the differential irrigation treatments in our experiment. Average values of potential evapotranspiration (ET_O) and precipitation in the region are 1482 mm and 500 mm, respectively, for the 2002–18 period (data recorded at the nearby of the study area, Los Molares station, 37° 10′ 34″ N, −5° 40′ 22″ W, 77 m above sea level; averages provided by the Regional Government of Andalusia). For the same period, average maximum ($T_{a, max}$) and minimum ($T_{a, min}$) air temperatures were 24.8 °C and 10.6 °C, respectively. The hottest months are July and August, whose $T_{a, max}$ values are over 40 °C. In addition, at least once per year between July and August, the vapor pressure deficit values reach over 7 kPa.

4.2.2. Irrigation and treatments

Two irrigation treatments were applied in 12 trees: 6 well-watered (WW) trees with a full irrigated (FI) regime, which were irrigated daily to replace 100% of the irrigation needs (IN), and another 6 water stressed (WS) trees subjected to a sustained deficit irrigation (SDI) regime, whose trees received 50% of IN (50 SDI). The IN were calculated daily based on the maximum potential crop evapotranspiration (ET_c) described in Allen et al. (1998) as IN = ET_c − P_e, being P_e the effective precipitation calculated as 75% of the precipitation recorded in the orchard. Further details can be found in Fernández et al. (2013). The SDI treatment was carried out from DOY 196; however, we applied an irrigation recovery on DOY 285 to see its effect on the trees. In addition, due to technical problems, an irrigation event occurred on

DOY 261. Each tree row was irrigated with one dripper line located close to the trunk with a 2 L h^{-1} dripper every 0.5 m.

To study the effect of fruit presence or absence, we applied two different treatments in each irrigation treatment: three trees with a presence of fruits (+) which are considered a control where the tree fruit load had not been modified, and three trees with an absence of fruits (−) in which all fruits have been detached from the tree. Fruit removal was performed on DOY 182 (July 1) before all the measurements and then the experiment started. The number of fruits per tree was estimated in eight adjacent trees. No significant differences were found between treatments: WW trees had 8786 ± 790 fruits and WS 10,124 ± 518 fruits. Moreover, in our study plot we have never seen any evidence of alternate bearing (see for example Fernández et al. (2013) and Hernandez-Santana et al. (2017) for a summary of the yield of the period 2010–12 and 2011–15, respectively).

4.2.3. Olive growing cycle

The olive growing cycle is widely known and a graphical representation of the most important processes and the times at which they occur in our study area can be found in Hernandez-Santana et al. (2017). The olive growing cycle starts in our experimental area in mid-February with the shoot growth. Bloom usually occurs in April, thus fruit growth starts in May and continues until mid-September, when fruit growth rate becomes slower than in the previous months. From the beginning of the fruit growth period, cell division in the fruit occurs, being maximum until July when starts to slow down until the end of August, when it is completely stopped. Maximum rate of pit hardening is normally detected in June and could be extended along July and August. Finally, ripening begins in September and lasts until harvest, which normally happens

at the end of October–beginning of November. Oil accumulation starts sometime after fruit growth in June and continues until harvest.

4.2.4. Gas exchange and leaf water potential measurements

Net photosynthesis rate (A_N) and stomatal conductance (g_s) values were measured weekly with a LI-6400 portable photosynthesis system (Li-Cor, Lincoln NE, USA) with a 2 cm × 3 cm standard chamber and ambient light and CO_2 conditions (400 p.p.m.). Measurements were taken at 10:00–11:00 h GMT during summer (DOY 191–261 inclusive) and 12:00–13:00 h GMT during the autumn (DOY 268–302 inclusive) period to reach the minimum and maximum daily A_N and g_s according to Fernández et al. (1997). Leaf gas exchange measurements were performed on three young, fully mature and developed leaves per tree from the southeast part of the canopy ~1.5 m above the ground. leaf–water potential at midday ($\Psi_{leaf, md}$) was measured with a Scholander-type pressure chamber (PMS Instrument Company, Albany, OR, USA) in two leaves per tree. Briefly, after collecting the leaves, they were enclosed in an open regular plastic bag and stored in an icebox with ice packs that were not touching the bagged leaves to avoid abrupt changes in leaf temperature that might result in condensation. This plastic bag was introduced in a closed, zip plastic bag into which a moistened paper towel was introduced. We also exhaled into this bag, so that high humidity and CO_2 conditions would prevent the occurrence transpiration. Measurements were conducted late in the afternoon. Full details of the procedure followed can be found in (Rodriguez-Dominguez et al., 2022).

4.2.5. Fresh fruit weight, dry weight, and oil content

Six fruits per studied tree were collected every 2 weeks. In the laboratory, the fruit fresh weight (FW) values were taken using an accurate

electronic balance (Balance XS105, Mettler Toledo, Columbus OH, USA). Then, fruits were immediately placed in an oven at 75 °C for at least 72 h until constant weight and their dry weight (DW) was recorded.

The oil content was measured from six fruits per studied tree every 2 weeks. The fruits were frozen, and at the end of the experiment, the oil extraction analyses were performed from fruit mesocarp tissue by the method used in Hara and Radin, (1978). Oil content (%) was determined by gravimetric quantification of total lipid weight after solvent evaporation in an Eppendorf® centrifugal vacuum concentrator Basic Model 5301 (Eppendorf, Hamburg, Germany).

4.2.6. Leaf osmotic potential measurements

Ten green and mature leaves per each tree were collected on DOY 219, 226, 233, 240, 254, 261, 268, 283 and 295 at 13:30 h. Specifically, in the WW+ and WS+ treatments, efforts were made to collect them near the fruits. Leaves were cut, covered with aluminium foil paper and immediately introduced in liquid nitrogen. Back in the laboratory, the samples were stored in a freezer at −80 °C until further analysis. To calculate the leaf osmotic potential (Ψ_π), we used two foliar 7 mm diameter disks per sample, between the midrib and margin obtained with a cork borer. Then, we punctured the fruit 15–20 times with forceps to equilibrate the sample. We used a PSYPRO Thermocouple Psychrometer Water Potential System (Wescor Inc., South Logan, UT, USA) and let the sample be in equilibrium ca 2 h before it was measured. Measurements were calculated by using the regression model proposed by Bartlett et al. (2012) based on temperature dependence for constant equilibrium of chemical processes.

4.2.7. Soluble sugars and starch analyses

Additional four green and mature leaves were collected on DOY 219, 254, 283 and 295 at 13:30 h. They were frozen immediately in liquid nitrogen and then stored at −80 °C. Then, they were lyophilized (VirTis BenchTop 2 K Freeze Dryer, SP Industries Inc. Warminster, PA, USA) for 48 h and their DW was recorded. For the extraction of soluble sugars from the polar fraction, 50 mg of DW were used and 20 volumes (1000 µl) of 80% EtOH +0.1% formic acid were added. The samples were incubated in a heating block at 80 °C with gentle shaking for 1 h, they were then centrifuged and the supernatant was reduced to the aqueous phase in an Eppendorf® centrifugal vacuum concentrator Basic Model 5301 (Eppendorf, Hamburg, Germany) at 50 °C. This process was repeated twice and the tubes were immediately frozen in liquid nitrogen and stored in a freezer overnight. The following day, they were resuspended in 20 volumes of sterile dH_2O.

The concentration of soluble sugars (glucose, myo-inositol, mannitol, galactose, fructose and sucrose) were determined by anion exchange chromatography using a sample dilution (sample:sterile dH_2O 1:100) but only glucose, myo-inositol and mannitol showed significant concentrations. Thus, glucose, myo-inositol and mannitol were the soluble sugars shown in this work. Chromatographic analyses of soluble sugars were conducted in a Metrohm (Herisau, Switzerland) 930 compact ICFlex ion chromatograph equipped with a pulsed amperometric detector (PAD). The chromatographic separation was performed on a Metrosep Carb 2 column (4 mm × 150 mm, Metrohm) equipped with a guard column (Metrosep Carb 2 Guard, 5 mm × 30 mm, Metrohm). Isocratic elution mode was applied using a mobile phase composed by a mixture of NaOH 0.3 M and CH_3COONa 0.01 M at a flow rate of 0.5 ml min−1 in a 17-min run at a column temperature of 30 °C, and an injection volume of 20 µl. The electrochemical detector was equipped with a gold

106

working electrode and a palladium reference electrode. The cell of the PAD was kept at 35 °C. Sugar identification and quantification were carried out using retention times and the related sugar calibration curve, respectively.

For starch quantification, glucose extraction from starch was performed. The pellet obtained in the previous process was washed twice with sterile dH2O, resuspended in nine volumes (450 µl) of sterile dH2O and stored at 4 °C overnight. The starch in the pellet was gelatinized by introducing the samples at 100 °C for 2 h. Once at room temperature, one volume (50 µl) of 1 M CH_3COONa, pH 4.5, containing 100 U ml−1 of α-amyloglucosidase was added to transform starch into glucose. It was checked using a Lugol solution (sterile dH_2O:Lugol 10:1). Then, the extracted glucose was determined as described before.

The contribution of soluble sugars to the osmotic potential was calculated from the concentation of each osmolite by using the Boyle–;van't Hoff relation as Aranda et al. (2021) and (Ranney et al. (1991). Briefly, osmotic potential = RDW × c × R × T, where RDW represents the ratio of leaf DW to leaf–water content (estimated as the difference between leaf fresh weight and DW), c is the concentration of each osmolyte, R is the gas constant and T is the temperature at 25 °C.

4.2.8. Turgor-related sensors

To study maximum daily changes in leaf turgor pressure, leaf turgor pressure sensors ('ZIM turgor sensors') were installed on one leaf in three WW+ and WW− trees. No leaf turgor pressure sensors were installed in WS trees because under water stress conditions leaves are in a turgorless state and out of the minimum range that they can measure (Ehrenberger et al., 2012). This is not a limitation in our study since if the turgor is too low, the conditions for fruit growing are not achieved, and the measurement of turgor is irrelevant

(Hernandez-Santana et al. (2021), for more information on this topic). The basis of these sensors consists of clamping the leaf between two metal pads with two magnets. The principle of the turgor-related sensors was described in detail by Westhoff et al. (2009) and Zimmermann et al. (2008). The relative leaf turgor pressure (P) is measured as a function of the pressure that the turgor sensor exerts on the leaf and is referred to as leaf patch pressure (P_p). The magnets exert a pressure on the leaf that it is counteracted by its turgor pressure. The higher the turgor pressure of the leaf, the lower the P_p (more details on the method in Zimmermann et al. (2008), Westhoff et al. (2009) and Ehrenberger et al. (2012). Therefore, the minimum daily value of the sensor ($P_{p, min}$) corresponds to the maximum daily turgor pressure of the leaf. Seasonal changes in $P_{p, min}$ are interpreted as changes in the maximum turgor of the leaf. To monitor more clearly the trend of these seasonal changes, the difference in Pp, min between two consecutive days was calculated ($\Delta P_{p, min}$). Positive values of ΔP_p , min indicate that the maximum turgor reached by the leaf every day is decreasing, and in the context of our study it would suggest that the osmotic potential is increasing due to a lower concentration of osmolytes in the leaf. The use of these sensors is not valid in the WS treatment when leaves are in a nearly turgorless state as defined by Ehrenberger et al. (2012). Under water stress conditions, like those imposed in the WS treatment, the conditions for fruit growth are not fulfilled, as demonstrated by Hernandez-Santana et al. (2021). Therefore, turgor sensors were only used to study the presence or absence of fruits in the WW treatment.

4.2.9. Statistical analyses

Data for A_N, g_s, Ψ_{leaf}, md and Ψ_π of each measurement day were analyzed by a two-way ANOVA, being water stress treatment (WW and WS) and the presence/absence of fruits (+ and −) the factors considered. Data for

fruit DW and oil content were analyzed by a one-way ANOVA. The assumptions of normality and homoscedasticity in the data were verified before performing an ANOVA. Statistical analyses were carried out using SigmaPlot® software (Systat Sotfware, San Jose, CA, USA).

4.3. Results

4.3.1. Fruit DW and oil content

Although differences between WW+ and WS+ trees were found in both fruit DW and oil content during some days in the studied period (Fig. 1), the synthesis of oil was less affected by water stress than the fruit DW. The increment rate of fruit DW occurred at a slower pace in the WS than in the WW treatment from DOY 220 to DOY 263, generating the differences between both irrigation treatments during the period of higher water stress. However, during that period, the rate of increment of oil content was similar in both treatments, suggesting that the plant promoted the oil synthesis process over fruit DW increment, and that the level of stress was not enough to impair it. After irrigation recovery, no differences were found between treatments in either variable.

4.3.2. Leaf gas exchange

Higher values of AN and gs were measured in WW than in WS trees, independently of the fruit presence (Fig. 2). Differences were as high as threefold between water treatments. When fruit treatments were compared within a single water treatment, no differences were found for the WS trees. However, significant differences emerged in the WW trees from DOY 260 to DOY 270, WW+ showing higher A_N and g_s than WW− trees. When the irrigation recovery was applied on DOY 285, we observed that, although there were still

differences between both irrigation treatments, these differences became smaller than in the previous period.
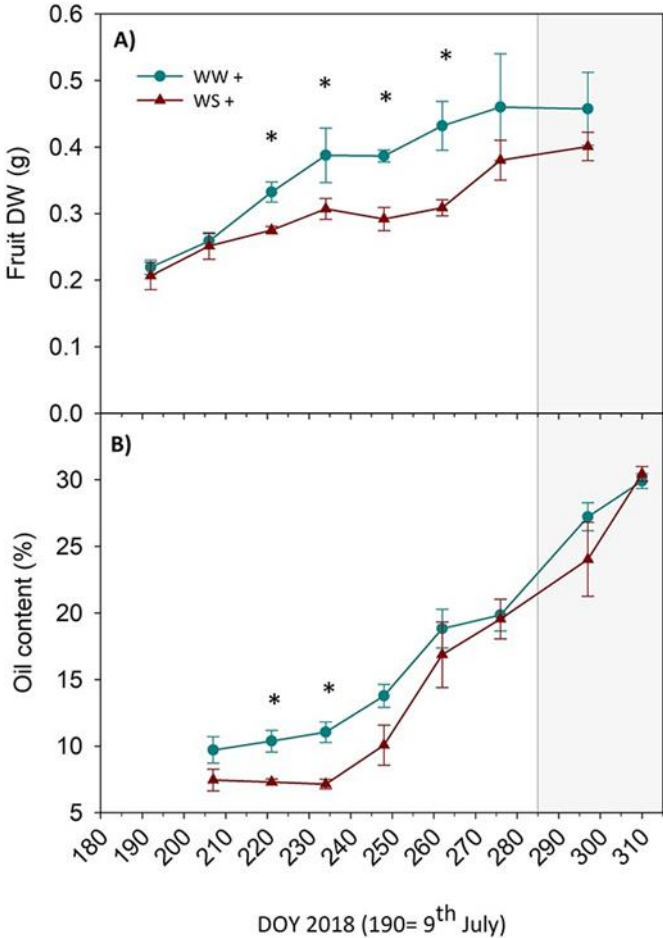
Fig. 1. Evolution of **(A)** fruit DW (g) and **(B)** total oil content (%) in WW (blue) and WS (red) trees with presence of fruits (+). Irrigation recovery, that is represented by a gray area, started at DOY 285 (12 October). Data are mean ± standard errors from six fruits per tree. Asterisks are shown when significant differences between irrigation treatments ($P \leq 0.05$) were found according to one-way ANOVA.
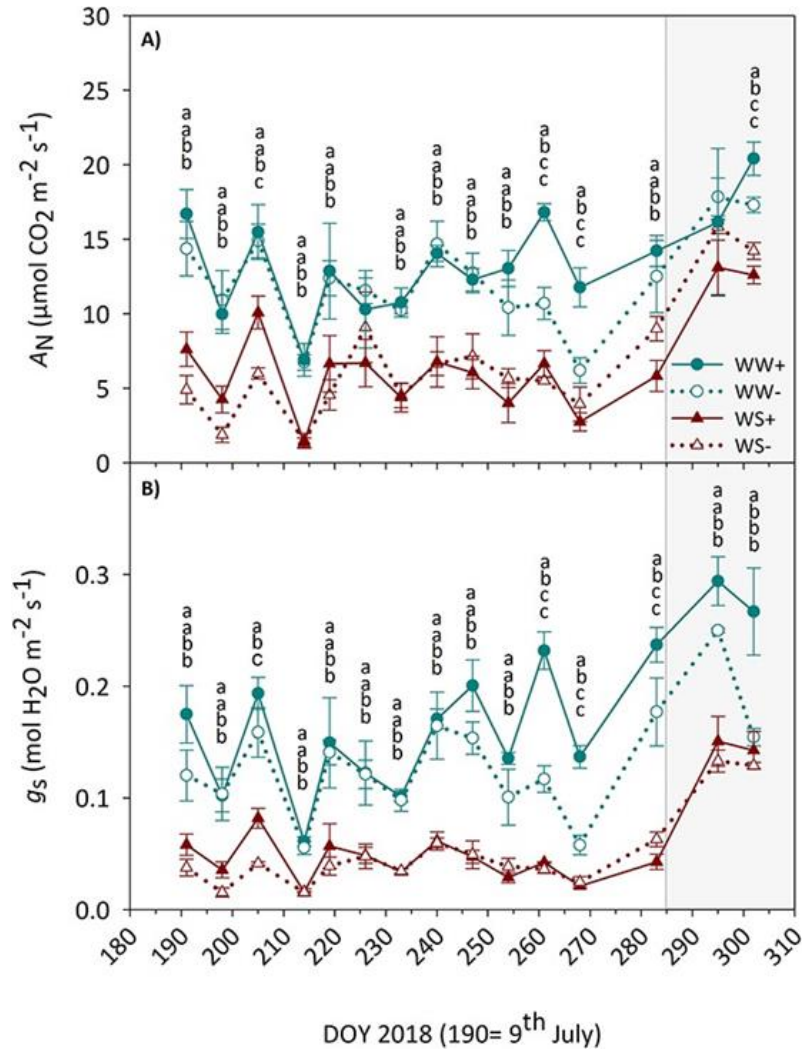
Fig. 2. Evolution from DOY 2018 190 to 310 (9 July–6 November 2018) of **(A)** photosynthesis rate (A_N (mmol CO_2 m^{-2} s^{-1})) and **(B)** stomatal conductance (g_s (mmol H_2O m^{-2} s^{-1})); in WW (blue) and WS (red) trees, presence of fruits (+) and absence of fruits (−). Irrigation recovery started at DOY 285 (12 October), and it is represented by a gray area. Data are mean ± SE from three different plots (1 tree = 1 plot) per treatment. Different letters indicate significant differences between irrigation treatments and fruit loads combined ($P \le 0.05$) according to two-way ANOVA. The order of the letters follows the order of the treatments in the legend. Letters are not shown when no differences were found.

4.3.3. Leaf-water and osmotic potential

We observed significant differences in $\Psi_{leaf,\,md}$ between WW and WS trees from DOY 226 to 285 (Fig. 3A). In most of the dates during the deficit irrigation period, $\Psi_{leaf,\,md}$ in WS+ was significantly more negative than in WS− trees. Differences disappeared when irrigation was recovered on DOY 285. The sudden increase of $\Psi_{leaf,\,md}$ on 260 was due to technical problems in the irrigation system, but the effects of the irrigation treatments were maintained as WW was still significantly less negative than WS.

Regarding Ψ_π, we found significant differences between the WW and WS trees from DOY 226 to DOY 283 (Fig. 3B). The WW trees presented higher leaf $\Psi\pi$, than the WS trees. However, in contrast to $\Psi_{leaf,\,md}$, we found differences between WW+ and WW− from DOY 261 onward, WW+ presenting higher Ψ_π values than trees without fruits. On the contrary, no differences between WS+ and WS− trees for most dates were observed. After irrigation recovery, differences in Ψ_π were maintained between WW+ and WW−, but Ψ_π from WS+ trees became significantly higher than in WS− trees.

4.3.4. Changes in soluble sugars and starch and relationship with leaf osmotic potential

The highest concentrations of soluble sugars and starch were measured in WS− trees (Fig. 4). In addition, leaves from trees without fruits presented higher concentrations of soluble sugars and starch than leaves from trees with fruits for both irrigation treatments. These differences were found in the period of deficit irrigation, and trends matched those found in leaf Ψ_π. This pattern was noticed mainly in myo-inositol and mannitol. Starch accumulated three- to fourfold in leaves of trees without fruits than in trees with fruits in both WW and WS treatments (Fig. 4D).

112
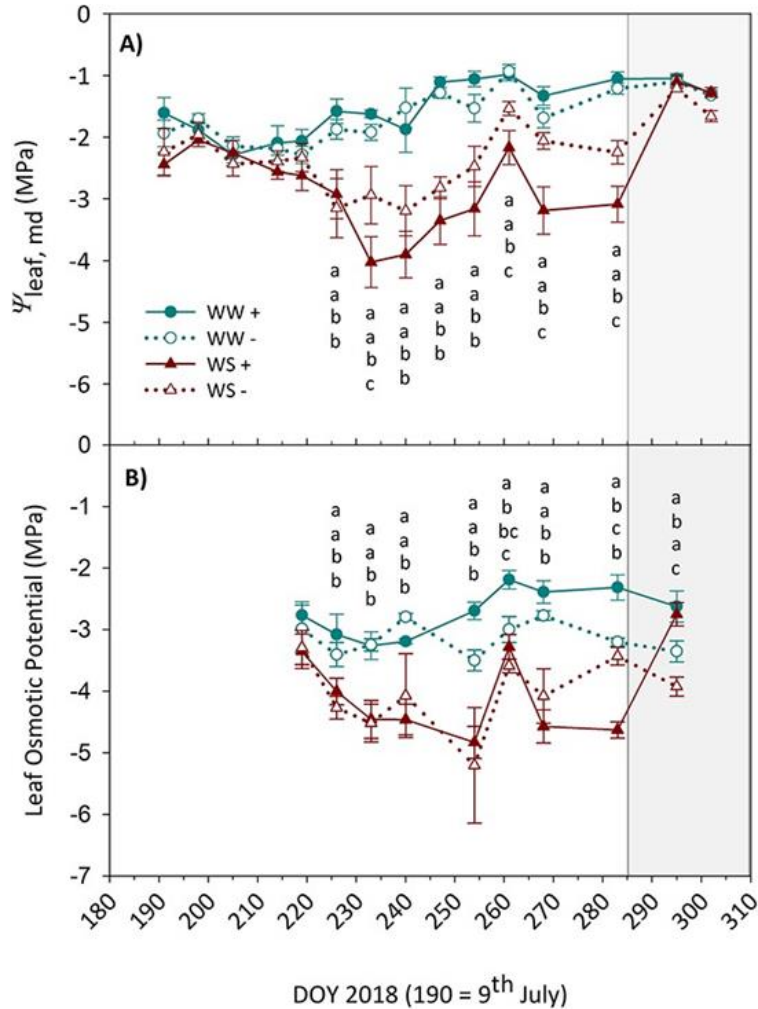
Fig. 3. Evolution from DOY 2018 190 to 310 (9 July–6 November 2018) of **(A)** leaf–water potential at midday ($\Psi_{leaf, md}$ (MPa)) and **(B)** leaf osmotic potential (Ψ_π (MPa)); in WW (blue) and WS (red) trees, with presence of fruits (+) and absence of fruits (−). Irrigation recovery started at DOY 285 (12 October) and it is represented by a gray area. Data are mean ± standard errors from two leaves per tree. Different letters indicate significant differences between irrigation treatments and fruit loads combined ($P \leq 0.05$) according to two-way ANOVA. The order of the letters follows the order of the treatments in the legend. Letters are not shown when no differences were found.

Effects of the presence of fruits on leaf gas exchange
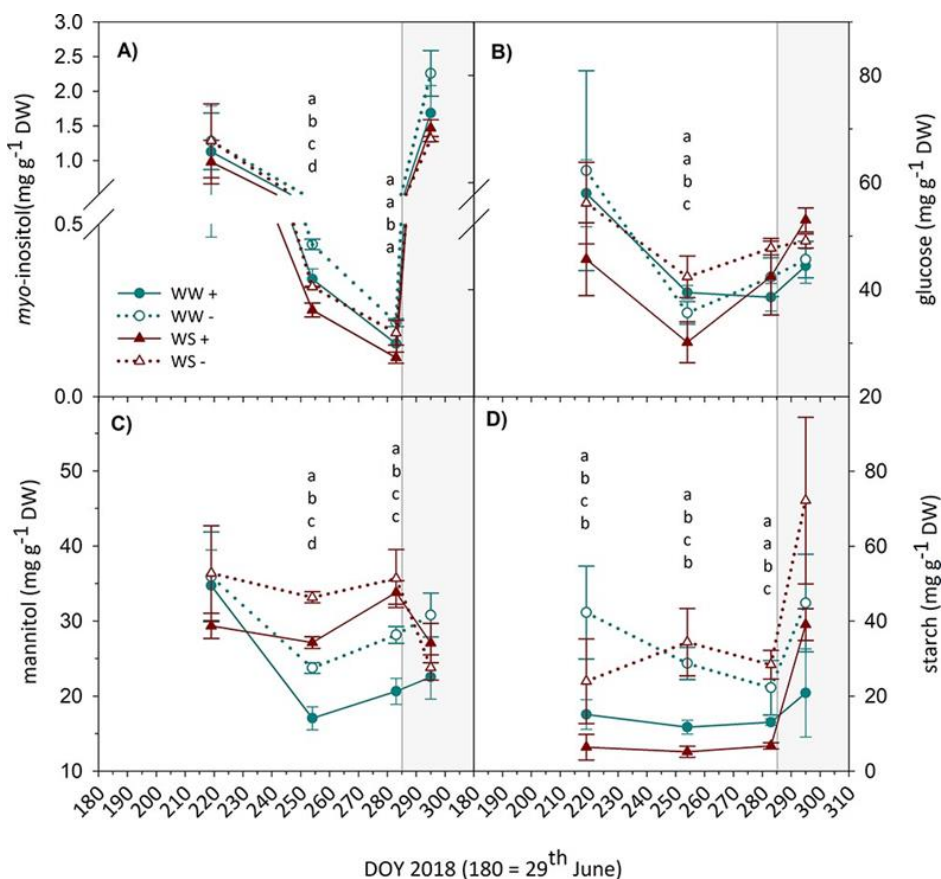
Fig. 4. Leaf soluble sugars (mg g^{-1} DW). (A) Myo-inositol, **(B)** glucose, **(C)** mannitol and **(D)** starch from DOY 2018, 219 to 295 (7 August to 22 October) in WW (blue) and WS (red) trees; and presence of fruits (+) and absence of fruits (−) trees. Irrigation recovery, which is represented by a gray area, started at DOY 285 (12 October). Data are mean ± standard errors from four leaves per tree. Different letters indicate significant differences between irrigation treatments and fruit loads combined (P ≤ 0.05) according to two-way ANOVA. The order of the letters follows the order of the treatments in the legend. Letters are not shown when no differences were found.

Our results show that mannitol was related to leaf Ψ_π (Fig. 5), especially at moderate values of Ψ_π (above −4 MPa). Lower Ψ_π values than −4 MPa did not correspond with higher concentrations of mannitol, suggesting that this sugar was not responsible for the lowest $\Psi\pi$ values measured. The contribution of mannitol to the osmotic potential estimated by Boyle−van't Hoff equation

114

showed that mannitol represented between 17 and 20% of the osmotic potential measured in the range of concentrations observed. A mannitol concentration of 20 mg g^{-1} DW represents −0.5 MPa, meanwhile a concentration of 35 mg g−1 DW represents −0.87 MPa.
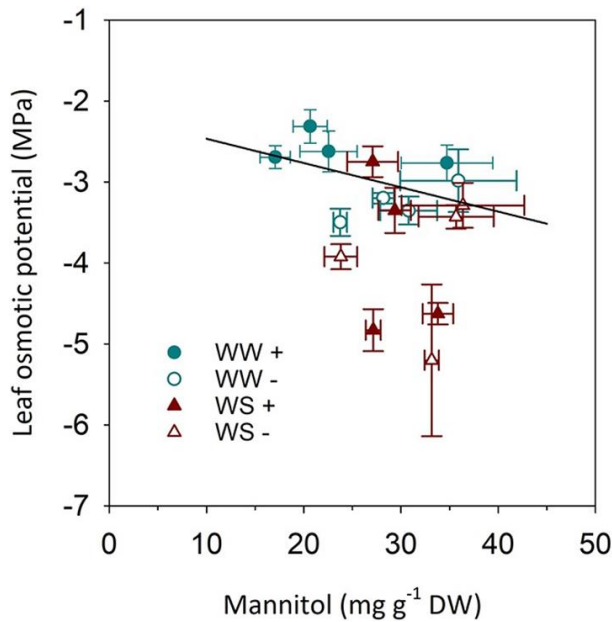
Fig. 5. Relationship between mannitol content (mg g^{-1} DW) and leaf osmotic potential (Ψ_π (MPa)) measured at midday in WW (blue) and WS (red) trees, presence of fruits (+) and absence of fruits (−). Data are mean ± standard errors from three trees per treatment. Every dot is one date from each treatment. Regression line is plotted using all values higher than −4 MPa ($R^2 = 0.25$ $P \leq 0.05$).

4.3.5. Dynamics of turgor estimated with turgor-related sensors

$P_{p, min}$ represents the maximum turgor that a leaf achieves in a day. Thus, in terms of turgor-related probes functioning, it means that the lower the value is, the higher the leaf turgor is (Fig. S1). In the studied period, fruitless trees, WW− (Fig. 6), showed a constant value of $P_{p, min}$, suggesting that no changes in maximum turgor occurred. However, a remarkable increase was

monitored in the WW+ trees, starting on DOY 254, indicating a reduction in the maximum turgor of the leaf. The same conclusion can be inferred independently from Fig. 3, where differences were found in Ψ_π with no changes in water potential. $P_{p,\,min}$ in WW+ was much higher than WW− during the period DOY 254–275. During those days, g_s (Fig. 2) and leaf Ψ_π (Fig. 3) were also significantly higher in WW+ than WW−.
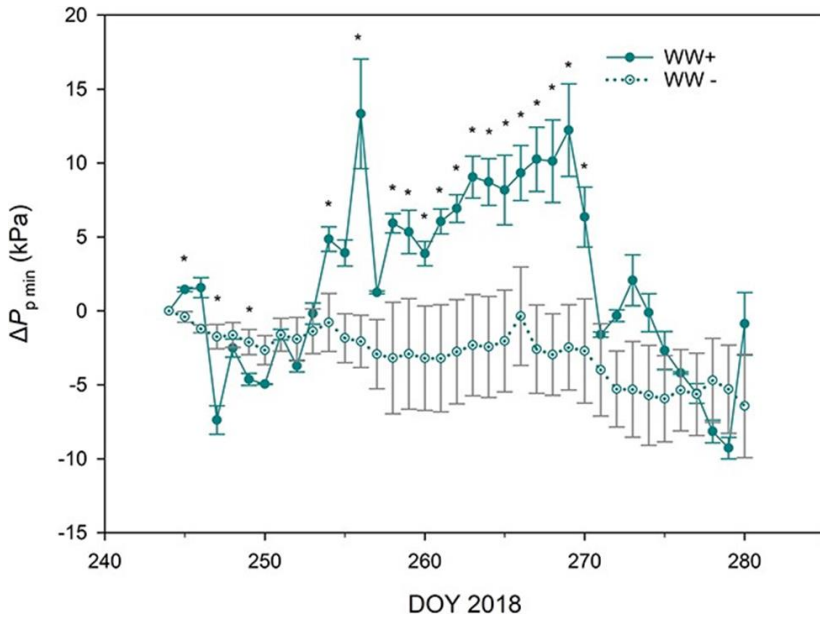
Fig. 6. Evolution of the maximum daily variation of leaf turgor ($\Delta P_{p,\,min}$ (kPa)) from DOY 2018, 244 to 280 (1 September–7 October) in WW (blue) trees with presence of fruits (+) and absence of fruits (−). Data are mean ± standard errors from three trees per treatment. Asterisks are shown when significant differences between irrigation treatments ($P \leq 0.05$) were found according to one-way ANOVA.

4.4. Discussion

According to our hypothesis, the decrease of g_s and A_N observed in WW− compared with WW+ (Fig.2) can be explained by sugar accumulation in the leaves (Fig. 4 and 5) as the dynamics of the studied variables were similar. When the export of sucrose is impaired due to the absence of fruits, sugars accumulate in the leaves of WW− trees because the photosynthesis produces more carbohydrates than demanded. This carbohydrates accumulation in WW− trees would have been produced by the accumulation of photosynthesis due to the lower demand of sugars in the tree generated by the absence of fruits. The absence of these major sinks (Hernandez-Santana et al., 2018; Ryan et al., 2018) impairs the sugars exportation by the phloem. The accumulated soluble sugars perform different functions such as the already mentioned inhibition of photosynthesis (Goldschmidt and Huber, 1992), the well-defined role in tree survival (Bustan et al., 2011; Tixier et al., 2018) and also a myriad of functions (metabolic, osmotic balance among different organs, etc.) that requires maintaining relatively high concentrations of soluble sugars at all times (Martínez-Vilalta et al., 2016). Some of these functions of great relevance to cope with water stress are osmoregulation (key to maintaining turgor) and maintenance of vascular integrity (xylem and phloem) (Sala et al., 2012). However, there are crucial aspects of these functions that are not yet fully understood (Adams et al., 2013; Hartmann and Trumbore, 2016; Martínez-Vilalta et al., 2016), and thus this work contributes to advance in the knowledge of the effect of temporal strong carbon sinks on the regulation of stomatal conductance and leaf turgor.

The acceptance of the hypothesis that sugars are the key regulating factor of the leaf gas exchange under these conditions of sink demand (i.e., fruit absence) means that non-stomatal limitations are the main constraints of photosynthesis under these circumstances (Dewar et al., 2022). In general, it is

difficult to distinguish whether leaf–water content or sugar concentration is triggering the regulation of photosynthesis since these two variables are intimately linked to each other (Hölttä et al., 2017). Sugar concentration can increase not only because sugars cannot be transported via phloem to other plant organs, but because lower water content increases sugar concentration in the liquid phase. However, a lower water content does not seem to be the cause in this study. Leaf osmotic potential was lower in WW− than in WW+, as there were differences in leaf gas exchange during that period. However, despite fruit removal decreasing g_s, and consequently transpiration, in WW− with respect to WW+, both treatments showed similar leaf–water potential. At the moderate water stress level measured in WW treatments in this study, it is known that olive leaves can maintain the relative water content constant along the season, even if there is osmotic adjustment (Diaz-Espejo et al., 2018). Thus, the water status of the plant does not seem to be playing a role in the downregulation of the leaf gas exchange, and thus the cause of this downregulation should be the lack of phloem transport of sugars.

Besides inhibiting photosynthesis and stomatal conductance, sugars accumulation drives changes in the leaf-water relations, which is reflected in the osmotic potential decrease (Fig. 3). Indeed, part of the soluble sugars measured in the leaves of this study corresponded to sugars that have been described to play an important role in osmotic adjustment in olive (Lo Bianco et al., 2013), such as mannitol (Flora and Madore, 1993; Tattini et al., 1996; Lo Bianco and Avellone, 2014; Lo Bianco and Scalisi, 2017). However, not all the changes in osmotic potential were produced by the observed increase in the concentration of mannitol, especially in WS trees (Fig. 5). In olive trees, it has been reported that, apart from soluble sugars, other organic compounds, such as proline, betaines or polyamines, are involved in the osmotic adjustment in response to abiotic stress (Gucci and Tattini, 1997). In our case, the strongest

correlation between leaf osmotic potential and mannitol occurred in the WW treatment, which corresponded to the highest values of osmotic potential. The concentrations of mannitol measured were calculated to contribute to around 20% to the osmotic potential, which aligns well with previous studies in olive trees (Dichio et al., 2009). The trend was similar for the high osmotic potential values of WS. However, at lower osmotic potential induced by more severe water stress, there was no correlation between leaf osmotic potential and mannitol. This lack of correlation could be explained by a greater contribution of other osmolytes as the ones already mentioned, present only under severe water stress conditions. Accordingly, for sugar accumulation trends (Fig. 4), we found greater starch concentrations in WW− than WW+. Different studies (Akinci and Losel, 2010; Thalmann and Santelia, 2017) suggest that starch is accumulated during the day, it is hydrolysed later on into organic acids and soluble sugars, which are transported during the night to guarantee carbon in the sink organs. Thus, starch can be a precursor of soluble sugars involved in osmotic and stomatal adjustment processes during abiotic stresses (Krasensky and Jonak, 2012; Horrer et al., 2016). These processes would explain the lower amount of starch in trees with fruits compared with trees without fruits, regardless of the treatment.

Contrary to what happens in WW, the sugar differences between WS− and WS+ trees resulted in no differences in the leaf gas exchange variables (Fig. 2) or osmotic potential (Fig. 3B). Under the severe water stress imposed, stomatal conductance and photosynthesis were at minimum values in both treatments, and thus the stomatal closure to prevent xylem disruption (Scoffoni et al., 2017) may have prevented the effect of stress caused by the presence of fruit from being observed, since it is probably of lesser magnitude than that caused by soil water deficit.

However, the presence of fruits in this water-limited treatment imposed an extra negative impact on the plant water status, as suggests the lower leaf–water potential. The lower $\Psi_{leaf,\,md}$ in WS+ than in WS− trees (Fig. 3) would have been likely produced by a preferential water movement towards the fruits due to their lower water potential than in the leaves, as observed in Fernandes et al. (2018). As a result, the leaf–water potential would have decreased more steeply in WS+ than in WS−.

Moreover, the leaves accumulated more soluble sugars and starch in WS− trees than WS+ trees (Fig. 4), similar to WW. In the case of mannitol, the concentration was overall higher in WS than in WW. According to Gersony et al. (2020), a lower xylem than phloem water potential would have occurred in WS compared with WW trees, which could have prevented the sugars exportation to sink organs of the plant to a greater extent than in WW. This difficulty in exporting sugars to fruits or other sink organs' could have contributed to the mannitol accumulation in the leaf. According to Gersony et al. (2020), this carbohydrate mobilization should happen during the night in water-stressed trees because large diurnal depressions in water potential may impede carbon export from leaves to other plant organs, such as fruits. As the xylem is the source of water for the phloem, when lower (more negative) potentials are recorded in the xylem, higher osmotic concentrations would be needed in the phloem to extract water from the xylem. Since xylem potentials partially recover at night, as seen in olive, movement of water from xylem to phloem would be more feasible at this time (Diaz-Espejo and Hernandez-Santana, 2017). Testing this hypothesis of sugar transportation at night is beyond the objective of our work.

Finally, the effect of the presence of fruits on leaf turgor of WW trees was monitored with leaf turgor sensors. Our explanation for the significant difference between WW− and WW+ in $\Delta P_{p,\,min}$ is that the higher osmotic

potential in WW+ compared with WW− together with the lack of differences in leaf–water potential between WW+ and WW− trees, lead to a lower turgor pressure in WW+ than in WW−. The major increase in $P_{p,min}$, which is the maximum turgor of the leaf in a day, occurred in the same period when most of the changes in osmotic and leaf gas exchange happened. There is sufficient theoretical background to associate it as cause–effect because active growing fruits use sugars to increase their osmotic potential as a mean of attracting water (Kramer and Boyer, 1995; Matthews and Shackel, 2005). The independent measurement of turgor with the leaf turgor sensors confirms the expected consequences of sugar dynamics in the leaves due to the fruit presence. However, the highest increment of $P_{p,min}$ in WW+ cannot be explained by an intense dry matter accumulation in the fruit in this period (Fig. 1). The higher demand for sugars from fruits to leaves corresponded to an increase of fruit oil synthesis (Fig. 1). This might have significant implications on the management of deficit irrigation strategies because with this method we could identify critical periods in terms of physiological processes related to the phenology of the crop in addition to the water stress produced by soil or atmosphere water deficit. Furthermore, our results reinforce the use of the leaf turgor sensors in physiological studies, providing more information than simply their use as indicator of water stress, and open new possibilities in ecophysiological studies. If according to the published works the leaf turgor sensors are a good proxy of actual turgor pressure (Zimmermann et al., 2008; Westhoff et al., 2009; Rüger et al., 2010a; Rüger et al., 2010b; Zimmermann et al., 2010; Ehrenberger et al., 2012), they can be used to derive the dynamics of parameters determining leaf–water relations, like the osmotic potential at full turgor (which corresponds to an increase in $P_{p,\ min}$). In our study, we hypothesized that the effect of sugar export from leaves to fruits would increase the leaf osmotic potential at full turgor, as we have demonstrated. The

change of the osmotic potential at full turgor has profound ecophysiological implications since it also involves the change in the turgor loss point (Bartlett et al., 2012), which deserves further verification in more species. In agronomy, regulated deficit irrigation strategies are designed considering the phenological stages when the crop is more sensitive to water stress or when a process needs to be promoted and facilitated (Fernández et al., 2013). Our results facilitate the identification of these sensitive periods, i.e., when fruits demand more sugars, using sensors which work in a continuous and automatic manner. Thus, the changes in the leaf–water relations are of such magnitude that they can be monitored and potentially used to manage a deficit irrigation strategy.

4.5. Conclusions

In this work, we have shown that fruits behave as strong water and carbon sink organs, and therefore their presence or absence is reflected at the leaf level in both leaf gas exchange regulation and water status. We conclude that under no water stress conditions, the impact of fruit absence on leaf–water relations is mainly explained by leaf sugar accumulation, which downregulates A_N and g_s compared with trees with high fruit loads. Sugars accumulation decreases the leaf osmotic potential but not the water potential and, therefore leaf turgor pressure is also affected. Interestingly, the water stress produced by the strong demand for carbon and water of a high fruit load can be tracked with the leaf turgor pressure sensors. In the future, this knowledge should be tested in trees with different fruit loads, and the use of turgor sensors could improve the application of irrigation strategies in some stages of the phenological cycle of the crop based on the sugar demand by fruits.

4.6. Supplementary material
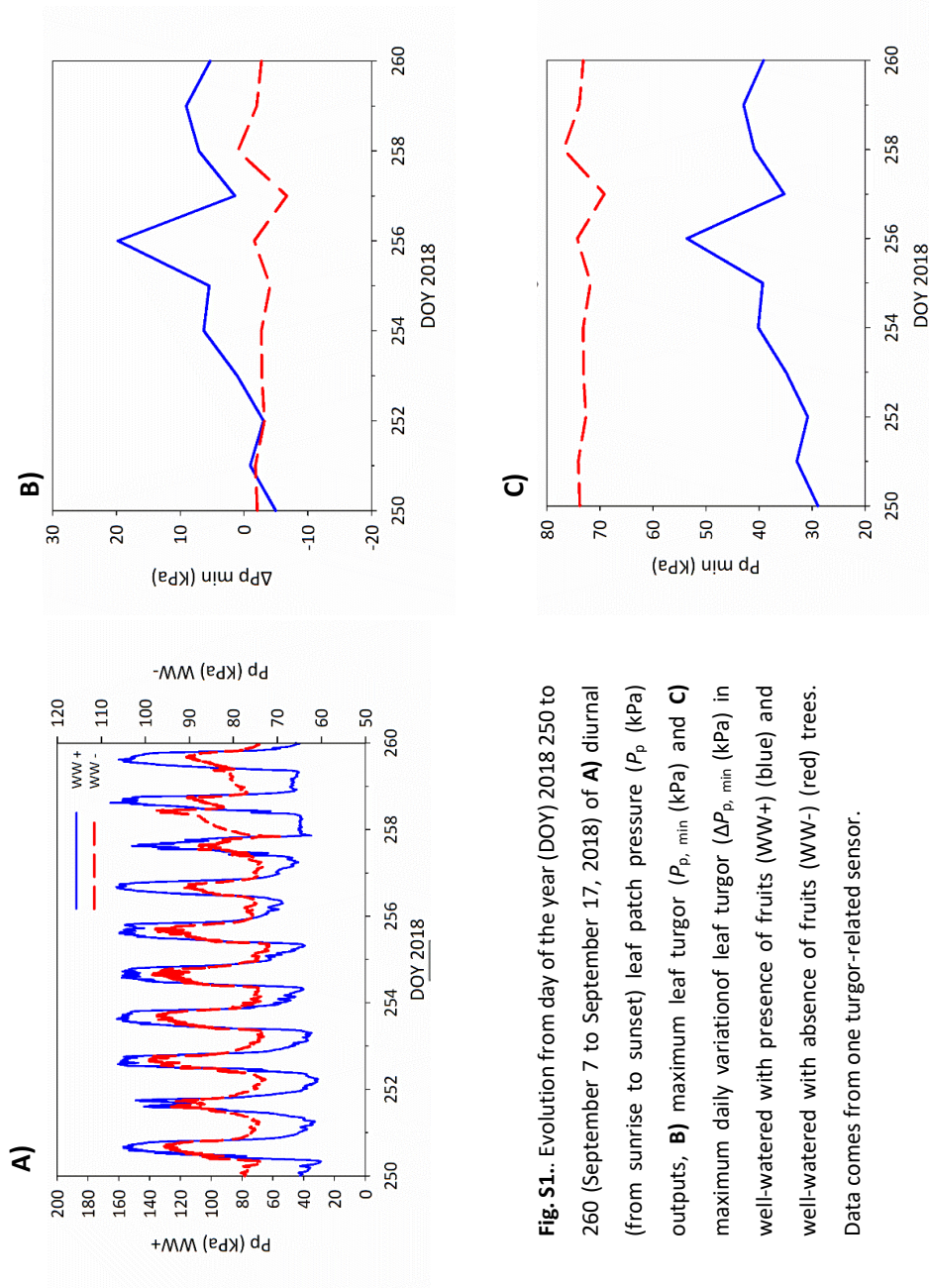
Fig. S1.. Evolution from day of the year (DOY) 2018 250 to 260 (September 7 to September 17, 2018) of **A)** diurnal (from sunrise to sunset) leaf patch pressure (P_p (kPa) outputs, **B)** maximum leaf turgor ($P_{p, min}$ (kPa)) and **C)** maximum daily variation of leaf turgor ($\Delta P_{p, min}$ (kPa)) in well-watered with presence of fruits (WW+) (blue) and well-watered with absence of fruits (WW–) (red) trees. Data comes from one turgor-related sensor.

CHAPTER 5:

CARBON SUPPLY AND WATER STATUS REGULATE FATTY ACID AND TRIACYLGLYCEROL BIOSYNTHESIS AT TRANSCRIPTIONAL LEVEL IN THE OLIVE MESOCARP
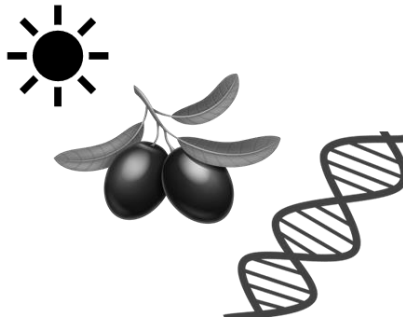
Published as:

Abstract

The relative contribution of carbon sources generated from leaves and fruits photosynthesis for triacylglycerol biosynthesis in the olive mesocarp and their interaction with water stress, was investigated. With this aim, altered carbon source treatments were combined with different irrigation conditions. A higher decrease in mesocarp oil content was observed in fruits under girdled and defoliated shoot treatment compared to darkened fruit conditions, indicating that both leaf and fruit photosynthesis participate on carbon supply for oil biosynthesis being leaves the main source. The carbon supply and water status, affected oil synthesis in the mesocarp, regulating the expression of *DGAT* and *PDAT* genes and implicating *DGAT1-1*, *DGAT2*, *PDAT1-1*, and *PDAT1-2* as the principal genes responsible for triacylglycerol biosynthesis. A major role was indicated for *DGAT2* and *PDAT1-2* in well-watered conditions. Moreover, polyunsaturated fatty acid content together with *FAD2-1*, *FAD2-2* and *FAD7-1* expression levels were augmented in response to modified carbon supply in the olive mesocarp. Furthermore, water stress caused an increase in *DGAT1-1*, *DGAT1-2*, *PDAT1-1*, and *FAD2-5* gene transcript levels. Overall, these data indicate that oil content and fatty acid composition in olive fruit mesocarp are regulated by carbon supply and water status, affecting the transcription of key genes in both metabolic pathways.

5.1. Introduction

Olive oil is a major edible oil mainly composed (95-98%) of triacylglycerols (TAG), which consist of a glycerol backbone esterified by three fatty acids. Its exceptional nutritional, organoleptic, and technological properties are due to its well-balanced fatty acid composition, as well as the presence of minor components, such as antioxidants and vitamins (Aparicio and Harwood, 2013). According to the European Commission Regulation (2003), oleic acid is the major fatty acid in olive oil (55–83%), while linoleic acid accounts for 4–21% and linolenic acid for less than 1%. In contrast, although the cultivar is the main determinant of olive oil fatty acid composition, environmental factors and culture conditions have also been linked to variations in the fatty acid profile (Beltrán et al., 2004). Many studies have evaluated the effect of different water regimes on olive oil yield and composition (Fernández, 2014; Gonçalves et al., 2020; Sánchez-Rodríguez et al., 2020), demonstrating that even if water stress decreases fruit yield (Moriana et al., 2003; Greven et al., 2009), fruit volume (Gómez-del-Campo et al., 2014), fresh weight, cell size (Rapoport et al., 2004), and the mesocarp/endocarp ratio (Gucci et al., 2009), olive oil content in the mesocarp is not affected (Costagli et al., 2003); however, the fatty acid composition can be slightly changed (Tovar et al., 2002; Gómez-Rico et al., 2007; Ahumada-Orellana et al., 2018; Hernández et al., 2018). In the processes of fruit growth and oil synthesis, photosynthesis and its limitation by water deficit play a key role since it is the main supplier of reduced carbon (Lawlor and Cornic, 2002).

The olive fruit is a drupe consisting of an exocarp, a mesocarp, and a woody endocarp, which consists of a woody shell enclosing one or, rarely, two seeds (Sanchez, 1994). Total fruit weight comprises 70-90% mesocarp, 9-27% endocarp, and 2-3% seed. Accumulation of oil in the fruit begins in the

mesocarp and the seed after the lignification of the endocarp, when both tissues are properly differentiated (Sanchez, 1994). At the usual harvest time for oil production, the mesocarp contains about 30% oil, while the seed has 27%, and no oil is deposited in the endocarp (Connor and Fereres, 2005). Because the mesocarp weight is very much higher than the seed weight, much more of a fruit's oil is in the mesocarp than in the seed. In fact, the fatty acid composition of the olive oil is similar to that of the mesocarp, but different from that of the seed (Hernández et al., 2016).

The ultimate precursor of carbon for TAG synthesis is CO_2, which is fixed during photosynthesis (Sanchez, 1994; Sánchez and Harwood, 2002). Notably, the olive mesocarp possesses the remarkable characteristic of having a high TAG content together with active chloroplasts, which enables it to fix CO_2 under photosynthetic conditions (Sanchez, 1994). Therefore, unlike oilseeds, there are two sources of carbohydrates for fruit growth and lipid biosynthesis in the olive mesocarp: (i) sugars imported from the phloem, coming in turn from the leaves, and (ii) sugars formed by photosynthesis in the fruit (Sánchez and Harwood, 2002). In both cases, sugars are catabolised in the fruit mesocarp via glycolysis to form pyruvate, which is converted into acetyl-CoA, the precursor of *de novo* fatty acid biosynthesis. Because photosynthesis in fruit, measured by CO_2 exchange, rarely reaches the compensation point, it has been suggested that the organ contribution to the carbon economy is rather modest (Blanke and Lenz, 1989). More recently, pioneering studies using olive fruit from the cultivar 'Picual' with an altered carbon supply strongly suggest that fruit photosynthesis contributes significantly to oil biosynthesis (Sánchez, 1995; Sánchez and Harwood, 2002).

Fatty acid biosynthesis in higher plants begins in the plastids, with oleoyl-ACP being the main product of plastidial fatty acid biosynthesis (Harwood, 2005). The synthesised acyl-ACPs can either be utilised within the

plastid for glycerolipid assembly, for glycerolipid assembly and further desaturation, or cleaved by specific thioesterases to free fatty acids, activated to acyl-CoAs, and exported to the cytosol. In this way, they are available in the endoplasmic reticulum for incorporation into membrane glycerolipids and to allow *de novo* TAG formation *via* the Kennedy pathway, where diacylglycerol acyltransferase (DGAT) is the enzyme that catalyses the final acylation of diacylglycerol (DAG) to yield TAG. DGAT1 enzymes have been mainly related to the accumulation of TAG in oilseeds, while DGAT2 is responsible for the incorporation of unusual fatty acids into TAG (Bates, 2016). Additionally, an alternative acyl-CoA independent reaction catalysed by the phospholipid:diacylglycerol acyltransferase (PDAT) has been described for TAG synthesis (Dahlqvist et al., 2000), which transfers an acyl group from phosphatidylcholine (PC) to DAG, producing TAG. Moreover, oleic acid can be further desaturated to linoleic and linolenic acids by the activity of membrane-bound fatty acid desaturases (FAD). FAD2 and FAD3 are located in the endoplasmic reticulum, and FAD6 and FAD7/8 are in the chloroplast. These enzymes differ not only in their cellular localisations but also in their lipid substrates and electron donor systems (Shanklin and Cahoon, 1998).

In olive, two *DGAT* genes (*OeDGAT1-1* and *OeDGAT2*) have been isolated and characterised, showing overlapping but distinct expression patterns during olive mesocarp growth (Banilas et al., 2011). Recently, we have cloned and characterised three olive *PDAT* genes (*OePDAT1-1*, *OePDAT1-2*, and *OePDAT2*) and their contribution to oil synthesis in olive fruit has been investigated (Hernández et al., 2021a). Furthermore, we have also identified two new *DGAT1* genes (*OeDGAT1-2* and *OeDGAT1-3*) in the olive genome (Unver et al., 2017). Concerning FAD, five genes encoding microsomal oleate desaturases (*OeFAD2-1* to *OeFAD2-5*) have been reported (Hernández et al., 2005; Hernández et al., 2020), whereas only one *OeFAD6* gene has been

identified to date (Banilas et al., 2005; Hernández et al., 2011). It has been suggested that *OeFAD2-2* and *OeFAD2-5* are the main genes determining the linoleic acid content in the olive mesocarp and therefore in the virgin olive oil (Hernández et al., 2019; Hernández et al., 2020). Four members of the olive linoleate desaturase gene family have been isolated and characterised, two microsomal (*OeFAD3A*, Banilas et al., 2007; *OeFAD3B*, Hernández et al., 2016) and two plastidial (*OeFAD7-1,* Poghosyan et al., 1999; *OeFAD7-2,* Hernández et al., 2016), with *OeFAD7-1* and *OeFAD7-2* as the main genes that contribute to the linolenic acid present in the olive oil (Hernández et al., 2016).

Water availability represents one of the main limitations in agriculture; therefore, the application of deficit irrigation strategies, and consequently water stress, on olive crops is unavoidable. Empirical evidence suggests that oil synthesis is less sensitive to water stress than other growth processes in the plant (Iniesta et al., 2009), including fruit growth (Hernandez-Santana et al., 2018), although the physiological basis for this is poorly known, and a better understanding of the regulation of oil synthesis by the water supply is needed. To understand the molecular mechanisms that regulate oil biosynthesis in the photosynthetic olive mesocarp under different water conditions, the main objectives of this study were: (i) to evaluate the relative contribution of the different carbon sources, generated by leaf and fruit photosynthesis, for TAG biosynthesis in the olive mesocarp, and their interaction with water stress and (ii) to study the regulatory mechanisms involved in these metabolic processes. To achieve these objectives, different olive fruit carbon source treatments (control, darkened fruit, and girdling and defoliated shoot) were employed and combined with two irrigation conditions (well-watered and water-stressed) to assess their effects on the mesocarp oil content and fatty acid composition. In addition, the effect of these treatments on the expression levels of genes

encoding TAG synthesising enzymes (DGAT and PDAT) and membrane-bound fatty acid desaturases (FAD2 and FAD7) was investigated in this tissue.

5.2. Materials and methods

5.2.1. Experimental orchard and climate conditions

This study was conducted in a commercial super-high-density olive orchard (*Olea europaea* L. cv. Arbequina), located in Utrera (Seville, southwest Spain) (37° 15' N, -5° 48' W), during the 2018 irrigation season from July to October. 'Arbequina' olive trees were 12-years-old, planted in a 4 m × 1.5 m formation (1,667 trees ha $^{-1}$) and in rows oriented north-northeast to south-southwest. The soil in the orchard had a sandy top layer and a bottom clay layer (Arenic Albaquaf; USDA 2010, https://www.nrcs.usda.gov/Internet/FSE_DOCUMENTS/nrcs142p2_050915.pdf). Further details on the orchard characteristics can be found in Fernández et al. (2013).

The Mediterranean climate is dominant in the region with mild rainy winters and hot, dry summers. Most of the annual rainfall occurs from late September to May. In the area, average values of potential evapotranspiration (ET$_O$) and precipitation were 1482 and 500 mm, respectively, for the 2002–2018 period (data recorded at the Los Molares station, Regional Government of Andalusia, near the study area). For that period, the average maximum ($T_{a, max}$) and minimum ($T_{a, min}$) air temperatures were 24.8 and 10.6°C, respectively. The hottest months are July and August, whose $T_{a, max}$ values over 40°C are recorded nearly every year, with peak values rarely over 45°C. Vapour pressure deficit (VPD) values over 7 KPa are reached once per year between July and August.

5.2.2. Irrigation and altered carbon source treatments

Two irrigation treatments were applied: a well-watered (WW) treatment, whose trees were irrigated daily at full irrigation (FI) to replace irrigation needs (IN), and a water-stressed (WS) treatment, whose trees were under a regulated deficit irrigation (RDI) regime and received 45% of IN during a five-week period after pit hardening finished, following the strategy described by Fernández et al. (2013). Each irrigation treatment was carried out in three 12 m × 16 m plots in a randomised design (n=3). There were 24 trees per plot with the measurements made in 2 central trees to avoid border effects. Dripper lines were close to the trunk, and each one had five 2 L h^{-1} drippers separated by 0.5 m. IN was calculated daily based on a simplified version of the stomatal conductance model evaluated in the same olive orchard and described in greater detail in Fernandes et al. (2018) and Hernandez-Santana et al. (2021).

In addition to the irrigation treatment, an altered carbon source treatment with three levels was applied to the fruit of two central trees of each irrigation treatment (WW and WS), starting immediately after the lignification of the stone at 12 weeks after flowering (WAF). Four similar shoots of those trees were selected to establish three different altered carbon source treatments to determine the carbon source: a control fruit treatment (C), in which the shoot and fruit were not altered; a darkened fruit treatment (D), in which the fruit of the shoot were covered from sunlight with a black fabric to avoid photosynthesis in the fruit but allow ventilation, and thus, the carbon source was only that via phloem from other parts of the plant; and a girdled and defoliated shoot treatment (G), in which the leaves of the shoot were detached and the bark of the shoot was girdled to the phloem, so the fruit were deprived of the external supply of photosynthates for their growth. Fruit temperature was measured with wired thermocouples in fruits bagged and sun

exposed, and no significant differences were found between both conditions. In all treatments, selected shoots had the same number of fruits, and the trees had the same number of fruit bearing shoots.

5.2.3. Sample collection

The olive fruit were harvested at three different developmental stages: immediately after pit hardening (12 WAF) when oil accumulation began, fully green (20 WAF) when the rate of TAG synthesis and oil accumulation was at its maximum, and turning (24 WAF) when the fruit changed colour from green to purple. For each biological replicate, 2 g of olive mesocarp tissue was collected from at least ten different olives harvested from the two central trees contained in each of the three plots and three treatments. The skin of the olive fruit was peeled off, and the mesocarp samples were quickly frozen in liquid nitrogen and stored at -80°C.

5.2.4. Plant-based sensors

5.2.4.1. Fruit dendrometers (fruit DW)

For each of three plots of an irrigation treatment, the diameter of one fruit in two trees was measured by dendrometer, giving a total of six monitored fruit per irrigation treatment. The fruit dendrometers were adapted using a linear potentiometer (model MM(R)10-11) with an internal spring return (Megatron Elektronik GmbH & Co., Munich, Germany) coupled to a sensor holder. The sensors were connected to a data logger (CR1000, Campbell Scientific Ltd., Shepshed, UK), which saved data of fruit equatorial diameter every 5 minutes. In addition, the equatorial diameter and fruit dry weight (DW) of six olives were measured in each plot where the trees were monitored every 15 days from May to October. With those data, a correlation of both variables

was performed to obtain a non-linear regression ($y = ax^b$) for WW and WS treatments (R^2=0.91 and R^2=0.84, respectively). Then, both equations were used to simulate fruit DW continuously from fruit dendrometer measurements (Fig. S1).

5.2.4.2. Sap flow sensors (Accumulated A_N)

One central tree for each plot was monitored with sap flow sensors (Tranzflo NZ Ltd., Palmerston North, New Zealand) using the compensation heat pulse (CHP) method (Green et al., 2003) to derive sap flux density (J_s, mm h^{-1}) values. In both irrigation treatments, one extra tree was monitored in one plot. Measurements were made every 30 min for the whole study period and controlled by a CR1000 datalogger connected to an AM25T multiplexer (Campbell, Campbell Scientific Ltd., Shepshed, UK).

J_s was measured at a depth 5 mm below the cambium for continuous gas exchange measurements. The process to obtain g_s from J_s measurements in olive is described in Hernandez-Santana et al. (2016), and the A_N modelling was performed as in Hernandez-Santana et al. (2018). Briefly, a regression was established between gs measured in new, sun-exposed leaves and J_s measured in the trunk of the same tree, divided by VPD values calculated from the weather station at the orchard. The J_s /VPD vs g_s calibration equations were established using 10–23 data points from each instrumented tree. The stomatal conductance values used for the equations were obtained from measurements of g_s and A_N, which were conducted on four clear days from May to August, every 30–60 min from dawn to noon, in three sun-exposed current-year leaves per instrumented tree. The data from measuring maximum g_s and A_N in two leaves per tree, conducted every other week in every tree instrumented with sap flow probes, from mid-July to the beginning of October, at 8:00-9:00 GMT in the same plots were also used. For the gas exchange measurements, two portable photosynthesis systems (Li-Cor 6400-XT, LI-COR,

Inc., Lincoln, NE, USA), with a 2 cm × 3 cm standard chamber, at ambient light and CO_2 conditions were used. g_s was simulated every 30 min to model A_N using the model by Farquhar et al. (1980), using the simulated g_s as the input. Details on the modelling and measurements needed to apply the model in this olive orchard can be found in Hernandez-Santana et al. (2018). Accumulated A_N was calculated by summing the quantity of simulated A_N every 30 min until the moment the value was shown.

5.2.5. Oil content and fatty acid composition

Two different methodologies were used to determine the oil content of olive mesocarp tissue. With respect to the complete period of olive fruit development and ripening, six fruit per tree from the two irrigation treatments were harvested every two weeks. Lipids were extracted from the mesocarp tissue by the method of Hara and Radin, (1978). Mesocarp oil content (%) was determined by gravimetric quantification of total lipid weight after solvent evaporation in a centrifugal vacuum concentrator Basic Model *5301* (*Eppendorf*, Hamburg, Germany).

In the case of irrigation and altered carbon source treatments, olive mesocarp samples (1.5 g) corresponding to each biological replicate were lyophilised (VirTis BenchTop 2 K Freeze Dryer, SP Industries Inc.), and the dry weight (DW) was determined. The lyophilised samples were ground in a mortar, and three aliquots of 100 mg DW were sampled for fatty acid analysis. Lipids were extracted as described by Hara and Radin, (1978). Fatty acid methyl esters were produced by acid-catalysed transmethylation (Garcés and Mancha, 1993) (Garcés and Mancha, 1993) and analysed by gas-liquid chromatography (Román et al., 2015). Heptadecanoic acid was used as an internal standard to calculate the fatty acid content in the samples. The mesocarp oil content (% DW) was calculated as the sum of the different fatty acids in 100 mg DW. The

fatty acid composition was expressed in mol per cent of the different fatty acids. Both types of data are presented as the means ± standard error (SE) of three biological replicates, each having three technical replicates.

5.2.6. Total RNA extraction and cDNA synthesis

Total RNA isolation was performed using 100 mg FW of frozen olive mesocarp tissue and the Spectrum™ Plant Total RNA kit (Sigma-Aldrich). Contaminating DNA was removed from RNA samples using a TURBO DNA-free kit (Ambion, USA). RNA quality was verified using a QIAxcel Advanced System (Qiagen), scoring RNA integrity using indicators such as RIS (RNA Integrity Score), and values between 6.5 and 7 were obtained. cDNA synthesis was carried out with the SuperScript™ III First-Strand Synthesis System (Invitrogen, Carlsbad, CA) according to (Hernández et al., 2009).

5.2.7. Quantitative real-time PCR

Gene expression analysis was performed by quantitative real-time PCR (qRT-PCR) using a CFX Connect real-time PCR System and iTaq Universal SYBR Green Supermix (BioRad, California, USA), as previously described by Hernández et al. (2019). Primers for gene-specific amplification were designed using the Primer3 program (http://bioinfo.ut.ee/primer3/) and the Gene Runner program (Supplementary Table S1). The housekeeping olive ubiquitin2 gene (*OeUBQ2*, AF429430) was used as an endogenous reference for normalisation (Hernández et al., 2009). The relative expression level of each gene was calculated using the equation $2^{-\Delta Ct}$, where $\Delta Ct = (Ct_{GOI} - Ct_{UBQ2})$ (Livak and Schmittgen, 2001; Pfaffl, 2004). This method has the advantage of making comparisons at the level of gene expression across developmental stages, treatments, and genes. The data are presented as means ± SE of three biological replicates, each having two technical replicates per 96-well plate.

138

5.2.8. Statistical analyses

The average of accumulated A_N, fruit DW, oil content, and relative gene expression values for each plot was calculated. Data for accumulated A_N and fruit DW were analysed by one-way analysis of variance (ANOVA), and oil content and relative gene expression were analysed by two-way ANOVA with $p < 0.05$ as a significance level. Statistical analyses were carried out using SigmaPlot ® software (Systat Sotfware, San Jose, CA). In the graphs, the vertical bars represent the SE of the mean of the plot of each treatment.

5.3. Results

5.3.1. Effect of different altered carbon source and irrigation treatments on the oil content and fatty acid composition of the olive fruit mesocarp

The dynamics of accumulated A_N and fruit DW during the development and ripening of olive fruit (cv. Arbequina) followed similar trends (Fig. 1A, B), with lower values for both variables in the WS treatment than for WW. While the increment rate of accumulated A_N (0.29 mol m-2 day-1) and fruit DW (0.0018 g day-1) was constant in WW for most of the studied period, the rate decreased (0.19 mol m^{-2} day^{-1} and 0.0002 g day^{-1} for accumulated A_N and fruit DW, respectively) when deficit irrigation started (DOY 196) in the WS treatment. Increment rates recovered after resuming irrigation (DOY 243) to nearly as high as those for the WW treatment (Fig. 1A, B). A similar pattern was observed for oil accumulation rates in the olive fruit mesocarp (Fig. 1C). The mesocarp oil accumulation rate for WS treatment was lower during the deficit irrigation period than for WW treatment, but the rate increment was higher in WS than in WW during irrigation recovery (4.52% day^{-1} in WS compared to 3.69 % day^{-1}

in WW), yielding a similar oil content in the mesocarp for both treatments at harvest.
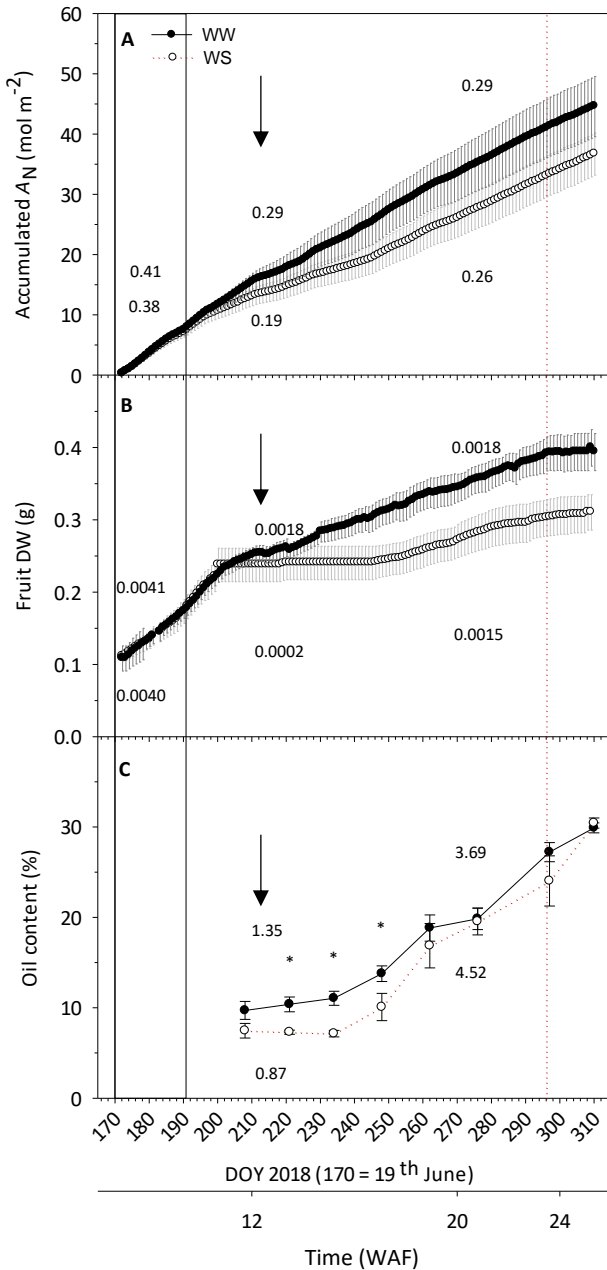
Fig. 1. Estimated daily accumulated photosynthesis (accumulated A_N) **(a)**, simulated daily fruit DW **(b)** and fruit oil content (% DW) in mesocarp tissue **(c)**. Numbers represent slope growth of the curve during different periods (accumulated A_N/day, fruit DW g/day and % oil content/day respectively). Well-watered trees (WW) and water-stressed trees (WS) are represented. Grey area is the deficit irrigation period (DOY 196–243), which occurred before the sampling dates 20 and 24 WAF. Vertical solid lines indicate the period of pit hardening (DOY 170–191), and vertical dotted line is the date where fruit ripening starts. The three times of sampling are indicated in WAF. Data are mean ± SE from three different plots. Asterisks means differences ($p \leq 0.05$) according to one-way ANOVA. The arrow indicates the beginning of the carbon source treatments.

140

When the different altered carbon source treatments were applied to olive fruit, a decrease in the oil content of the fruit mesocarp compared to C was observed, although at different extent (Fig. 2). In WW conditions, G fruit showed the highest reduction of mesocarp oil content at both times, whereas D fruit exhibited a diminution that was statistically significant at 20 WAF but not at 24 WAF. Regarding WS treatment, a stronger decrease for D fruit and milder reduction in G fruit for both 20 and 24 WAF was found compared to WW treatment. In contrast, the mesocarp oil content of C and G fruit was not significantly different between WW and WS treatments at 20 and 24 WAF (Fig. 2). D fruit in WS conditions exhibited a lower oil content in the mesocarp compared to WW treatment. Interestingly, D and G treatments accelerated fruit ripening, especially in the case of G fruit (Fig. S2). However, this effect was slowed under water stress.

Fig. 2. Oil content (% DW) in mesocarp tissue of olives (cv. Arbequina) grown under different altered carbon source conditions: control (C), darkened fruits (D) and girdled and defoliated shoots (G); and two different irrigation treatments: well-watered (WW) and water-stressed (WS). The deficit irrigation period occurred before the sampling dates 20 and 24 WAF. At the indicated times, mesocarp oil content was analysed as described in Matherial and methods. Data are mean ± SE from three biological replicates. Capital letters determine significant differences ($p \leq 0.05$) between both irrigation treatments within each fruit altered carbon source treatment and fruit development period according to two-way ANOVA. Lowercase letters determine significant differences ($p \leq 0.05$) between fruit treatments according to two-way ANOVA.
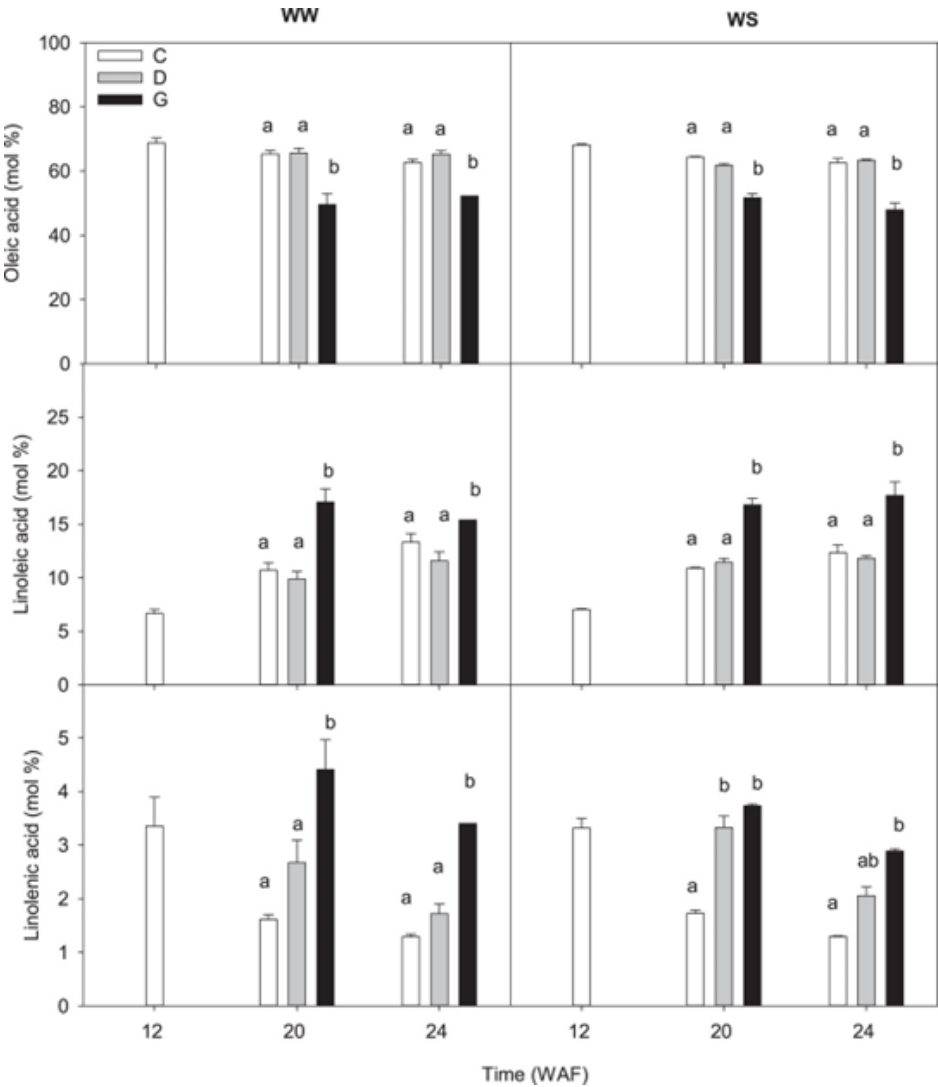
Fig. 3. Oleic, linoleic and linolenic acids percentage in the mesocarp tissue of olives (cv. Arbequina) grown under different altered carbon source conditions: control (C), darkened fruits (D) and girdled and defoliated shoots (G); and two different irrigation treatments: well-watered (WW) and water-stressed (WS). The deficit irrigation period occurred before the sampling dates 20 and 24 WAF. At the indicated times, fatty acid composition was analysed as described in Materials and methods. Data are mean ± SE from three biological replicates. Letters determine significant differences ($p \leq 0.05$) between fruit altered carbon sources according to two-way ANOVA.

Furthermore, different altered carbon source conditions and levels of water stress were studied to determine their effect on the unsaturated fatty acid composition of the olive fruit mesocarp (Fig. 3). The altered carbon source treatment substantially affected the fatty acid profile. In WW at 20 WAF, a significant reduction of oleic acid together with an increase in the linoleic and linolenic acid content was detected in the mesocarp of G fruit relative to C and D fruit. Similarly, this occurred in the WS treatment at 20 WAF, except for the linolenic acid content. In this case, its content was not only increased in G fruit mesocarp but also in the mesocarp of fruit from the D treatment. Overall, similar trends were observed at 24 WAF in the different altered carbon source and irrigation treatments, except for linolenic acid in the WS treatment, where the D and G treatments showed no significant differences. However, no differences were observed in the fatty acid composition of olive fruit mesocarp when comparing the two irrigation treatments.

5.3.2. Expression levels of genes encoding TAG synthesising enzymes in the olive fruit mesocarp under different altered carbon source and irrigation conditions

To examine the effect of the different altered carbon source and irrigation treatments on the expression of the genes involved in the last step of TAG synthesis, the transcript levels of *DGAT* and *PDAT* genes in the olive fruit mesocarp were determined by qRT-PCR. Since no significant differences were found in oil content and fatty acid composition between 20 and 24 WAF stages, we decided to analyse gene expression only at 20 WAF.

Fig. 4. Relative transcript abundance of olive DGAT genes in the mesocarp tissue of olives (cv. Arbequina) grown under different altered carbon source conditions: control (C), darkened fruits (D) and girdled and defoliated shoots (G); and two different irrigation treatments: well-watered (WW) and water-stressed (WS). The deficit irrigation period occurred before the sampling dates 20 and 24 WAF. At the indicated times, relative transcript abundance was determined by qRT-PCR as described in Materials and methods. Data are mean ± SE from three biological replicates. Capital letters determine significant differences ($p \leq 0.05$) between both irrigation treatments within each fruit carbon source according to two-way ANOVA. Lowercase letters determine significant differences ($p \leq 0.05$) between fruit altered carbon sources according to two-way ANOVA. Letters are not shown when significant differences were not found.

144

With respect to the different altered carbon source treatments and concerning the analysed *DGAT* genes (Fig. 4), only *DGAT2* transcript levels decreased significantly in the G treatment compared to C and D in WW conditions at 20 WAF. In the case of WS treatment, D fruit mesocarp showed a significant decrease of *DGAT1-1* expression levels compared to C, while G conditions produced a strong reduction in the mesocarp transcript levels not only for *DGAT1-1* but also for *DGAT2* compared to C. Interestingly, when comparing WS conditions with WW treatment, a significant increase in the expression levels of *DGAT1-1* and *DGAT1-2* genes was observed at 20 WAF in C fruit mesocarp, and the *DGAT1-2* gene also had significantly increased mesocarp transcript levels in the G treatment. Expression of the *DGAT1-3* gene was not detected in any condition.

In relation to *PDAT* genes (Fig. 5), only significant changes were detected in the transcript levels of the *PDAT1-1* gene. Regarding altered carbon source conditions, in the WS treatment, a strong decrease in its expression levels was observed in D and G fruit mesocarp with respect to C. When WW and WS conditions were compared, a strong increase in *PDAT1-1* transcript levels was detected in the mesocarp of C fruit. Expression of the *PDAT2* gene was not observed in any case.

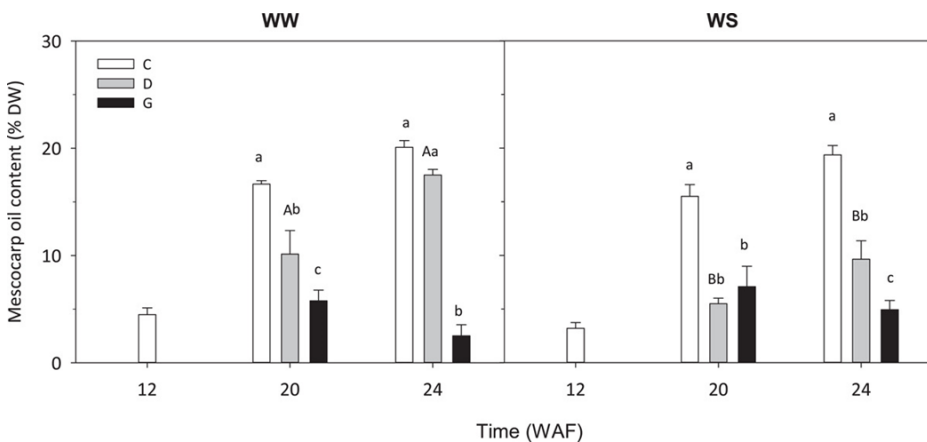**Fig. 5.** Relative transcript abundance of olive PDAT genes in the mesocarp tissue of olives (cv. Arbequina) grown under different altered carbon source conditions: control (C), darkened fruits (D) and girdled and defoliated shoots (G); and two different irrigation treatments: well-watered (WW) and water-stressed (WS). The deficit irrigation period occurred before the sampling dates 20 and 24 WAF. At the indicated times, relative transcript abundance was determined by qRT-PCR as described in Materials and methods. Data are mean ± SE from three biological replicates. Capital letters determine significant differences ($p \leq 0.05$) between both irrigation treatments within each fruit carbon source according to two-way ANOVA. Lowercase letters determine significant differences ($p \leq 0.05$) between fruit altered carbon sources according to two-way ANOVA. Letters are not shown when significant differences were not found.

5.3.3. Transcript levels of membrane-bound fatty acid desaturase genes in the olive fruit mesocarp under different altered carbon source and irrigation treatments

The effect of different altered carbon source and irrigation conditions on the expression levels of oleate and linoleate desaturase genes in the olive fruit mesocarp was also analysed. In particular, the transcript levels of *FAD2* and *FAD7* genes were determined, since they have been demonstrated as the main genes responsible for the linoleic and linolenic acid synthesis, respectively, in this tissue (Hernández et al., 2009; Hernández et al., 2016; Hernández et al., 2020; Hernández et al., 2021b).

In the case of *FAD2* genes (Fig. 6) and altered carbon source treatments, under the WW treatment, D and G fruit mesocarp showed a significant increase in *FAD2-2* gene expression levels compared to C, with that increase higher for G than for D fruit mesocarp. In WW conditions, the mesocarp of G fruit also showed a significant increment in *FAD2-1* transcript levels compared to that of C and D fruit. Concerning the WS regime, *FAD2-2* showed higher expression in G fruit mesocarp than in C and D, while *FAD2-5* exhibited a significant reduction of its expression levels in the mesocarp from D and G treatments compared to C. When comparing the same altered carbon source treatment but under WW or WS conditions, *FAD2-1* had increased transcript levels in D fruit mesocarp but decreased in G, D and G fruit mesocarp had decreased expression of *FAD2-2*, and C had increased expression of *FAD2-5* in the mesocarp. Expression of *FAD2-3* and *FAD2-4* genes was not detected in any condition.
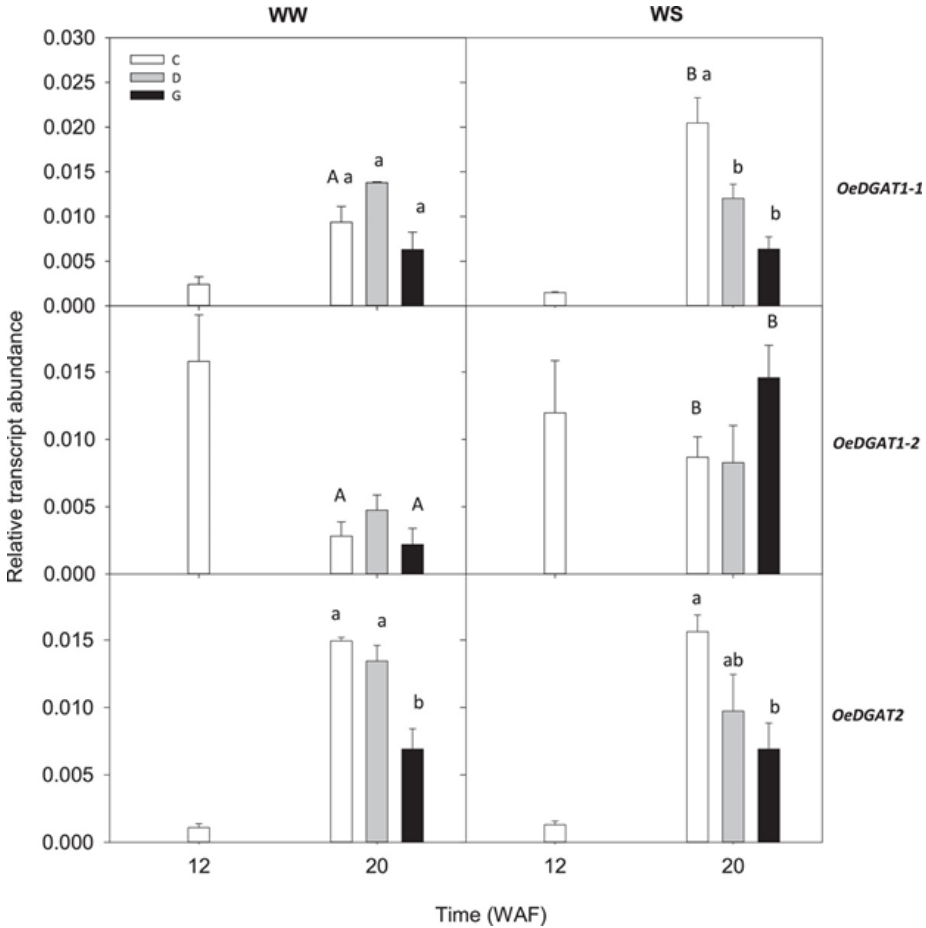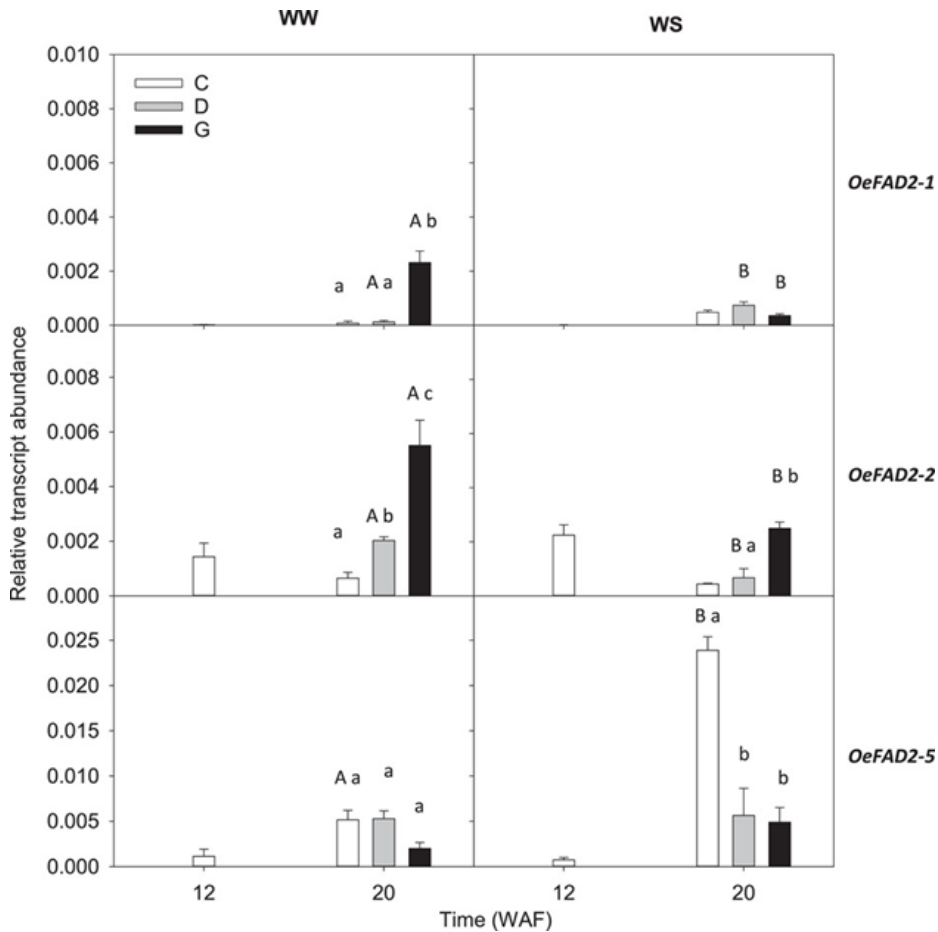
Fig. 6. Relative transcript abundance of olive FAD2 genes in the mesocarp tissue of olives (cv. Arbequina) grown under different altered carbon source conditions: control (C), darkened fruits (D) and girdled and defoliated shoots (G); and two different irrigation treatments: well-watered (WW) and water-stressed (WS). The deficit irrigation period occurred before the sampling dates 20 and 24 WAF. At the indicated times, relative transcript abundance was determined by qRT-PCR as described in Materials and methods. Data are mean ± SE from three biological replicates. Capital letters determine significant differences ($p \leq 0.05$) between both irrigation treatments within each fruit carbon source according to two-way ANOVA. Lowercase letters determine significant differences ($p \leq 0.05$) between fruit altered carbon sources according to two-way ANOVA. Letters are not shown when significant differences were not found.

Regarding *FAD7* genes (Fig. 7), no differences in their mesocarp transcript levels were found in fruit under WW or WS conditions at 20 WAF for any of the altered carbon source treatments. However, when the WS regime was compared to WW conditions, a significant increase in *FAD7-1* expression was observed in G fruit mesocarp.
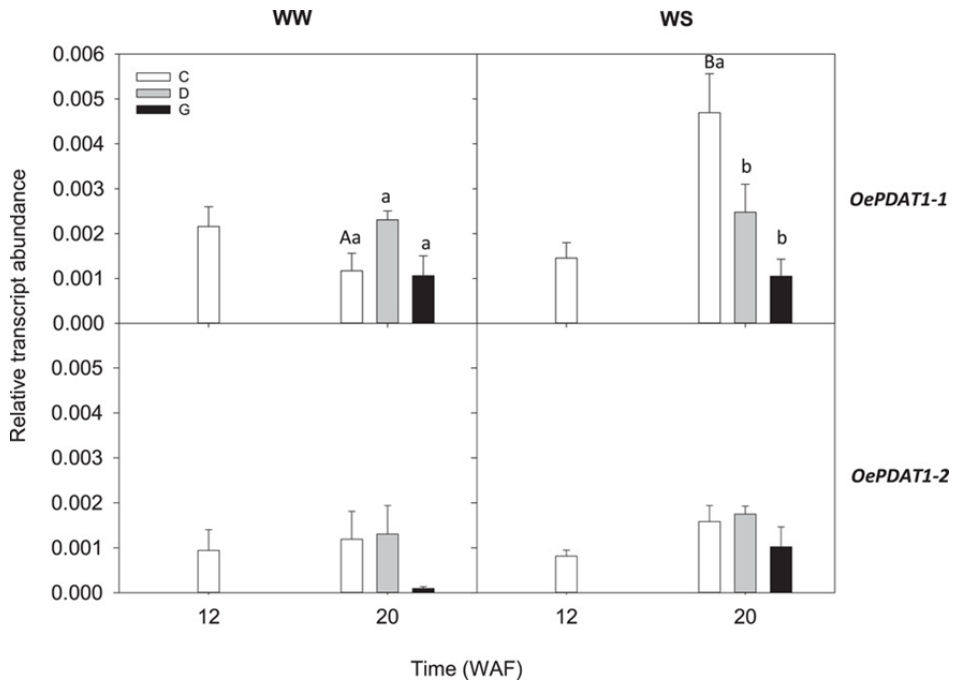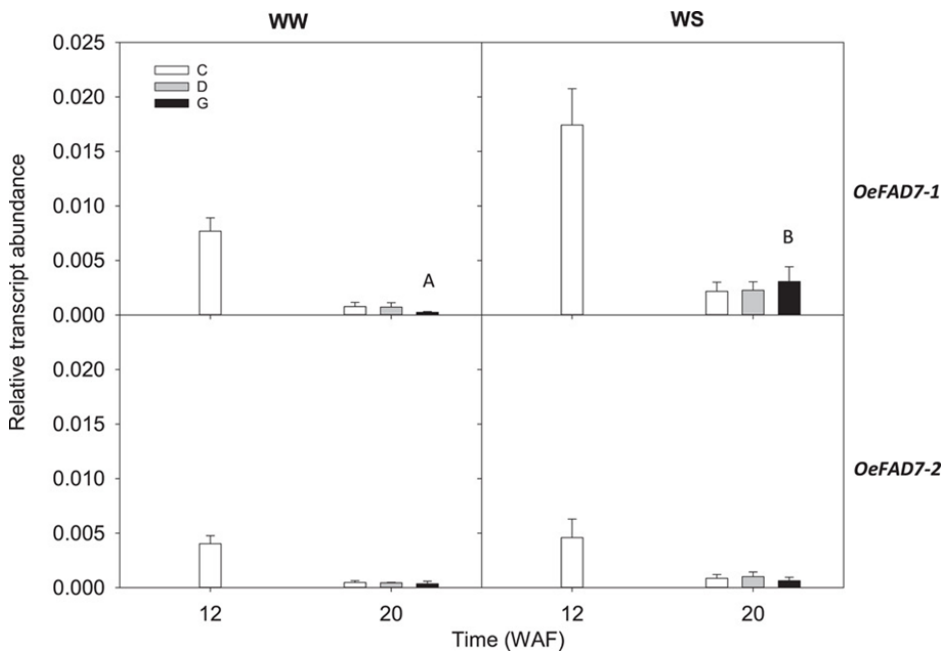

Fig. 7. Relative transcript abundance of olive FAD7 genes in the mesocarp tissue of olives (cv. Arbequina) grown under different altered carbon source conditions: control (C), darkened fruits (D) and girdled and defoliated shoots (G); and two different irrigation treatments: well-watered (WW) and water-stressed (WS). The deficit irrigation period occurred before the sampling dates 20 and 24 WAF. At the indicated times, relative transcript abundance was determined by qRT-PCR as described in Materials and methods. Data are mean ± SE from three biological replicates. Capital letters determine significant differences ($p \leq 0.05$) between both irrigation treatments within each fruit carbon source according to one-way ANOVA. Lowercase letters determine significant differences ($p \leq 0.05$) between fruit altered carbon sources according to two-way ANOVA. Letters are not shown when significant differences were not found.

5.4. Discussion

Our work provides novel insights into the regulation of TAG accumulation and fatty acid composition in response to carbon source availability and water stress in a photosynthetic oil fruit mesocarp. The two treatments (altered carbon source and irrigation) produced a range of carbon availability for the synthesis of TAG, which together with the regulation of key gene transcript levels allowed us to progress our understanding of olive oil synthesis and its response to water stress.

As a methodological consideration, we cannot discard that the removal of phloem in the girdled and defoliated shoot treatment affected other processes than just the transport of sugars to the fruit. Phloem has an important signalling role facilitating electrical signals (Sukhov et al., 2019), as well as the transport of some chemical molecules, including phytohormones (Jorgensen et al., 1998). However, most of the processes of fruit development are regulated and performed from the fruit itself (Giovannoni, 2004; Pesaresi et al., 2014).

5.4.1. Leaf and fruit photosynthesis participate in the carbon supply for oil biosynthesis in olive fruit mesocarp, with a major contribution of photoassimilates imported from the leaves

To examine the origin of the carbon source, generated from leaf and fruit photosynthesis, for TAG synthesis and oil content in the olive fruit mesocarp, different altered carbon sources conditions were applied. As shown in Fig. 2, a reduction in the oil content was found in the mesocarp of olive fruit from D and G altered carbon source treatments compared to the control. These results showed that not only the import of photoassimilates from leaves but also fruit photosynthesis contribute to oil biosynthesis in olive mesocarp, since oil accumulation was observed in both carbon source treatments. However,

150

although fruit photosynthesis is important, it is not an alternative to carbon import. In accordance with our results, transcriptomic studies performed in the avocado mesocarp showed high transcript levels for Rubisco and PEPc, suggesting a role for fruit photosynthesis in the carbon supply for oil biosynthesis in this oil fruit (Kilaru et al., 2015).

In addition, the higher decrease in the mesocarp oil content detected in G fruit related to D fruit in WW conditions indicated a major contribution of leaf photosynthesis with respect to fruit photosynthesis. This is true even in the case that the reduction observed in the mesocarp of D fruit could be partially due to the inactivation of acetyl-CoA carboxylase, which catalysed the first committed and the only light-regulated step of *de novo* fatty acid synthesis in plants (Ye et al., 2020). In contrast to our results, a similar contribution to oil synthesis was reported for heterotrophic and autotrophic olives from the 'Picual' cultivar (Sánchez, 1995; Sánchez and Harwood, 2002). This discrepancy could be explained because in those studies, the autotrophic treatment of defoliating leaves from the same branch as the fruit was not accompanied by phloem girdling. This is essential to prevent the import of photoassimilates from leaves from other branches of the olive tree, as it is shown in Fig. S2 where no significant differences in oil content were found between control and defoliated shoot treatment. In addition, the distinct magnitude of the decrease in oil content caused by the altered carbon source treatments could also be due to the use of a different cultivar. In this sense, it has been recently demonstrated that the effect of light availability on olive fruit development is cultivar-dependent (Reale et al., 2019).

In contrast, the WS treatment relative to the WW regime enhanced the reduction in oil content observed in the mesocarp of D olives, whereas in G olive mesocarp the detected decrease was attenuated (Fig. 2). These data show that water stress affects the carbon supply for oil synthesis in olive mesocarp

more severely in the case of the photoassimilates from leaves than in that involving fruit photosynthesis. This result can be explained by the lower water status of water stressed plants, which reduced their capacity to transport sugars via the phloem from leaves to fruit (Martre et al., 2011), illustrating the importance of imported carbon in the fruit for oil synthesis. Consistently, no differences existed in the mesocarp oil content between WW and WS in G fruit since they do not rely on the carbon imported from leaves. It is also remarkable how the sum of both D and G mesocarp oil content equals C in all situations (Fig. 2), confirming that the source of carbon for oil biosynthesis in the olive mesocarp was from both fruit and leaf photosynthesis.

5.4.2. The oil content of olive mesocarp is not affected by water stress without altered carbon source treatments

The imposed water stress without altered carbon source treatments reduced the carbon assimilation rate estimated at the leaf level (Fig. 1A) and decreased the fruit size (Fig. 1B), but the mesocarp oil content was not affected (Fig. 1C, 2). It is important to note that the water stress treatment was imposed for five weeks starting at 10 WAF. Afterwards, full irrigation was resumed some 2-3 weeks before the sampling at 20 WAF. One of the most intriguing aspects when applying regulated deficit irrigation strategies in olive is that a significant reduction of irrigation is not usually proportionally reflected in the reduction of oil yield (Iniesta et al., 2009; Hernandez-Santana et al., 2017; Hernandez-Santana et al., 2018). The tolerance of olive fruit to water stress has been explained by the lower sensitivity of oil synthesis processes to water deficit than other processes, such as vegetative growth (Hernandez-Santana et al., 2017). A complementary explanation for the maintenance of the mesocarp oil content in WS compared to WW is that oil synthesis could have used the spare

carbon that was not used for fruit growth. Growth and oil synthesis are the major carbon sinks of the fruit. However, the factor impairing fruit growth may have been the water status of the fruit (Dell'Amico et al., 2012; Girón et al., 2015; Fernandes et al., 2018), as an increasing number of works have demonstrated that the water status is more growth limiting than carbon availability (Fatichi et al., 2014; Körner, 2015; Steppe et al., 2015). The fruit growth inhibition produced by water factors, in turn, would have resulted in extra carbon available for other biosynthetic routes in the mesocarp, such as fatty acid biosynthesis and TAG accumulation.

5.4.3. Carbon supply and water status affect oil synthesis in the olive mesocarp, regulating DGAT and PDAT transcript levels

The specific contribution of DGAT and PDAT enzymes to the synthesis of TAG is a key point to elucidate the mechanisms that regulate oil accumulation in oil crops, and their specific involvement is dependent on the species (Chapman and Ohlrogge, 2012). In olive, since there are no mutants available, a different approach was employed by altering the carbon supply to the fruit, together with two different irrigation regimes, to examine if the detected changes in mesocarp oil content correlated with alterations in the transcript levels of the corresponding *DGAT* and *PDAT* genes in this tissue.

In WW plants, the decrease in the mesocarp oil content noted in G fruit (Fig. 2) was parallel to the reduction in the expression levels of *DGAT2* and *PDAT1-2* genes detected in this tissue (Fig. 4). In the case of WS olives, the diminution in oil content measured in D fruit mesocarp (Fig. 2) coincided with the observed decrease of the *DGAT1-1*, *DGAT2*, *PDAT1-1*, and *PDAT1-2* transcript levels in the mesocarp (Fig. 4, 5), while the reduction in oil content

noted in G fruit mesocarp correlated with the diminution of *DGAT1-1*, *DGAT2*, and *PDAT1-1* expression levels observed in this tissue.

These results implicate *DGAT1-1*, *DGAT2*, *PDAT1-1* and *PDAT1-2* as the genes that could be involved in TAG biosynthesis and oil accumulation in the olive mesocarp, with a major role for *DGAT2* and *PDAT1-2* in conditions of no water stress. The participation of *DGAT1-1* and *DGAT2* genes in the synthesis of TAG in this tissue has been previously reported for cultivar Koroneiki (Banilas et al., 2011). In addition, in the 'Picual' and 'Arbequina' mesocarp, it has been proposed that the incorporation of linoleic acid into TAG may occur preferentially via the Kennedy pathway, with a minor contribution of PDAT activity (Hernández et al., 2020). However, according to our data, not only *DGAT* but also *PDAT* genes could participate in oil synthesis and accumulation in the mesocarp of olive fruit in conditions of altered carbon supply and water stress, with DGAT and PDAT enzymes cooperating to guarantee the synthesis of TAG. In accordance with these results, the contribution of PDAT1-2 to the synthesis of TAG in olive fruit mesocarp has been recently described (Hernández et al., 2021a). In addition, previous studies indicated that PDAT may also contribute to TAG biosynthesis in olive callus culture (Hernández et al., 2008). In oilseeds, an overlapping role for *DGAT* and *PDAT* in oil accumulation has been proposed (Zhang et al., 2009). Remarkably, the *DGAT* and *PDAT* genes involved in this regulation of oil synthesis encode enzymes located at the final step of the TAG biosynthetic pathway without affecting membrane lipid biosynthesis. Furthermore, our results suggest that TAG synthesis is a priority for oil fruit mesocarp even under water stress conditions. Fruit play a role in disseminating the seeds to accumulate storage substances to attract animals and enhance the success of disseminating the matured seeds. Therefore, mesocarp oil accumulation rather than fruit size might be a better option for the plant.

154

Our data also indicate that both carbon supply and water status affect oil synthesis in the olive mesocarp, regulating the transcription of *DGAT* and *PDAT* genes. In this sense, the MYB96 transcription factor has been reported to activate *DGAT1* and *PDAT1* expression in Arabidopsis seeds (Lee et al., 2018). Interestingly, Arabidopsis MYB96 triggers not only drought-related traits, such as stomatal closure (Seo et al., 2009), but also regulates ABA-dependent TAG biosynthesis in vegetative tissues as carbon and energy storage, to further ensure plant growth and development under long-term drought stress conditions (Lee et al., 2019).

Conversely, the substantial increase detected for *DGAT1-1*, *DGAT1-2*, and *PDAT1-1* gene expression levels in C fruit mesocarp at 20 WAF under WS treatment compared to WW conditions (Fig. 4 and 5) indicates that these genes were transcriptionally upregulated by water stress. In opposition to the effect of water stress in C fruit mesocarp, no significant changes were found between WW and WS in the transcript level of *DGAT* and *PDAT* genes in D fruit mesocarp, and only one gene, *DGAT1-2*, was significantly upregulated in the mesocarp of G fruit. The upregulation of these genes seemed to be related to water stress and not to the imposition of altered carbon source conditions, as suggested by their expression under WW conditions. However, it is worth noting that both water stress and altered carbon source treatments have the reduction of available carbon in common.

5.4.4. Modifying the carbon supply alters FAD2 an FAD7 expression levels and unsaturated fatty acid composition in the olive mesocarp

The carbon availability not only affected the oil content of the mesocarp but also its fatty acid composition. The alterations observed in the

unsaturated fatty acid content were accompanied by changes in the transcript levels of the membrane-bound fatty acid desaturase genes responsible for their desaturation, indicating that the source of carbon supply for fatty acid biosynthesis regulates FADs at the transcriptional level in olive mesocarp.

In the case of WW fruit, the diminution in the oleic acid percentage and the increase in linoleic and linolenic acid seen in the mesocarp of G olives (Fig. 3) correlated with the observed augmentation in the mesocarp *FAD2-1* and *FAD2-2* transcript levels (Fig. 6). Regarding WS olives, the decrease in oleic acid together with the augmentation in linoleic and linolenic acid in G fruit mesocarp was parallel to the detected increase in the expression levels of *FAD2-2* and *FAD7-1* genes detected in this tissue (Fig. 3, 6, and 7).

Therefore, *FAD2-1*, *FAD2-2*, and *FAD7-1* were the fatty acid desaturase genes that could be responsible for the changes in the unsaturated fatty acid composition observed in response to the altered carbon supply in the olive mesocarp. The expression of these genes could be increased in response to the new carbon supply conditions to ensure the correct redistribution of available carbon. In oilseeds, two different transcription factors were reported to regulate the expression of *FAD2* genes, such as bHLH in sesame (Kim et al., 2007) and Dof11 in rapeseed (Sun et al., 2018). However, no similar information has been reported in oil fruit.

Additionally, in C fruit mesocarp at 20 WAF under WS conditions, a high increase of *FAD2-5* transcript levels was detected in comparison with the WW treatment (Fig. 6). In a previous study, a reduction in *FAD2-5* gene expression levels during olive mesocarp development was observed under water stress (30 RDI) (Hernández et al., 2020). Together, these results suggest that *FAD2-5* is the olive *FAD2* gene regulated by water supply. However, the dissimilar responses detected could be due to the different water treatments and the distinct climatic conditions in the years of the two studies. In addition, it has

been reported that drought stress increased *FAD2* expression in mandarin seedlings (Gimeno et al., 2009) and purslane leaves (D'Andrea et al., 2015), whereas osmotic stress enhanced the transcription of *FAD2* in lima bean leaves (Zhang et al., 2011) and Arabidopsis seedlings (Zhang et al., 2012). Furthermore, FAD7 has also been reported to be involved in drought resistance, since the antisense expression of an Arabidopsis *FAD7* gene in transgenic tobacco plants reduced drought tolerance (Im et al., 2002).

Although changes in the percentage of fatty acid composition in the olive fruit mesocarp were small, their role might be crucial for the plant since changes in the degree of fatty acid desaturation relate to the activation of intracellular signalling in response to abiotic stress. Polyunsaturated fatty acids, such as linoleic and linolenic acids, are precursors of oxylipins, including stress-related phytohormones, such as jasmonic acid (JA), which are involved in the mechanisms of the stress response (Wasternack and Feussner, 2018).

5.5. Conclusions

In the present study, a stronger reduction in the oil content of mesocarp tissue was detected in olive fruit under girdled and defoliated shoot treatment compared to darkened fruit conditions. This indicates that even though both leaf and fruit photosynthesis participate in the carbon supply for oil biosynthesis in olive fruit mesocarp, the major contribution of photoassimilates is imported from the leaves. Our results also demonstrated that carbon supply and water status affect oil synthesis and fatty acid composition in the olive mesocarp, regulating the transcript levels of *DGAT*, *PDAT*, and *FAD* genes. In particular, *DGAT1-1*, *DGAT2*, *PDAT1-1*, and *PDAT1-2* seemed to be the genes involved in TAG biosynthesis and oil accumulation in this tissue, with a major role for *DGAT2* and *PDAT1-2* in well-watered conditions. In addition, *FAD2-1*, *FAD2-2*, and *FAD7-1* transcript levels and

polyunsaturated fatty acid content increased in olive fruit mesocarp in response to the altered carbon supply. Moreover, *DGAT1-1*, *DGAT1-2*, *PDAT1-1*, and *FAD2-5* gene expression levels in olive mesocarp were transcriptionally upregulated by water stress. This study represents a significant advance in the understanding of the molecular mechanisms regulating TAG synthesis and composition in the olive mesocarp. In the future, this information will allow the development of molecular markers for the marker-assisted selection of new olive cultivars with increased oil content in olive fruit. Furthermore, these results provide for a better understanding of how olive mesocarp TAG content and composition are affected by water deficit, permitting us to choose a better irrigation strategy and to decide how much and when water stress can be imposed, which is critical to obtain olive oil with the highest yield and quality with minimum irrigation.

5.6. Supplemental material
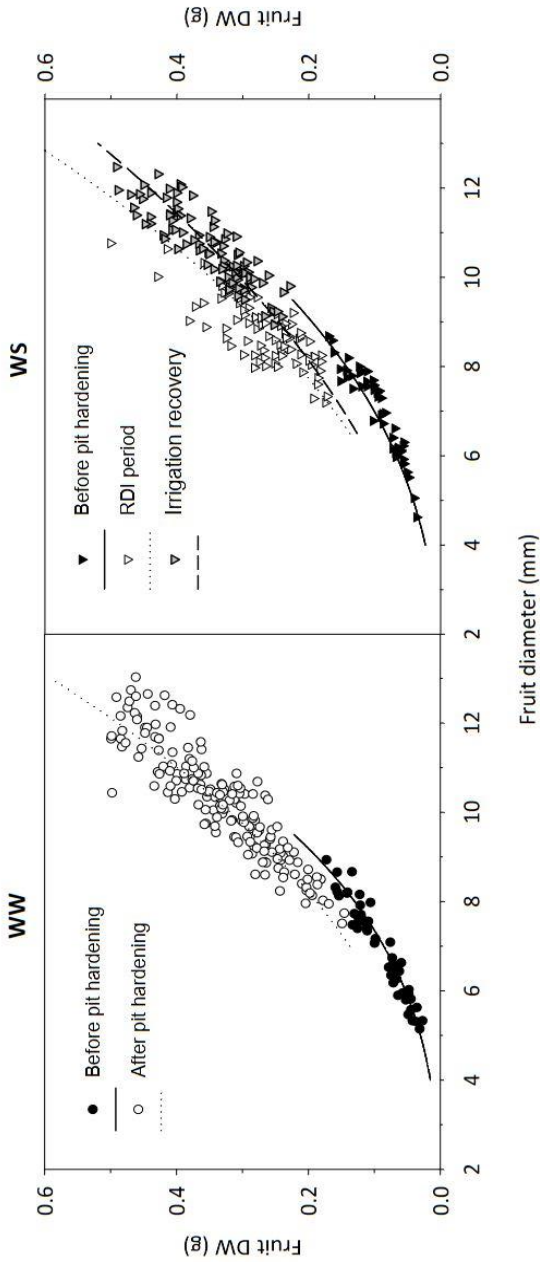
Fig. S1. Relationship between fruit diameter (mm) and fruit DW (g) measured every two weeks from May to November in well-watered (WW) and water stressed (WS) trees. Non-linear regression lines ($y = ax^b$) were fitted to each fruit stages. In WW trees, solid and dotted lines are the correlation before and after pit hardening (R^2=0.92 / R^2=0.87), respectively. In WS trees, solid, dotted and dashed lines are the correlation before pit hardening, during RDI period and irrigation recovery (R^2=0.9 / R^2=0.63 / R^2=0.77), respectively.
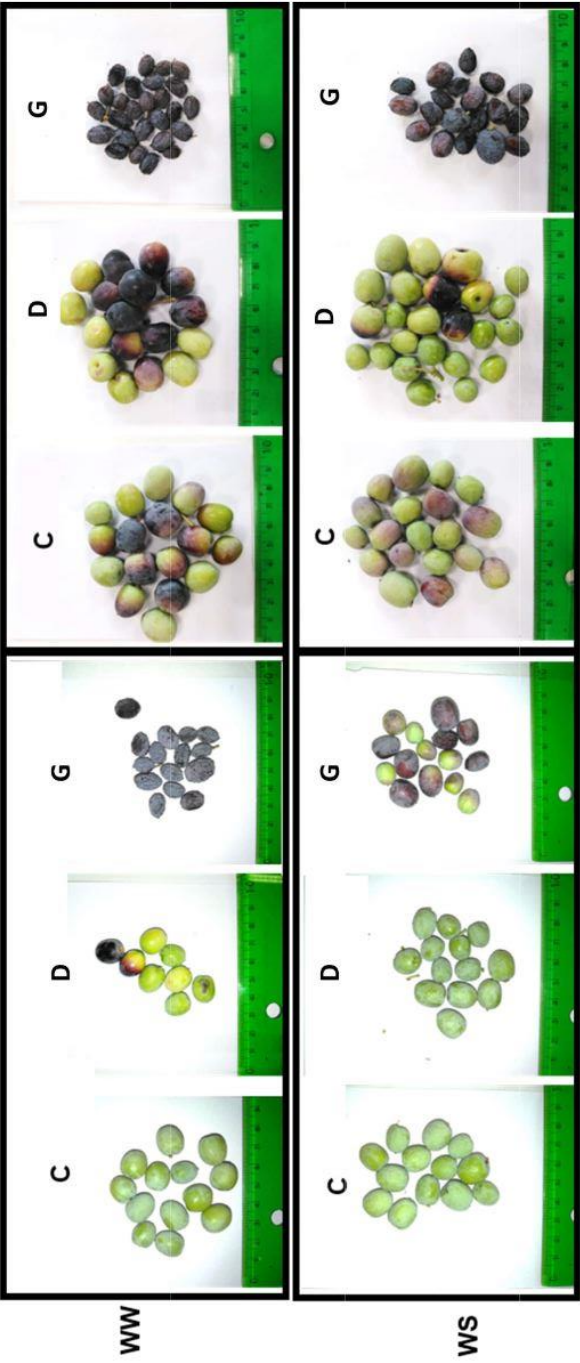
Fig. S2. Developmental and ripening changes of olives (cv. Arbequina) grown under different altered carbon source conditions: control (C), darkened fruits (D), and girdled and defoliated shoots (G); and two different irrigation treatments: well-watered (WW) and water-stressed (WS). Olives were harvested at the indicated times.
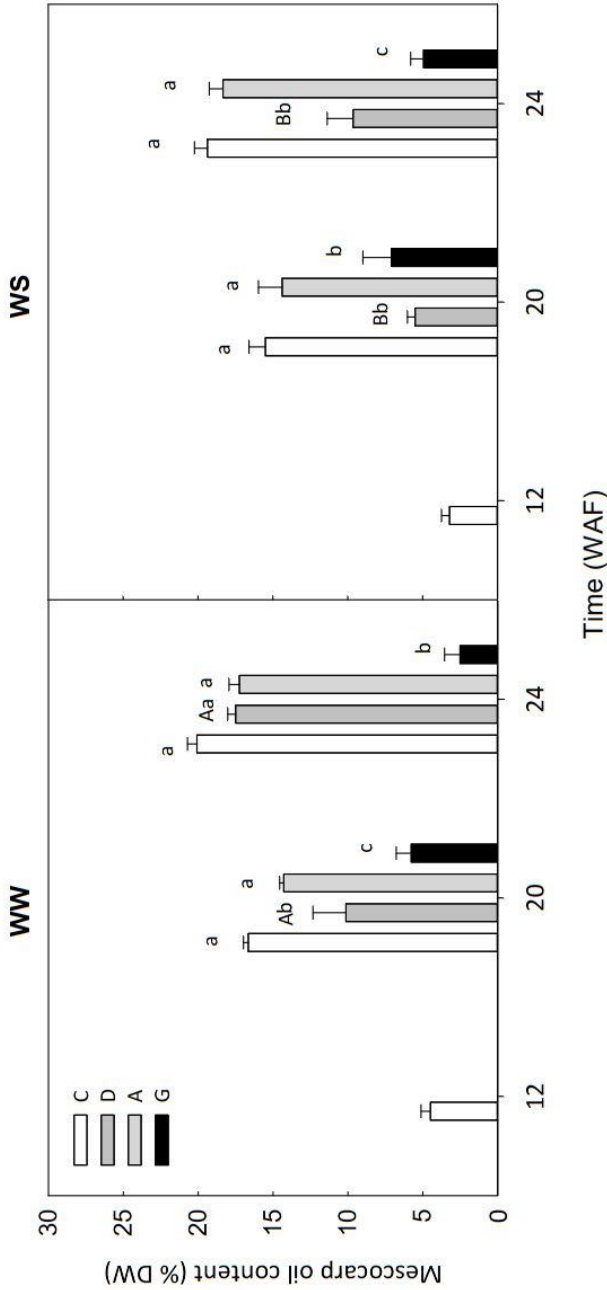
Fig. S3. Oil content (% DW) in mesocarp tissue of olives (cv. Arbequina) grown under different altered carbon source conditions: control (C), darkened fruits (D), autotrophic (A), and girdled and defoliated shoots (G); and two different irrigation treatments: well-watered (WW) and water-stressed (WS). The deficit irrigation period occurred prior to the sampling dates 20 and 24 WAF. At the indicated times, mesocarp oil content was analysed as described in Materials and Methods. Data are mean ± SE from three biological replicates. Capital letters determine significant differences (p ≤ 0.05) between both irrigation treatments within each fruit carbon source treatment and fruit development period according to two-way ANOVA. Lowercase letters determine significant differences (p ≤ 0.05) between fruit treatments according to two-way ANOVA

Table S1. Primer pair sequences and genes accession numbers used for qRT-PCR.

Gene	Accession no.	Sequence	Amplicon size (bp)	Reference
OeDGAT1-1	AAS01606	Forward: 5'-GTGATTCCATTGGGGGTACA-3' Reverse: 5'-TCGTTCCCTTCATGTCTCGT-3'	120	This work
OeDGAT1-2	XM_023007864	Forward: 5'-AATGGTGGGAAACATGGTGT-3' Reverse: 5'-ATTCGGATTGTTGGAGCTGT-3'	128	This work
OeDGAT1-3	XM_023026784	Forward: 5'-TGGAATGCGAAAACCGTTGAA-3' Reverse: 5'-AAATAGCACTTCCCCTCGGT-3'	121	This work
OeDGAT2	GU357635	Forward: 5'-CATGGGCAGTTTGTCGAAG-3' Reverse: 5'-TCACGGGGAATTTATTTTGG-3'	191	This work
OePDAT1-1	MZ614942	Forward: 5'-AATTGCTGCTGGGGCTAAG-3' Reverse: 5'-CCCGGCTCAAGTTATAGAGGT-3'	105	Hernández et al. (2021a)
OePDAT1-2	MZ614943	Forward: 5'-TCAAATGTCGGAAAGGATT-3' Reverse: 5'-TTTGGGGAATATGGTTGACAC-3'	143	Hernández et al. (2021a)
OePDAT2	MZ614944	Forward: 5'-CGAAGAAAGAGGCCAAGAAA-3' Reverse: 5'-GCATTCAAACATCCCCATTAG-3'	149	Hernández et al. (2021a)
OeFAD2-1	AY733076	Forward: 5'-AGTCACAGACGACACCATTCC-3' Reverse: 5'-CGTTCAAGGCCAAGTACAGAG-3'	175	Hernández et al. (2009)
OeFAD2-2	AY733077	Forward: 5'-CTTGTGGGCTTTACCGTCTC-3' Reverse: 5'-AGGGAGGGATGTGTATGCTG-3'	130	Hernández et al. (2009)
OeFAD2-3	MN103339	Forward: 5'-TCTTATGTTGTATGGAGTGAAG-3' Reverse: 5'-ACATTCCTCACAAGCACACC-3'	117	Hernández et al. (2020)
OeFAD2-4	MN103340	Forward: 5'-GGATGTGCCAAGGCTGTATC-3' Reverse: 5'-CACGAAAAGTATGGACCAAGG-3'	142	Hernández et al. (2020)
OeFAD2-5	MN103341	Forward: 5'-CCGAATGTCTGTCCCTTCC-3' Reverse: 5'-GCGGTATGGCTTTCTTGAGTT-3'	110	Hernández et al. (2020)
OeFAD7-1	DQ788674	Forward: 5'-TGGTACAGGGGAAAGGAATG-3' Reverse: 5'-GCTGCTTCGGTTGCTTCTAC-3'	164	Hernández et al. (2016)
OeFAD7-2	KP893695	Forward: 5'-GCAACAGAGGCAGCTAAACC-3' Reverse: 5'-GGTTGGGGTCAGTTTGGTAG-3'	163	Hernández et al. (2016)
OeUBQ2	AF429430	Forward: 5'-AATGAAGTCTGTCTCCTTTGG-3' Reverse: 5'-AAGGGAAATCCCATCAACG-3'	132	Hernández et al. (2009)
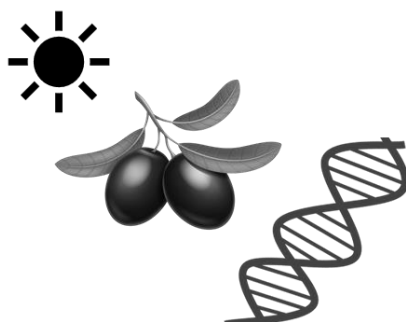
CHAPTER 6:

GENERAL DISCUSSION

The ultimate goal of this PhD Thesis is to understand the plant and fruit physiological mechanisms limiting fruit and oil yield in response to water deficit. This objective was assessed in olive trees at different scales (tree, fruit, leave) using a multidisciplinary approach (agronomy, ecophysiology and molecular biology (Fig. 1). In this last Chapter we discuss the results of the different chapters all together and their main implications.
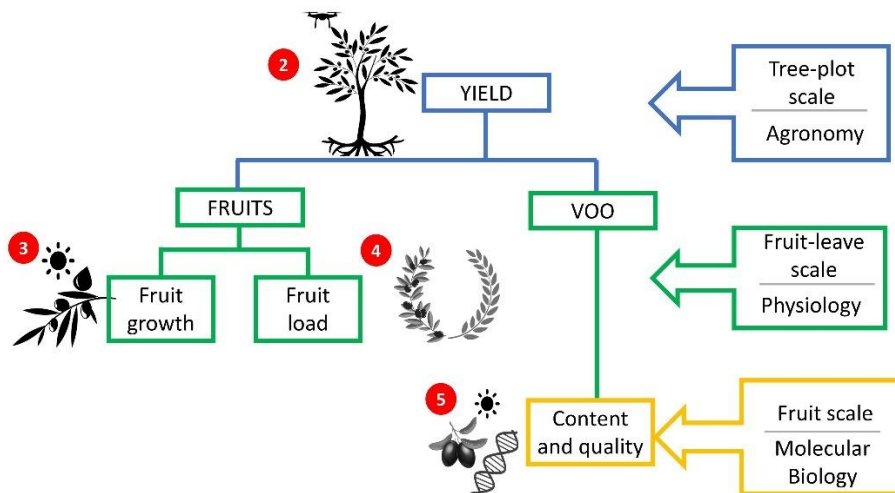
Fig. 1.: Schematic representation of the connections between the topics studied in the different chapters (red numbers) studied in this PhD. Thesis.

6.1. The tree-plot scale: The fruit yield variability

We have observed that there is a variability on fruit and VOO yield despite being subjected to the same amount of water. Our novelty study at agronomic level (**Chapter 2**) has allowed us to identify the main factors involved in fruit and VOO yield combining the use of remote sensing techniques and the application of statistical models. Based on the results obtained, we

have observed that this variability in yield is directly determined by several factors. First, the tree size is an important factor to consider. Tree size can be understood as canopy volume together with leaf area. Larger trees can hold a potentially larger yield because they could have more number of shoots with floral buds that will produce fruits (Galán et al., 2008), and also because they could have a larger leaf area that translates into a greater amount of photoassimilates available for fruit (Hernandez-Santana et al., 2017).

Therefore, one of the main goals that we have achieved in our study (**Chapter 2**), has been the obtaining of agronomic parameters from remote sensing techniques such as tree size (canopy volume, leaf area, number of shoots with fruits), the status of the crop (NDVI, canopy temperature) and the fruit physiological development (fruit growth and oil accumulation and having been able to relate them to estimate fruit and VOO yield from statistical models.

6.2. The fruit-leaf scale: The fruit growth and the fruit load

Unlike more empirical deficit irrigation management methods (e.g. crop coefficient method, artificial intelligence, etc.), this PhD. Thesis is based on the hypothesis that to improve productivity using less water, we first must understand the physiology of the plant. Specifically, in this PhD. Thesis we focused our effort on studying the most important player on production which is the fruit. Surprisingly, it had been much less studied that the leaf physiology or the tree as a whole and thus, the results of PhD. Thesis represent a relevant advance in the knowledge of the response of fruit growth to water deficit as well as the oil biosynthesis that also occurs in this organ. Thus, in this PhD. Thesis we developed two different experiments **(Chapter 3 and 4)** to explore in depth the relevance of some of the factors analysed in **chapter 2** but from a physiological perspective.

168

In the first experiment **(Chapter 3)**, the objective was to examine in an integrated way the relative importance of water and C for fruit growth limitation as a function of soil water deficit and fruit growth period. With the unique database obtained with different sensors and flow cytometry, we found that the relative importance to limit fruit growth of photosynthesis is greater during periods of more intense cell division, while turgor hours are of greater importance during periods when cell division virtually ceases and fruit growth depends primarily on cell expansion, being its lost the major variable explaining growth limitation. Our results join a growing body of evidence (Fatichi et al., 2014; Körner, 2015; Steppe et al., 2015) that calls for a shift from modelling plant growth from a C-centered viewpoint to one based on variables related to the water status of the plant, such as turgor.

Another important factor for fruit yield is the number of shoots with fruits (**Chapter 2**), which is closely related to the fruit load of a tree. It has been shown that trees with high fruit loads consume higher amount of water and present higher transpiration rates than trees with lower fruit loads (Naor et al., 2013; Bustan et al., 2016) which makes any deficit irrigation strategy extremely difficult to apply precisely in large orchards with tree variability. In **Chapter 4**, we confirmed that trees with fruits showed higher stomatal conductance than the ones without fruits as it had been shown before, but importantly, we proposed an explanation and a method to estimate the stress level that fruit loads could produce in the trees. The fruits, as sink organs, would demand high concentrations of soluble sugars, decreasing them in the leaves. On the contrary, the soluble sugars in the trees without fruits would be accumulated in the leaves, downregulating A_N, which in turn, would downregulate g_s. Moreover, the soluble sugar accumulation would make osmotic potential more negative, attracting more water, which in turn, would increase turgor. This effect of fruit sink demand on turgor can be tracked with

the ZIM turgor sensor which would allow the identification of the onset of fruit sugar demand and the impact of high fruit load on the water relations of the tree. The more fruit on the tree, the greater the negative effect on leaf turgor measured with ZIM turgor sensors. In this way, through this method we would be able to detect the periods in which there is more water stress in the tree produced by soil water deficit, but also by the strong demand for carbon and water of a high fruit load.

In both chapters, turgor measured by means of ZIM turgor sensors was the most relevant variable in the processes studied. The loss of cell turgor is a key indicator of water stress in plants, as it has important effects on several key processes for plant water relations (Kramer and Boyer 1995). The leaf water potential at turgor loss has been proved to be consistently related to water supply within and across biomes, demonstrating its good performance as an indicator of drought tolerance, being osmotic potential a major driver (Bartlett et al. 2012). Its complex role on stomatal regulation is also undeniable (Buckley 2019). In this Doctoral Thesis, we use a proxy of bulk turgor to identify the effect of fruit sink demand on plant water relations and also use it as a means to quantify growth limitation due to water stress, increasing the possibilities that the study of this variable has for both the field of physiology and agronomy.

6.3. The fruit scale: The oil content and quality

Unlike fruit growth, deficit irrigation does not have a negative effect on fatty acid biosynthesis (Costagli et al., 2003). In addition, a RDI management implies changes in the olive oil composition improving its quality as it has been observed in several works (Tovar et al., 2002; Gómez-Rico et al., 2007; Ahumada-Orellana et al., 2018; Hernández et al., 2018). For the metabolic pathways involved in oil biosynthesis to continue to function, we have found

that water status and carbon source play a coordinated role (**Chapter 5**). Through a novel and multidisciplinary experimental design that included sensors, ecophysiological measurements and molecular analysis, it was possible to identify that water stress and the modification of the C source increased the relative expression of some genes involved in the oil biosynthesis pathway, which would explain the low effect of water deficit on oil composition and quantity. The advance that this work represents is huge since it could allow selecting a better irrigation strategy and deciding how much and when to impose water stress in order to obtain a higher yield and quality olive oil with the minimum amount of water.

6.4. Major implications and future perspectives

In this PhD Thesis, we have joined agronomy, physiology and molecular biology to try to give a broader vision of regulated deficit irrigation management from the point of view of the most important organ of the tree for yield, the fruit. Studying the fruit from different disciplines has led us to understand how it grows, how it biosynthesizes oil and what relationships it maintains with the tree, obtaining novel results with relevant implications.

To do this, we have related the leaf turgor (measured in continuous by sensors) to the fruit growth and fruit load, which has direct implications for regulated deficit irrigation strategies. In both **chapters 3 and 4**, the results highlight turgor as a variable extremely relevant for the ultimate objective of this PhD Thesis. Regarding fruit growth, the turgor loss was the main fruit growth limitation and regarding the effect of fruit number, the turgor tracking would allow to detect the effect of fruit sinks. Besides the undeniable importance of turgor in numerous physiological processes, the method used in this PhD Thesis, the ZIM turgor sensors, emerges as a promising approach for deficit irrigation management, but in a completely different way to which they

have been used to the moment. Up to now, ZIM turgor sensors have been used to schedule deficit irrigation based on probes states (Padilla-Díaz et al., 2016; Martínez-Gimeno et al., 2017). However, the use of these states have been challenged due to the observer effect (Fernandes et al., 2017) or the fact that they do not allow the calculation of crop water needs compared to other methods (Hernandez-Santana et al., 2019b). However, in more recent works, ZIM turgor sensors have been started to be used with a more physiological perspective with promising results (Rodriguez-Dominguez et al., 2019). Our results add further evidence to a physiological-based approach of ZIM turgor sensors and opens new possibilities of breakthrough applications in agriculture. The fact that ZIM turgor sensors detect, through the monitoring of a variable related to leaf turgor, the water stress produced by soil water deficit and the effect by the strong demand for water and carbon by the fruit in specific phenological periods, makes them an excellent tool for stress detection. In that way, the ZIM turgor sensore use which could allow the inclusion of the effect of the fruit load in the amount of irrigation to apply. Furthermore, as proposed in **Chapter 3** and other works (Fatichi et al., 2014; Körner, 2015; Steppe et al., 2015; Coussement et al., 2021), turgor loss plays an important role in limiting plant growth and thus, its use can indicate whether growth limitation is occurring. This is of great relevance since one of the main effects that irrigation is intended to have is basically to eliminate the limitations of fruit growth caused by soil water deficit. Therefore, the physiological-based use of the ZIM turgor sensors, overcomes the high level of empiricism with which they had been used so far, which was preventing them from being used reliably on a more generalized way. This corroborates our initial hypothesis (increasing water productivity in crop production demands physiological knowledge) and makes the extrapolation of automatic data processing and interpretation much easier. Moreover, this method opens the

172

possibility to create models capable of developing irrigation strategies based on the water needs of each tree, which would allow minimizing the variability observed between individuals at the plot level.

Furthermore, we have expanded the knowledge about the molecular mechanisms involved in oil biosynthesis and its quality under water stress conditions and different carbon sources. We have obtained that the major carbon source contribution for oil biosynthesis comes from the leaves despite fruit photosynthesis being also important. It is known that, in higher plants, triacylglycerol (TAG) are synthesized by the sequential addition of fatty acids in the Kennedy pathway and this happens in the final rate-limiting step catalyzed by the acyl-Coa:diacylglycerol acyltransferase (DGAT) and, alternatively, by an acyl-Coa independent reaction catalyzed by the phospholipid:diacylglycerol acyltransferase (PDAT). In chapter 5, we discovered that carbon supply and water status affected mesocarp oil content, regulating the relative expression levels of olive DGAT and PDAT genes and pointing to OeDGAT1-1, OeDGAT2, OePDAT1-1, and OePDAT1-2 as the principal genes involved in TAG biosynthesis, with a major role for OeDGAT2 and OePDAT1-2 in well-watered conditions. Furthermore, water stress caused an increase in olive mesocarp DGAT1-1, DGAT1-2, and PDAT1-1 gene transcript levels. Under future perspectives of water stress conditions, these facts open up a new possibility within the irrigation management. New olive varieties, whose relative expression of PDAT and DGAT genes would be higher, could be enhanced to continuing olive biosynthesis with a huge impact on alimentary industry increasing virgin olive oil yield and its quality.

CHAPTER 7:

CONCLUSIONS

CONCLUSIONES

7.1. Conclusions

The conclusions obtained in accordance with the objectives of this doctoral thesis are as follows:

- The use of unmanned aerial vehicles allows the study of the canopy size distribution in the farm and therefore, provide us with a valuable tool to manage irrigation more precisely.

- The case of the olive tree with two different market products, fruits and oil, shows that the factors contributing to crop yield vary depending on the process studied, and the irrigation treatment applied. If confirmed in future studies under other growing conditions, this result suggests that we must focus our monitoring efforts on different variables depending on the irrigation strategy we are implementing or the final product we are interested in.

- Fruit growth decline does not necessarily indicate C limitation, as traditionally assumed. Rather, it was concluded, that under water stress, a reduction in the time of turgor-driven cell expansion has a greater and more immediate impact on fruit growth than smaller reductions in photosynthesis, consistent with the sink limitation hypothesis suggested. The turgor-driven time necessary for growth can be followed in an automatic manner with leaf turgor sensors.

- Photosynthesis plays a key role in growth because it is the base for building the carbon skeletons, required by plants to build up their structures specially during periods of intense cell division.

- The sink strength of fruits for carbon and water explains the downregulation of photosynthesis and stomatal conductance in the absence of fruits, under well-watered conditions. The fruit absence

contributes to sugar accumulation in the leaves, which down-regulates photosynthesis, and in turn, stomatal conductance.

- Leaf sugar accumulation produced by the absence of fruits also provokes the decrease of leaf osmotic potential, but not the water potential, which in turn, increases leaf turgor. These changes in leaf turgor can be identified with leaf turgor sensors, which, together with the use of determining turgor-driven time to growth, makes them a promising tool for managing irrigation to consider fruit growth and sugar demand as well as different fruit loads in a continuous manner.

- The main contribution of photoassimilates for oil biosynthesis in the mesocarp of olive fruit comes from the leaf, as compared to the fruit photosynthesis.

- The source of carbon supply and water status affects oil synthesis and fatty acid composition in the olive mesocarp by regulating the transcript levels of *DGAT*, *PDAT* and *FAD* genes. In particular, *DGAT1-1*, *DGAT2*, *PDAT1-1* and *PDAT1-2* appeared to be the genes involved in triacylglycerol biosynthesis and oil accumulation in this tissue, with an important role for *DGAT2* and *PDAT1-2* under well-watered conditions.

- Transcript levels of *FAD2-1*, *FAD2-2* and *FAD7-1* genes and polyunsaturated fatty acid content increased in the olive mesocarp in response to different carbon supplies. In addition, the expression levels of *DGAT1-1*, *DGAT1-2*, *PDAT1-1* and *FAD2-5* genes in the olive mesocarp were transcriptionally up-regulated by water stress.

7.2. Conclusiones

Las conclusiones obtenidas de acuerdo con los objetivos de esta tesis doctoral son las siguientes:

- El uso de vehículos aéreos no tripulados permite el estudio de la distribución del tamaño del dosel en la finca y, por tanto, proporcionarnos una valiosa herramienta para gestionar el riego con mayor precisión.

- El caso del olivo con dos productos de mercado diferentes, frutos y aceite, muestra que los factores que contribuyen al rendimiento del cultivo varían en función del proceso estudiado, y del tratamiento de riego aplicado. De confirmarse en futuros estudios bajo otras condiciones de cultivo, este resultado sugiere que debemos centrar nuestros esfuerzos de control en diferentes variables dependiendo de la estrategia de riego que estemos aplicando o del producto final que nos interese.

- La disminución del crecimiento del fruto no indica necesariamente una limitación de carbono, como se suponía hasta ahora. Más bien, bajo estrés hídrico, un menor número de horas de expansión celular impulsada por turgencia tiene un impacto mayor y más inmediato en el crecimiento del fruto que pequeñas reducciones en la fotosíntesis, lo que es consistente con la hipótesis de limitación por sumidero. Las horas de turgencia necesarias para el crecimiento pueden seguirse de forma automática a través de sensores de turgencia foliar.

- La fotosíntesis desempeña un papel clave en el crecimiento porque es la base para construir los esqueletos de carbono, necesarios para que las plantas construyan sus estructuras especialmente durante los periodos de intensa división celular.

- En buenas condiciones de riego, el efecto sumidero de carbono y agua que ejercen los frutos explica la disminución de la fotosíntesis y de la conductancia estomática en ausencia de estos. La ausencia de frutos contribuye a la acumulación de azúcares en las hojas, lo que regula a la baja la fotosíntesis y, a su vez, la conductancia estomática.

- La acumulación de azúcares en las hojas producida por la ausencia de frutos también provoca la disminución del potencial osmótico en la hoja, pero no del potencial hídrico, lo que a su vez aumenta la turgencia en esta. Estos cambios en la turgencia de la hoja pueden identificarse con sensores de turgencia foliar, lo que, junto con el uso de la determinación del número de horas de crecimiento impulsado por la turgencia, los convierte en una herramienta prometedora para la gestión del riego que considere el crecimiento de los frutos y la demanda de azúcares, así como las diferentes cargas de frutos de forma continua.

- La principal contribución de fotoasimilados para la biosíntesis de aceite en el mesocarpio del fruto del olivo proviene de la hoja, en comparación con la fotosíntesis procedente del fruto.

- La fuente de suministro de carbono y el estado hídrico afectan a la biosíntesis de aceite y a la composición de ácidos grasos en el mesocarpio del fruto del olivo mediante la regulación de los niveles de transcripción de los genes *DGAT*, *PDAT* y *FAD*. En particular, *DGAT1-1*, *DGAT2*, *PDAT1-1* y *PDAT1-2* parecen ser los genes implicados en la biosíntesis de triacilglicerol y la acumulación de aceite en este tejido, con un papel importante para *DGAT2* y *PDAT1-2* en cbuenas condiciones de riego.

- Los niveles de transcripción de los genes *FAD2-1*, *FAD2-2* y *FAD7-1* y el contenido en ácidos grasos poliinsaturados aumentaron en el

"

mesocarpio del fruto del olivo en respuesta a diferentes suministros de carbono. Además, los niveles de expresión de los genes *DGAT1-1*, *DGAT1-2*, *PDAT1-1* y *FAD2-5* en el mesocarpio de la aceituna se regulan transcripcionalmente al alza debido al estrés hídrico.

REFERENCES

Adams WW, Muller O, Cohu CM, Demmig-Adams B (2013) May photoinhibition be a consequence, rather than a cause, of limited plant productivity? Photosynth Res **117**: 31–44

Ahmed N, Ward JD, Saint CP (2014) Can integrated aquaculture-agriculture (IAA) produce "more crop per drop"? Food Secur **6**: 767–779

Ahumada-Orellana LE, Ortega-Farías S, Searles PS (2018) Olive oil quality response to irrigation cut-off strategies in a super-high density orchard. Agric Water Manag **202**: 81–88

Akinci S, Losel DM (2010) The effects of water stress and recovery periods on soluble sugars and starch content in cucumber cultivars. Fresenius Environ Bull **19**: 164–171

Albarracín V, Hall AJ, Searles PS, Rousseaux MC (2017) Responses of vegetative growth and fruit yield to winter and summer mechanical pruning in olive trees. Sci Hortic (Amsterdam) **225**: 185–194

Alegre S, Marsal J, Mata M, Arbonés A, Girona J, Tovar MJ (2002) Regulated deficit irrigation in olive trees (*Olea europaea* L. cv. Arbequina) for oil production. Acta Hortic. International Society for Horticultural Science (ISHS), Leuven, Belgium, pp 259–262

Allen RG, Pereira LS, Raes D, Smith M, Ab W (1998) Crop evapotranspiration. Guidelines for computing crop water requirements. FAO Irrig Drain Pap Rome **56**: 300

Angelopoulos K, Dichio B, Xiloyannis C (1996) Inhibition of photosynthesis in olive trees (Olea europaea L.) during water stress and rewatering. J Exp Bot **47**: 1093–1100

Aparicio R, Harwood J (2013) Handbook of olive oil: Analysis and properties, 2nd editio. Handb Olive Oil Anal Prop. doi: 10.1007/978-1-4614-7777-8

Aranda I, Cadahía E, Fernández De Simón B (2021) Specific leaf metabolic changes that underlie adjustment of osmotic potential in response to drought by four Quercus species. Tree Physiol **41**: 728–743

Ballester C, Castel J, Intrigliolo DS, Castel JR (2013a) Response of Navel Lane Late citrus trees to regulated deficit irrigation: Yield components and fruit composition. Irrig Sci **31**: 333–341

Ballester C, Castel J, Jiménez-Bello MA, Castel JR, Intrigliolo DS (2013b) Thermographic measurement of canopy temperature is a useful tool for predicting water deficit effects on fruit weight in citrus trees. Agric Water

Manag **122**: 1–6

Banilas G, Karampelias M, Makariti I, Kourti A, Hatzopoulos P (2011) The olive DGAT2 gene is developmentally regulated and shares overlapping but distinct expression patterns with DGAT1. J Exp Bot **62**: 521–532

Banilas G, Moressis A, Nikoloudakis N, Hatzopoulos P (2005) Spatial and temporal expressions of two distinct oleate desaturases from olive (*Olea europaea* L.). Plant Sci **168**: 547–555

Banilas G, Nikiforiadis A, Makariti I, Moressis A, Hatzopoulos P (2007) Discrete roles of a microsomal linoleate desaturase gene in olive identified by spatiotemporal transcriptional analysis. Tree Physiol **27**: 481–490

Bartlett MK, Scoffoni C, Sack L (2012) The determinants of leaf turgor loss point and prediction of drought tolerance of species and biomes: A global meta-analysis. Ecol Lett **15**: 393–405

Bates PD (2016) Understanding the control of acyl flux through the lipid metabolic network of plant oil biosynthesis. Biochim Biophys Acta (BBA)-Molecular Cell Biol Lipids **1861**: 1214–1225

Bellvert J, Marsal J, Girona J, Gonzalez-Dugo V, Fereres E, Ustin SL, Zarco-Tejada PJ (2016) Airborne thermal imagery to detect the seasonal evolution of crop water status in peach, nectarine and Saturn peach orchards. Remote Sens **8**: 1–17

Beltrán G, Del Rio C, Sánchez S, Martínez L (2004) Influence of harvest date and crop yield on the fatty acid composition of virgin olive oils from cv. Picual. J Agric Food Chem **52**: 3434–3440

Ben-David E, Kerem Z, Zipori I, Weissbein S, Basheer L, Bustan A, Dag A (2010) Optimization of the Abencor system to extract olive oil from irrigated orchards. Eur J Lipid Sci Technol **112**: 1158–1165

Ben-Gal A, Kool D, Agam N, van Halsema GE, Yermiyahu U, Yafe A, Presnov E, Erel R, Majdop A, Zipori I, et al (2010) Whole-tree water balance and indicators for short-term drought stress in non-bearing 'Barnea' olives. Agric Water Manag **98**: 124–133

Blanke MM, Lenz F (1989) Fruit photosynthesis. Plant Cell Environ **12**: 31–46

Blonquist JM, Norman JM, Bugbee B (2009) Automated measurement of canopy stomatal conductance based on infrared temperature. Agric For Meteorol **149**: 1931–1945

Buckley TN (2019) How do stomata respond to water status? New Phytol **224**: 21–36

Bustan A, Avni A, Lavee S, Zipori I, Yeselson Y, Schaffer AA, Riov J, Dag A (2011) Role of carbohydrate reserves in yield production of intensively cultivated oil olive (Olea europaea L.) trees. Tree Physiol **31**: 519–530

Bustan A, Dag A, Yermiyahu U, Erel R, Presnov E, Agam N, Kool D, Iwema J, Zipori I, Ben-Gal A (2016) Fruit load governs transpiration of olive trees. Tree Physiol **36**: 380–391

Calderón R, Navas-Cortés JA, Lucena C, Zarco-Tejada PJ (2013) High-resolution airborne hyperspectral and thermal imagery for early detection of Verticillium wilt of olive using fluorescence, temperature and narrow-band spectral indices. Remote Sens Environ **139**: 231–245

Caruso G, Gucci R, Urbani S, Esposto S, Taticchi A, Di Maio I, Selvaggini R, Servili M (2014) Effect of different irrigation volumes during fruit development on quality of virgin olive oil of cv. Frantoio. Agric Water Manag **134**: 94–103

Caruso G, Palai G, Gucci R, Priori S (2022a) Remote and Proximal Sensing Techniques for Site-Specific Irrigation Management in the Olive Orchard. Appl Sci. doi: 10.3390/app12031309

Caruso G, Palai G, Marra FP, Caruso T (2021) High-resolution UAV imagery for field olive (Olea europaea L.) phenotyping. Horticulturae **7**: 1–16

Caruso G, Palai G, Tozzini L, Gucci R (2022b) Using Visible and Thermal Images by an Unmanned Aerial Vehicle to Monitor the Plant Water Status, Canopy Growth and Yield of Olive Trees (cvs. Frantoio and Leccino) under Different Irrigation Regimes. Agronomy. doi: 10.3390/agronomy12081904

Caruso G, Zarco-Tejada PJ, González-Dugo V, Moriondo M, Tozzini L, Palai G, Rallo G, Hornero A, Primicerio J, Gucci R (2019) High-resolution imagery acquired from an unmanned platform to estimate biophysical and geometrical parameters of olive trees under different irrigation regimes. PLoS One **14**: 1–19

de Castro AI, Rallo P, Suárez MP, Torres-Sánchez J, Casanova L, Jiménez-Brenes FM, Morales-Sillero A, Jiménez MR, López-Granados F (2019) High-Throughput System for the Early Quantification of Major Architectural Traits in Olive Breeding Trials Using UAV Images and OBIA Techniques. Front Plant Sci **10**: 1–17

Chalmers DJ, Mitchell PD, van Heek L (1981) Control of peach tree growth and productivity by regulated water supply, tree density and summer pruning. J Am Soc Hortic Sci **106**: 307–312

References

Chapman KD, Ohlrogge JB (2012) Compartmentation of triacylglycerol accumulation in plants. J Biol Chem **287**: 2288–2294

Conde C, Delrot S, Gerós H (2008) Physiological, biochemical and molecular changes occurring during olive development and ripening. J Plant Physiol **165**: 1545–1562

Connor DJ, Fereres E (2005) The physiology of adaptation and yield expression in olive. Hortic Rev (Am Soc Hortic Sci) **31**: 155–229

Costagli G, Gucci R, Rapoport HF (2003) Growth and development of fruits of olive 'Frantoio' under irrigated and rainfed conditions. J Hortic Sci Biotechnol **78**: 119–124

Coussement JR, Villers SLY, Nelissen H, Inzé D, Steppe K (2021) Turgor-time controls grass leaf elongation rate and duration under drought stress. Plant Cell Environ **44**: 1361–1378

D'Andrea RM, Triassi A, Casas MI, Andreo CS, Lara MV (2015) Identification of genes involved in the drought adaptation and recovery in *Portulaca oleracea* by differential display. Plant Physiol Biochem **90**: 38–49

Dag A, Bustan A, Avni A, Tzipori I, Lavee S, Riov J (2010) Timing of fruit removal affects concurrent vegetative growth and subsequent return bloom and yield in olive (Olea europaea L.). Sci Hortic (Amsterdam) **123**: 469–472

Dag A, Kerem Z, Yogev N, Zipori I, Lavee S, Ben-David E (2011) Influence of time of harvest and maturity index on olive oil yield and quality. Sci Hortic (Amsterdam) **127**: 358–366

Dahlqvist A, Ståhl U, Lenman M, Banas A, Lee M, Sandager L, Ronne H, Stymne S (2000) Phospholipid:diacylglycerol acyltransferase: An enzyme that catalyzes the acyl-CoA-independent formation of triacylglycerol in yeast and plants. Proc Natl Acad Sci U S A **97**: 6487–6492

Dell'Amico J, Moriana A, Corell M, Girón IF, Morales D, Torrecillas A, Moreno F (2012) Low water stress conditions in table olive trees (*Olea europaea* L.) during pit hardening produced a different response of fruit and leaf water relations. Agric Water Manag **114**: 11–17

Dewar R, Hölttä T, Salmon Y (2022) Exploring optimal stomatal control under alternative hypotheses for the regulation of plant sources and sinks. New Phytol **233**: 639–654

Dhankher OP, Foyer CH (2018) Climate resilient crops for improving global food security and safety. Plant Cell Environ **41**: 877–884

Diaz-Espejo A, Buckley TN, Sperry JS, Cuevas M V., de Cires A, Elsayed-Farag

S, Martin-Palomo MJ, Muriel JL, Perez-Martin A, Rodriguez-Dominguez CM, et al (2012) Steps toward an improvement in process-based models of water use by fruit trees: A case study in olive. Agric Water Manag **114**: 37–49

Diaz-Espejo A, Fernández JE, Torres-Ruiz JM, Rodriguez-Dominguez CM, Perez-Martin A, Hernandez-Santana V (2018) Chapter 18 - The olive tree under water stress: fitting the pieces of response mechanisms in the crop performance puzzle. *In* IFG& VHD Zuazo, ed, Water scarcity Sustain. Agric. semiarid Environ., I.F. Garcı. London: Academic Press, pp 439–479

Diaz-Espejo A, Hafidi B, Fernandez JE, Palomo MJ, Sinoquet H (2002) Transpiration and photosynthesis of the olive tree: a model approach. Acta Hortic. International Society for Horticultural Science (ISHS), Leuven, Belgium, pp 457–460

Diaz-Espejo A, Hernandez-Santana V (2017) The phloem-xylem consortium: Until death do them part. Tree Physiol **37**: 847–850

Diaz-Espejo A, Nicolás E, Fernández JE (2007) Seasonal evolution of diffusional limitations and photosynthetic capacity in olive under drought. Plant, Cell Environ **30**: 922–933

Díaz-Espejo A, Walcroft AS, Fernández JE, Hafidi B, Palomo MJ, Girón IF (2006) Modeling photosynthesis in olive leaves under drought conditions. Tree Physiol **26**: 1445–1456

Dichio B, Margiotta G, Xiloyannis C, Bufo SA, Sofo A, Cataldi TRI (2009) Changes in water status and osmolyte contents in leaves and roots of olive plants (Olea europaea L.) subjected to water deficit. Trees - Struct Funct **23**: 247–256

Doležel J, Greilhuber J, Suda J (2007) Estimation of nuclear DNA content in plants using flow cytometry. Nat Protoc **2**: 2233–2244

Domingo R, Ruiz-Sánchez MC, Sánchez-Blanco MJ, Torrecillas A (1996) Water relations, growth and yield of Fino lemon trees under regulated deficit irrigation. Irrig Sci **16**: 115–123

Egea G, Padilla-Díaz CM, Martinez-Guanter J, Fernández JE, Pérez-Ruiz M (2017) Assessing a crop water stress index derived from aerial thermal imaging and infrared thermometry in super-high density olive orchards. Agric Water Manag **187**: 210–221

Ehrenberger W, Rüger S, Rodríguez-Domínguez CM, Díaz-Espejo A, Fernández JE, Moreno J, Zimmermann D, Sukhorukov VL, Zimmermann U (2012) Leaf patch clamp pressure probe measurements on olive leaves in a

nearly turgorless state. Plant Biol **14**: 666–674

European Commission Regulation (2003) European Commission Regulation EC1989/2003. Off J Eur Union **L295**: 57–77

FAO (2009) High Level Expert Forum—How to Feed the World in 2050. Rome 12-13 October

Farquhar GD, von Caemmerer S, Berry JA (1980) A biochemical model of photosynthetic CO2 assimilation in leaves of C3 species. Planta **149**: 78–90

Fatichi S, Leuzinger S, Körner C (2014) Moving beyond photosynthesis: From carbon source to sink-driven vegetation modeling. New Phytol **201**: 1086–1095

Fatichi S, Pappas C, Zscheischler J, Leuzinger S (2019) Modelling carbon sources and sinks in terrestrial vegetation. New Phytol **221**: 652–668

Fereres E, Soriano MA (2007) Deficit irrigation for reducing agricultural water use. J Exp Bot **58**: 147–159

Fernandes RDM, Cuevas MV, Diaz-Espejo A, Hernandez-Santana V (2018) Effects of water stress on fruit growth and water relations between fruits and leaves in a hedgerow olive orchard. Agric Water Manag **210**: 32–40

Fernandes RDM, Cuevas MV, Hernandez-Santana V, Rodriguez-Dominguez CM, Padilla-Díaz CM, Fernández JE (2017) Classification models for automatic identification of daily states from leaf turgor related measurements in olive. Comput Electron Agric **142**: 181–189

Fernandes RDM, Egea G, Hernandez-Santana V, Diaz-Espejo A, Fernández JE, Perez-Martin A, Cuevas M V. (2021) Response of vegetative and fruit growth to the soil volume wetted by irrigation in a super-high-density olive orchard. Agric Water Manag. doi: 10.1016/j.agwat.2021.107197

Fernández JE (2014) Understanding olive adaptation to abiotic stresses as a tool to increase crop performance. Environ Exp Bot **103**: 158–179

Fernández JE, Diaz-Espejo A, D'Andria R, Sebastiani L, Tognetti R (2008) Potential and limitations of improving olive orchard design and management through modelling. Plant Biosyst - An Int J Deal with all Asp Plant Biol **142**: 130–137

Fernández JE, Diaz-Espejo A, Romero R, Hernandez-Santana V, García JM, Padilla-Díaz CM, Cuevas M V. (2018) Precision Irrigation in Olive (Olea europaea L.) Tree Orchards. Water Scarcity Sustain Agric Semiarid Environ. doi: 10.1016/b978-0-12-813164-0.00009-0

Fernández JE, Moreno F, Girón IF, Blázquez OM (1997) Stomatal control of water use in olive tree leaves. Plant Soil **190**: 179–192

Fernández JE, Moreno F, Martín-Palomo MJ, Cuevas MV, Torres-Ruiz JM, Moriana A (2011) Combining sap flow and trunk diameter measurements to assess water needs in mature olive orchards. Environ Exp Bot **72**: 330–338

Fernández JE, Perez-Martin A, Torres-Ruiz JM, Cuevas M V., Rodriguez-Dominguez CM, Elsayed-Farag S, Morales-Sillero A, García JM, Hernandez-Santana V, Diaz-Espejo A (2013) A regulated deficit irrigation strategy for hedgerow olive orchards with high plant density. Plant Soil **372**: 279–295

Fernández JEE, Alcon F, Diaz-Espejo A, Hernandez-Santana V, Cuevas MV V. (2020) Water use indicators and economic analysis for on-farm irrigation decision: A case study of a super high density olive tree orchard. Agric Water Manag **237**: 106074

Fishman S, Génard M (1998) A biophysical model of fruit growth: Simulation of seasonal and diurnal dynamics of mass. Plant, Cell Environ **21**: 739–752

Flexas J, Carriquí M, Nadal M (2018) Gas exchange and hydraulics during drought in crops: Who drives whom? J Exp Bot **69**: 3791–3795

Flora LL, Madore MA (1993) Stachyose and mannitol transport in olive (Olea europaea L.). Planta **189**: 484–490

Galán C, García-Mozo H, Vázquez L, Ruiz L, Díaz De La Guardia C, Domínguez-Vilches E (2008) Modeling olive crop yield in Andalusia, Spain. Agron J **100**: 98–104

Galindo A, Cruz ZN, Rodríguez P, Collado-González J, Corell M, Memmi H, Moreno F, Moriana A, Torrecillas A, Pérez-López D (2016) Jujube fruit water relations at fruit maturation in response to water deficits. Agric Water Manag **164**: 110–117

Garcés R, Mancha M (1993) One-step lipid extraction and fatty acid methyl esters preparation from fresh plant tissues. Anal Biochem **211**: 139–143

García-Tejero I, Jiménez-Bocanegra JA, Martínez G, Romero R, Durán-Zuazo VH, Muriel-Fernández JL (2010) Positive impact of regulated deficit irrigation on yield and fruit quality in a commercial citrus orchard [Citrus sinensis (L.) Osbeck, cv. salustiano]. Agric Water Manag **97**: 614–622

García JM, Cuevas M V., Fernández JE (2013) Production and oil quality in 'Arbequina' olive (Olea europaea, L.) trees under two deficit irrigation strategies. Irrig Sci **31**: 359–370

References

García JM, Morales-Sillero A, Pérez-Rubio AG, Diaz-Espejo A, Montero A, Fernández JE (2017) Virgin olive oil quality of hedgerow 'Arbequina' olive trees under deficit irrigation. J Sci Food Agric **97**: 1018–1026

Génard M, Dauzat J, Franck N, Lescourret F, Moitrier N, Vaast P, Vercambre G (2008) Carbon allocation in fruit trees: From theory to modelling. Trees - Struct Funct **22**: 269–282

Génard M, Fishman S, Vercambre G, Huguet JG, Bussi C, Besset J, Habib R (2001) A biophysical analysis of stem and root diameter variations in woody plants. Plant Physiol **126**: 188–202

Gersony JT, Hochberg U, Rockwell FE, Park M, Gauthier PP, Holbrook NM (2020) Leaf carbon export and non-structural carbohydrates in relation to diurnal water dynamics in mature oak trees. Plant Physiol **183**: 1612–1621

Gifford RM, Evans LT (1981) Photosynthesis, carbon partitioning, and yield. Annu Rev Plant Physiol **32**: 485–509

Gimeno J, Gadea J, Forment J, Pérez-Valle J, Santiago J, Martínez-Godoy MA, Yenush L, Bellés JM, Brumós J, Colmenero-Flores JM, et al (2009) Shared and novel molecular responses of mandarin to drought. Plant Mol Biol **70**: 403–420

Giorio P, Sorrentino G, D'Andria R (1999) Stomatal behaviour, leaf water status and photosynthetic response in field-grown olive trees under water deficit. Environ Exp Bot **42**: 95–104

Giovannoni JJ (2004) Genetic regulation of fruit development and ripening. Plant Cell **16**: 170–180

Girón IF, Corell M, Galindo A, Torrecillas E, Morales D, Dell'Amico J, Torrecillas A, Moreno F, Moriana A (2015) Changes in the physiological response between leaves and fruits during a moderate water stress in table olive trees. Agric Water Manag **148**: 280–286

Goldewijk KK, Beusen A, Doelman J, Stehfest E (2017) Anthropogenic land use estimates for the Holocene - HYDE 3.2. Earth Syst Sci Data **9**: 927–953

Goldhamer DA, Viveros M, Salinas M (2006) Regulated deficit irrigation in almonds: Effects of variations in applied water and stress timing on yield and yield components. Irrig Sci **24**: 101–114

Goldschmidt EE, Huber SC (1992) Regulation of photosynthesis by end-product accumulation in leaves of plants storing starch, sucrose, and hexose sugars. Plant Physiol **99**: 1443–1448

Gómez-del-Campo M, Pérez-Expósito MÁ, Hammami SBMM, Centeno A,

Rapoport HF (2014) Effect of varied summer deficit irrigation on components of olive fruit growth and development. Agric Water Manag **137**: 84–91

Gómez-Rico A, Salvador MD, Moriana A, Pérez D, Olmedilla N, Ribas F, Fregapane G (2007) Influence of different irrigation strategies in a traditional Cornicabra cv. olive orchard on virgin olive oil composition and quality. Food Chem **100**: 568–578

Gonçalves A, Silva E, Brito C, Martins S, Pinto L, Dinis LT, Luzio A, Martins-Gomes C, Fernandes-Silva A, Ribeiro C, et al (2020) Olive tree physiology and chemical composition of fruits are modulated by different deficit irrigation strategies. J Sci Food Agric **100**: 682–694

Grant OM, Chaves MM, Jones HG (2006) Optimizing thermal imaging as a technique for detecting stomatal closure induced by drought stress under greenhouse conditions. Physiol Plant **127**: 507–518

Green S, Clothier B, Jardine B (2003) Theory and practical application of heat pulse to measure sap flow. Agron J **95**: 1371–1379

Greenspan MD, Schultz HR, Matthews MA (1996) Field evaluation of water transport in grape berries during water deficits. Physiol Plant **97**: 55–62

Greven M, Neal S, Green S, Dichio B, Clothier B (2009) The effects of drought on the water use, fruit development and oil yield from young olive trees. Agric Water Manag **96**: 1525–1531

Grömping U (2006) Relative importance for linear regression in R: The package relaimpo. J Stat Softw **17**: 1–27

Gucci R, Caruso G, Gennai C, Esposto S, Urbani S, Servili M (2019) Fruit growth, yield and oil quality changes induced by deficit irrigation at different stages of olive fruit development. Agric Water Manag **212**: 88–98

Gucci R, Lodolini E, Rapoport HF (2007) Productivity of olive trees with different water status and crop load. J Hortic Sci Biotechnol **82**: 648–656

Gucci R, Lodolini EM, Rapoport HF (2009) Water deficit-induced changes in mesocarp cellular processes and the relationship between mesocarp and endocarp during olive fruit development. Tree Physiol **29**: 1575–1585

Gucci R, Tattini M (1997) Salinity tolerance in olive. Hortic Rev (Am Soc Hortic Sci) **21**: 177–214

Hacket-Pain AJ, Lageard JGA, Thomas PA (2017) Drought and reproductive effort interact to control growth of a temperate broadleaved tree species (Fagus sylvatica). Tree Physiol **37**: 744–754

References

Hara A, Radin NS (1978) Lipid extraction of tissues with a low-toxicity solvent. Anal Biochem **90**: 420–426

Hartmann H, Trumbore S (2016) Understanding the roles of nonstructural carbohydrates in forest trees - from what we can measure to what we want to know. New Phytol **211**: 386–403

Harwood JL (2005) Fatty acid biosynthesis. Plant lipids Biol. Util. Manip., Murphy, D. Blackwell Publishing, Oxford, UK, pp 27–101

Harwood JL, Yaqoob P (2002) Nutritional and health aspects of olive oil. Eur J Lipid Sci Technol **104**: 685–697

Hernandez-Santana V, Diaz-Rueda P, Diaz-Espejo A, Raya-Sereno MD, Gutiérrez-Gordillo S, Montero A, Perez-Martin A, Colmenero-Flores JM, Rodriguez-Dominguez CM (2019a) Hydraulic traits emerge as relevant determinants of growth patterns in wild olive genotypes under water stress. Front Plant Sci **10**: 1–15

Hernandez-Santana V, Fernandes RDM, Perez-Arcoiza A, Fernández JE, Garcia JM, Diaz-Espejo A (2018) Relationships between fruit growth and oil accumulation with simulated seasonal dynamics of leaf gas exchange in the olive tree. Agric For Meteorol **256**–**257**: 458–469

Hernandez-Santana V, Fernández JE, Cuevas M V., Perez-Martin A, Diaz-Espejo A (2017) Photosynthetic limitations by water deficit: Effect on fruit and olive oil yield, leaf area and trunk diameter and its potential use to control vegetative growth of super-high density olive orchards. Agric Water Manag **184**: 9–18

Hernandez-Santana V, Fernández JE, Diaz-Espejo A (2019b) Irrigation scheduling in a high-density olive orchard from estimated stomatal conductance. Acta Hortic **1253**: 449–456

Hernandez-Santana V, Fernández JE, Rodriguez-Dominguez CM, Romero R, Diaz-Espejo A (2016a) The dynamics of radial sap flux density reflects changes in stomatal conductance in response to soil and air water deficit. Agric For Meteorol **218**–**219**: 92–101

Hernandez-Santana V, Perez-Arcoiza A, Gomez-Jimenez MC, Diaz-Espejo A (2021) Disentangling the link between leaf photosynthesis and turgor in fruit growth. Plant J **107**: 1788–1801

Hernandez-Santana V, Rodriguez-Dominguez CM, Fernández JE, Diaz-Espejo A (2016b) Role of leaf hydraulic conductance in the regulation of stomatal conductance in almond and olive in response to water stress. Tree Physiol **36**: 725–735

194

Hernández ML, Guschina IA, Martínez-Rivas JM, Mancha M, Harwood JL (2008) The utilization and desaturation of oleate and linoleate during glycerolipid biosynthesis in olive (*Olea europaea* L.) callus cultures. J Exp Bot **59**: 2425–2435

Hernández ML, Mancha M, Martínez-Rivas JM (2005) Molecular cloning and characterization of genes encoding two microsomal oleate desaturases (FAD2) from olive. Phytochemistry **66**: 1417–1426

Hernández ML, Moretti S, Sicardo MD, García Ú, Pérez A, Sebastiani L, Martínez-Rivas JM (2021a) Distinct Physiological Roles of Three Phospholipid:Diacylglycerol Acyltransferase Genes in Olive Fruit with Respect to Oil Accumulation and the Response to Abiotic Stress. Front Plant Sci **12**: 1–16

Hernández ML, Padilla MN, Mancha M, Martínez-Rivas JM (2009) Expression analysis identifies FAD2-2 as the olive oleate desaturase gene mainly responsible for the linoleic acid content in virgin olive oil. J Agric Food Chem **57**: 6199–6206

Hernández ML, Padilla MN, Sicardo MD, Mancha M, Martínez-Rivas JM (2011) Effect of different environmental stresses on the expression of oleate desaturase genes and fatty acid composition in olive fruit. Phytochemistry **72**: 178–187

Hernández ML, Sicardo MD, Alfonso M, Martínez-Rivas JM (2019) Transcriptional regulation of stearoyl-acyl carrier protein desaturase genes in response to abiotic stresses leads to changes in the unsaturated fatty acids composition of olive mesocarp. Front Plant Sci **10**: 251

Hernández ML, Sicardo MD, Arjona PM, Martínez-Rivas JM (2020) Specialized functions of olive FAD2 gene family members related to fruit development and the abiotic stress response. Plant Cell Physiol **61**: 427–441

Hernández ML, Sicardo MD, Belaj A, Martínez-Rivas JM (2021b) The Oleic/Linoleic acid ratio in olive (*Olea europaea* L.) fruit mesocarp is mainly controlled by OeFAD2-2 and OeFAD2-5 genes together with the different specificity of extraplastidial acyltransferase enzymes. Front Plant Sci **12**: 1–10

Hernández ML, Sicardo MD, Martínez-Rivas JM (2016) Differential contribution of endoplasmic reticulum and chloroplast ω-3 fatty acid desaturase genes to the linolenic acid content of olive (*Olea europaea*) fruit. Plant Cell Physiol **57**: 138–151

Hernández ML, Velázquez-Palmero D, Sicardo MD, Fernández JE, Diaz-Espejo

A, Martínez-Rivas JM (2018) Effect of a regulated deficit irrigation strategy in a hedgerow 'Arbequina' olive orchard on the mesocarp fatty acid composition and desaturase gene expression with respect to olive oil quality. Agric Water Manag **204**: 100–106

Herold A (1980) Regulation of photosynthesis by sink activity: the missing link. New Phytol **86**: 131–144

Hilty J, Muller B, Pantin F, Leuzinger S (2021) Plant growth: the What, the How, and the Why. New Phytol **232**: 25–41

Hilty J, Pook C, Leuzinger S (2019) Water relations determine short time leaf growth patterns in the mangrove Avicennia marina (Forssk.) Vierh. Plant Cell Environ **42**: 527–535

Hölttä T, Lintunen A, Chan T, Mäkelä A, Nikinmaa E (2017) A steady-state stomatal model of balanced leaf gas exchange, hydraulics and maximal source-sink flux. Tree Physiol **37**: 851–868

Horrer D, Flütsch S, Pazmino D, Matthews JSA, Thalmann M, Nigro A, Leonhardt N, Lawson T, Santelia D (2016) Blue light induces a distinct starch degradation pathway in guard cells for stomatal opening. Curr Biol **26**: 362–370

Hsiao TC, Acevedo E, Fereres E, Henderson DW (1976) Water stress, growth and osmotic adjustment: Philos. Trans R Soc London Serv Bull **273**: 471–500

Hyndman R, Athanasopoulos G, Bergmeir C, Caceres G, Chhay L, O'Hara-Wild M, Petropoulos F, Razbash S, Wang E, Yasmeen F (2020) forecast: Forecasting Functions for Time Series and Linear Models. R package version 8.13. Available: https://pkg. robjhyndman.com/forecast\

Im YJ, Han O, Chung GC, Cho BH (2002) Antisense expression of an *Arabidopsis* omega-3 fatty acid desaturase gene reduces salt/drought tolerance in transgenic tobacco plants. Mol Cells **13**: 264–271

Iniesta F, Testi L, Orgaz F, Villalobos FJ (2009) The effects of regulated and continuous deficit irrigation on the water use, growth and yield of olive trees. Eur J Agron **30**: 258–265

Jorgensen RA, Atkinson RG, Forster RLS, Lucas WJ (1998) An RNA-based information superhighway in plants. Science (80-) **279**: 1486–1487

Jurado JM, Ortega L, Cubillas JJ, Feito FR (2020a) Multispectral mapping on 3D models and multi-temporal monitoring for individual characterization of olive trees. Remote Sens **12**: 1–26

Jurado JM, Ramos MI, Enríquez C, Feito FR (2020b) The impact of canopy reflectance on the 3D structure of individual trees in a Mediterranean Forest. Remote Sens **12**: 1–21

Kelly G, Moshelion M, David-Schwartz R, Halperin O, Wallach R, Attia Z, Belausov E, Granot D (2013) Hexokinase mediates stomatal closure. Plant J **75**: 977–988

Kilaru A, Cao X, Dabbs PB, Sung HJ, Rahman MM, Thrower N, Zynda G, Podicheti R, Ibarra-Laclette E, Herrera-Estrella L, et al (2015) Oil biosynthesis in a basal angiosperm: transcriptome analysis of Persea americana mesocarp. BMC Plant Biol **15**: 203

Kim MJ, Kim J-K, Shin JS, Suh MC (2007) The SebHLH transcription factor mediates trans-activation of the SeFAD2 gene promoter through binding to E- and G-box elements. Plant Mol Biol **64**: 453–466

Körner C (2013) Growth controls photosynthesis - mostly. Nov Acta Leopoldina NF **Vol. 114**: 273–283

Körner C (2015) Paradigm shift in plant growth control. Curr Opin Plant Biol **25**: 107–114

Körner C (2003) Carbon limitation in trees. J Ecol **91**: 4–17

Kozlowski TT (1972) Water deficits and plant growth. *In* TT Kozlowsk, ed, Shrinking and swelling of plant tissues. New York: Academic Press, pp 1–64

Kramer PJ, Boyer JS (1995) Water relations of plants and soils. Academic Press, San Diego

Krasensky J, Jonak C (2012) Drought, salt, and temperature stress-induced metabolic rearrangements and regulatory networks. J Exp Bot **63**: 1593–1608

Lavee S (1996) Biology and physiology of the olive. *In* JM Blazquez, ed, World Olive Encycl. Plaza and Janes S. M. Barcelona, Spain, pp 61–105

Lawlor DW, Cornic G (2002) Photosynthetic carbon assimilation and associated metabolism in relation to water deficits in higher plants. Plant Cell Environ **25**: 275–294

Lee HG, Kim H, Suh MC, Kim HU, Seo PJ (2018) The MYB96 transcription factor regulates triacylglycerol accumulation by activating DGAT1 and PDAT1 expression in arabidopsis seeds. Plant Cell Physiol **59**: 1432–1442

Lee HG, Park ME, Park BY, Kim HU, Seo PJ (2019) The Arabidopsis MYB96 transcription factor mediates ABA-dependent triacylglycerol

accumulation in vegetative tissues under drought stress conditions. Plants **8**: 296

Livak KJ, Schmittgen TD (2001) Analysis of relative gene expression data using real-time quantitative PCR and the 2-ΔΔCT method. Methods **25**: 402–408

Lo Bianco R, Avellone G (2014) Diurnal regulation of leaf water status in high- and low-mannitol olive cultivars. Plants **3**: 196–208

Lo Bianco R, Panno G, Avellone G (2013) Characterization of Sicilian Olive Genotypes by Multivariate Analysis of Leaf and Fruit Chemical and Morphological Properties. J Agric Sci **5**: 229–245

Lo Bianco R, Scalisi A (2017) Water relations and carbohydrate partitioning of four greenhouse-grown olive genotypes under long-term drought. Trees - Struct Funct **31**: 717–727

Lockhart JA (1965) An analysis of irreversible plant cell elongation. J Theor Biol **8**: 264–275

Longchamps L, Tisseyre B, Taylor J, Sagoo L, Momin A, Fountas S, Manfrini L, Ampatzidis Y, Schueller JK, Khosla R (2022) Yield sensing technologies for perennial and annual horticultural crops: a review. Precis Agric **23**: 2407–2448

Loureiro J (2009) Flow cytometric approaches to study plant genomes. Ecosistemas **18**: 103–108

Martín-Vertedor AI, Rodríguez JMP, Losada HP, Castiel EF (2011a) Interactive responses to water deficits and crop load in olive (olea europaea L., cv. Morisca) I. - Growth and water relations. Agric Water Manag **98**: 941–949

Martín-Vertedor AI, Rodríguez JMP, Losada HP, Castiel EF (2011b) Interactive responses to water deficits and crop load in olive (Olea europaea L., cv. Morisca). II: Water use, fruit and oil yield. Agric Water Manag **98**: 950–958

Martínez-Gimeno MA, Castiella M, Rüger S, Intrigliolo DS, Ballester C (2017) Evaluating the usefulness of continuous leaf turgor pressure measurements for the assessment of Persimmon tree water status. Irrig Sci **35**: 159–167

Martínez-Vilalta J, Sala A, Asensio D, Galiano L, Hoch G, Palacio S, Piper FI, Lloret F (2016) Dynamics of non-structural carbohydrates in terrestrial plants: A global synthesis. Ecol Monogr **86**: 495–516

Martínez JM, Muñoz E, Alba J, Lanzón A (1975) Report about the use of the "Abencor" analyzer. Grasas y Aceites **26**: 379–385

Martre P, Bertin N, Salon C, Génard M (2011) Modelling the size and composition of fruit, grain and seed by process-based simulation models. New Phytol **191**: 601–618

Maselli F, Chiesi M, Brilli L, Moriondo M (2012) Simulation of olive fruit yield in Tuscany through the integration of remote sensing and ground data. Ecol Modell **244**: 1–12

Matthews MA, Shackel KA (2005) Growth and water transport in fleshy fruit. Vasc. Transp. plants. Elsevier Academic Press, pp 181–197

Matyssek R, Fromm J, Rennenberg H, Roloff A (2010) Biologie der Bäume: von der Zelle zur globalen Ebene. UTB Ulmer, Stuttgart

McAdam SAM, Brodribb TJ (2016) Linking Turgor with ABA Biosynthesis: Implications for Stomatal Responses to Vapor Pressure Deficit across Land Plants. Plant Physiol **171**: 2008–2016

McFadyen LM, Hutton RJ, Barlow EWR (1996) Effects of crop load on fruit water relations and fruit growth in peach. J Hortic Sci **71**: 469–480

Melgar JC, Mohamed Y, Navarro C, Parra MA, Benlloch M, Fernández-Escobar R (2008) Long-term growth and yield responses of olive trees to different irrigation regimes. Agric Water Manag **95**: 968–972

Mengmeng D, Noboru N, Atsushi I, Yukinori S, Du MM, Noguchi N, Itoh A, Shibuya Y (2017) Multi-temporal monitoring of wheat growth by using images from satellite and unmanned aerial vehicle. Int J Agric Biol Eng **10**: 1–13

Mills T, Behboudian M, Clothier B (1996) Water Relations, Growth, and the Composition of 'Braeburn' Apple Fruit under Deficit Irrigation Materials and Methods. J Amer Soc Hort Sci **121**: 286–291

Mitchell PJ, O'Grady AP, Tissue DT, Worledge D, Pinkard EA (2014) Co-ordination of growth, gas exchange and hydraulics define the carbon safety margin in tree species with contrasting drought strategies. Tree Physiol **34**: 443–458

Morales-Sillero A, Pérez AG, Casanova L, García JM (2017) Cold storage of 'Manzanilla de Sevilla' and 'Manzanilla Cacereña' mill olives from super-high density orchards. Food Chem **237**: 1216–1225

Morandi B, Losciale P, Manfrini L, Zibordi M, Anconelli S, Galli F, Pierpaoli E, Corelli Grappadelli L (2014) Increasing water stress negatively affects pear fruit growth by reducing first its xylem and then its phloem inflow. J Plant Physiol **171**: 1500–1509

References

Morandi B, Rieger M, Grappadelli LC (2007) Vascular flows and transpiration affect peach (Prunus persica Batsch.) fruit daily growth. J Exp Bot **58**: 3941–3947

Moriana A, Orgaz F, Pastor M, Fereres E (2003) Yield responses of a mature olive orchard to water deficits. J Am Soc Hortic Sci **128**: 425–431

Moriana A, Villalobos FJ, Fereres E (2002) Stomatal and photosynthetic responses of olive (Olea europaea L.) leaves to water deficits. Plant, Cell Environ **25**: 395–405

Morison JIL, Baker NR, Mullineaux PM, Davies WJ (2008) Improving water use in crop production. Philos Trans R Soc B Biol Sci **363**: 639–658

Muller B, Pantin F, Génard M, Turc O, Freixes S, Piques M, Gibon Y (2011) Water deficits uncouple growth from photosynthesis, increase C content, and modify the relationships between C and growth in sink organs. J Exp Bot **62**: 1715–1729

Naor A, Schneider D, Ben-Gal A, Zipori I, Dag A, Kerem Z, Birger R, Peres M, Gal Y, Schneider D, et al (2013) The effects of crop load and irrigation rate in the oil accumulation stage on oil yield and water relations of 'Koroneiki' olives. Irrig Sci **31**: 781–791

Orgaz F, Fereres E (2008) Riego. El Cultiv. del olivo. pp 337–362

Orgaz F, Testi L, Villalobos FJ, Fereres E (2006) Water requirements of olive orchards–II: determination of crop coefficients for irrigation scheduling. Irrig Sci **24**: 77–84

Ortuño MF, García-Orellana Y, Conejero W, Ruiz-Sánchez MC, Alarcón JJ, Torrecillas A (2006) Stem and leaf water potentials, gas exchange, sap flow, and trunk diameter fluctuations for detecting water stress in lemon trees. Trees - Struct Funct **20**: 1–8

Padilla-Díaz CM, Rodriguez-Dominguez CM, Hernandez-Santana V, Perez-Martin A, Fernandes RDM, Montero A, García JM, Fernández JE (2018) Water status, gas exchange and crop performance in a super high density olive orchard under deficit irrigation scheduled from leaf turgor measurements. Agric Water Manag **202**: 241–252

Padilla-Díaz CM, Rodriguez-Dominguez CM, Hernandez-Santana V, Perez-Martin A, Fernández JE (2016) Scheduling regulated deficit irrigation in a hedgerow olive orchard from leaf turgor pressure related measurements. Agric Water Manag **164**: 28–37

Paul MJ, Foyer CH (2001) Sink regulation of photosynthesis. J Exp Bot **52**: 1383–

1400

Perez-Arcoiza A, Hernández ML, Sicardo MD, Hernandez-Santana V, Diaz-Espejo A, Martinez-Rivas JM (2022) Carbon supply and water status regulate fatty acid and triacylglycerol biosynthesis at transcriptional level in the olive mesocarp. Plant Cell Environ **45**: 2366–2380

Perez-Martin A, Michelazzo C, Torres-Ruiz JM, Flexas J, Fernández JE, Sebastiani L, Diaz-Espejo A (2014) Regulation of photosynthesis and stomatal and mesophyll conductance under water stress and recovery in olive trees: Correlation with gene expression of carbonic anhydrase and aquaporins. J Exp Bot **65**: 3143–3156

Pesaresi P, Mizzotti C, Colombo M, Masiero S (2014) Genetic regulation and structural changes during tomato fruit development and ripening. Front Plant Sci **5**: 1–14

Pfaffl MW (2004) Quantification strategies in real-time PCR. *In* A-Z of Quantitative PCR, ed, Bustin, S.A. International University Line, La Jolla, pp 87–112

Poghosyan ZP, Haralampidis K, Martsinkovskaya AI, Murphy DJ, Hatzopoulos P (1999) Developmental regulation and spatial expression of a plastidial fatty acid desaturase from *Olea europaea*. Plant Physiol Biochem **37**: 109–119

Rallo P, Rapoport HF (2001) Early growth and development of the olive fruit mesocarp. J Hortic Sci Biotechnol **76**: 408–412

Ranney TG, Bassuk NL, Whitlow TH (1991) Osmotic Adjustment and Solute Constituents in Leaves and Roots of Water-stressed Cherry (Prunus) Trees. J Am Soc Hortic Sci **116**: 684–688

Rapoport HF (2008) 'Botánica y morfología'. *In* D Barranco, ed, El Cultiv. del olivo, 6th ed. Madrid: Mundi-Prensa, pp 37–62

Rapoport HF, Costagli G, Gucci R (2004) The effect of water deficit during early fruit development on olive fruit morphogenesis. J Am Soc Hortic Sci **129**: 121–127

Reale L, Nasini L, Cerri M, Regni L, Ferranti F, Proietti P (2019) The influence of light on olive (*Olea europaea* L.) fruit development is cultivar dependent. Front Plant Sci **10**: 385

Rodriguez-Dominguez CM, Brodribb TJ (2020) Declining root water transport drives stomatal closure in olive under moderate water stress. New Phytol **225**: 126–134

References

Rodriguez-Dominguez CM, Buckley TN, Egea G, de Cires A, Hernandez-Santana V, Martorell S, Diaz-Espejo A (2016) Most stomatal closure in woody species under moderate drought can be explained by stomatal responses to leaf turgor. Plant Cell Environ **39**: 2014–2026

Rodriguez-Dominguez CM, Forner A, Martorell S, Choat B, Lopez R, Peters JMR, Pfautsch S, Mayr S, Carins-Murphy MR, McAdam SAM, et al (2022) Leaf water potential measurements using the pressure chamber: Synthetic testing of assumptions towards best practices for precision and accuracy. Plant Cell Environ 2037–2061

Rodriguez-Dominguez CM, Hernandez-Santana V, Buckley TN, Fernández JE, Diaz-Espejo A (2019) Sensitivity of olive leaf turgor to air vapour pressure deficit correlates with diurnal maximum stomatal conductance. Agric For Meteorol **272**–**273**: 156–165

Román Á, Hernández ML, Soria-García Á, López-Gomollón S, Lagunas B, Picorel R, Martínez-Rivas JM, Alfonso M (2015) Non-redundant contribution of the plastidial FAD8 ω-3 desaturase to glycerolipid unsaturation at different temperatures in *Arabidopsis*. Mol Plant **8**: 1599–1611

Rosati A, Paoletti A, Al Hariri R, Morelli A, Famiani F (2018) Resource investments in reproductive growth proportionately limit investments in whole-tree vegetative growth in young olive trees with varying crop loads. Tree Physiol **38**: 1267–1277

Rosecrance RC, Krueger WH, Milliron L, Bloese J, Garcia C, Mori B (2015) Moderate regulated deficit irrigation can increase olive oil yields and decrease tree growth in super high density 'Arbequina' olive orchards. Sci Hortic (Amsterdam) **190**: 75–82

Rossi F, Manfrini L, Venturi M, Corelli Grappadelli L, Morandi B (2022) Fruit transpiration drives interspecific variability in fruit growth strategies. Hortic Res **9**: 1–10

Rotondi A, Bendini A, Cerretani L, Mari M, Lercker G, Toschi TG (2004) Effect of olive ripening degree on the oxidative stability and organoleptic properties of cv. Nostrana di Brisighella extra virgin olive oil. J Agric Food Chem **52**: 3649–3654

Ruane J, Sonnino A, Steduto P, Deane C (2008) Coping with water scarcity : What role for biotechnologies ? L Water Discuss Pap 5–17

Rüger S, Ehrenberger W, Arend M, Geßner P, Zimmermann G, Zimmerann D, Bentrup FW, Nadler A, Raveh E, Sukhorukv VL, et al (2010a) Comparative

monitoring of temporal and spatial changes in tree water status using the non-invasive leaf patch clamp pressure probe and the pressure bomb. Agric Water Manag **98**: 283–290

Rüger S, Netzer Y, Westhoff M, Zimmermann D, Reuss R, Ovadiya S, Gessner P, Zimmermann G, Schwartz A, Zimmermann U (2010b) Remote monitoring of leaf turgor pressure of grapevines subjected to different irrigation treatments using the leaf patch clamp pressure probe. Aust J Grape Wine Res **16**: 405–412

Ruiz-Sanchez MC, Domingo R, Castel JR (2010) Review. deficit irrigation in fruit trees and vines in spain. Spanish J Agric Res. doi: 10.5424/sjar/201008s2-1343

Ryan MG, Oren R, Waring RH (2018) Fruiting and sink competition. Tree Physiol **38**: 1261–1266

Sala A, Woodruff DR, Meinzer FC (2012) Carbon dynamics in trees: Feast or famine? Tree Physiol **32**: 764–775

Sánchez-Rodríguez L, Kranjac M, Marijanović Z, Jerković I, Pérez-López D, Carbonell-Barrachina ÁA, Hernández F, Sendra E (2020) "Arbequina" olive oil composition is affected by the application of regulated deficit irrigation during pit hardening stage. JAOCS, J Am Oil Chem Soc **97**: 449–462

Sanchez J (1994) Lipid photosynthesis in olive fruit. Prog Lipid Res **33**: 97–104

Sánchez J (1995) Olive Oil Biogenesis. Contribution of Fruit photosynthesis. *In* J-C Kader, P Mazliak, eds, Plant Lipid Metab. Springer Netherlands, Dordrecht, pp 564–566

Sánchez J, Harwood JL (2002) Biosynthesis of triacylglycerols and volatiles in olives. Eur J Lipid Sci Technol **104**: 564–573

Scoffoni C, Albuquerque C, Brodersen C, Townes S V, John GP, Bartlett MK, Buckley TN, McElrone AJ, Sack L (2017) Outside-xylem vulnerability, not xylem embolism, controls leaf hydraulic decline during dehydration. Plant Physiol **173**: 1197–1210

Seo PJ, Xiang F, Qiao M, Park JY, Lee YN, Kim SG, Lee YH, Park WJ, Park CM (2009) The MYB96 transcription factor mediates abscisic acid signaling during drought stress response in *Arabidopsis*. Plant Physiol **151**: 275–289

Shanklin J, Cahoon EB (1998) Desaturation and related modifications of fatty acids. Annu Rev Plant Biol **49**: 611–641

Sinclair TR (1998) Historical changes in harvest index and crop nitrogen

accumulation. Crop Sci **38**: 638–643

Singh P, Pandey PC, Petropoulos GP, Pavlides A, Srivastava PK, Koutsias N, Deng KAK, Bao Y (2020) 8 - Hyperspectral remote sensing in precision agriculture: present status, challenges, and future trends. *In* PC Pandey, PK Srivastava, H Balzter, B Bhattacharya, GPBT-HRS Petropoulos, eds, Earth Obs. Elsevier, pp 121–146

Steppe K, Sterck F, Deslauriers A (2015) Diel growth dynamics in tree stems: Linking anatomy and ecophysiology. Trends Plant Sci **20**: 335–343

Sukhov V, Sukhova E, Vodeneev V (2019) Long-distance electrical signals as a link between the local action of stressors and the systemic physiological responses in higher plants. Prog Biophys Mol Biol **146**: 63–84

Sun Q, Xue J, Lin L, Liu D, Wu J, Jiang J, Wang Y (2018) Overexpression of soybean transcription factors GmDof4 and GmDof11 significantly increase the oleic acid content in seed of *Brassica napus* L. Agronomy **8**: 222

Tardieu F, Granier C, Muller B (2011) Water deficit and growth. Co-ordinating processes without an orchestrator? Curr Opin Plant Biol **14**: 283–289

Tattini M, Gucci R, Romani A, Baldi A, Everard JD (1996) Changes in non-structural carbohydrates in olive (Olea europaea) leaves during root zone salinity stress. Physiol Plant **98**: 117–124

Taylor CA, Rising J (2021) Tipping point dynamics in global land use. Environ Res Lett. doi: 10.1088/1748-9326/ac3c6d

Team RC (2021) R: A language and environment for statistical computing [Computer software, version 4.1. 0].

Thalmann M, Santelia D (2017) Starch as a determinant of plant fitness under abiotic stress. New Phytol **214**: 943–951

Tixier A, Orozco J, Roxas AA, Earles JM, Zwieniecki MA (2018) Diurnal variation in nonstructural carbohydrate storage in trees: Remobilization and vertical mixing. Plant Physiol **178**: 1602–1613

Torres-Ruiz JM, Cochard H, Choat B, Jansen S, López R, Tomášková I, Padilla-Díaz CM, Badel E, Burlett R, King A, et al (2017) Xylem resistance to embolism: presenting a simple diagnostic test for the open vessel artefact. New Phytol **215**: 489–499

Torres-Ruiz JM, Diaz-Espejo A, Morales-Sillero A, Martín-Palomo MJ, Mayr S, Beikircher B, Fernández JE (2013) Shoot hydraulic characteristics, plant water status and stomatal response in olive trees under different soil

water conditions. Plant Soil **373**: 77–87

Torres-Ruiz JM, Diaz-Espejo A, Perez-Martin A, Hernandez-Santana V (2015) Role of hydraulic and chemical signals in leaves, stems and roots in the stomatal behaviour of olive trees under water stress and recovery conditions. Tree Physiol **35**: 415–424

Tovar MJ, Romero MP, Alegre S, Girona J, Motilva MJ (2002) Composition and organoleptic characteristics of oil from 'Arbequina' olive (*Olea europaea* L.) trees under deficit irrigation. J Sci Food Agric **82**: 1755–1763

Trapletti A, Hornik K (2020) tseries: time series analysis and computational finance. R package version 0.10–48. Available: https://CRAN.R-project.org/package=tseries

Trentacoste ER, Contreras-Zanessi O, Beyá-Marshall V, Puertas CM (2018) Genotypic variation of physiological and morphological traits of seven olive cultivars under sustained and cyclic drought in Mendoza, Argentina. Agric Water Manag **196**: 48–56

Trentacoste ER, Puertas CM, Sadras VO (2010) Effect of fruit load on oil yield components and dynamics of fruit growth and oil accumulation in olive (Olea europaea L.). Eur J Agron **32**: 249–254

Unver T, Wu Z, Sterck L, Turktas M, Lohaus R, Li Z, Yang M, He L, Deng T, Escalante FJ, et al (2017) Genome of wild olive and the evolution of oil biosynthesis. Proc Natl Acad Sci U S A **114**: E9413–E9422

Wasternack C, Feussner I (2018) The oxylipin pathways: biochemistry and function. Annu Rev Plant Biol **69**: 363–386

Westhoff M, Reuss R, Zimmermann D, Netzer Y, Gessner A, Gessner P, Zimmermann G, Wegner LH, Bamberg E, Schwartz A, et al (2009) A non-invasive probe for online-monitoring of turgor pressure changes under field conditions. Plant Biol (Stuttg) **11**: 701–712

Xiong D, Nadal M (2020) Linking water relations and hydraulics with photosynthesis. Plant J **101**: 800–815

Ye Y, Fulcher YG, Sliman DJ, Day MT, Schroeder MJ, Koppisetti RK, Bates PD, Thelen JJ, van Doren SR (2020) The BADC and BCCP subunits of chloroplast acetyl-CoA carboxylase sense the pH changes of the light-dark cycle. J Biol Chem **295**: 9901–9916

Zarco-Tejada PJ, Diaz-Varela R, Angileri V, Loudjani P (2014) Tree height quantification using very high resolution imagery acquired from an unmanned aerial vehicle (UAV) and automatic 3D photo-reconstruction methods. Eur J Agron **55**: 89–99

Zhang J, Liu H, Sun J, Li B, Zhu Q, Chen S, Zhang H (2012) Arabidopsis fatty acid desaturase FAD2 is required for salt tolerance during seed germination and early seedling growth. PLoS One **7**: e30355

Zhang M, Fan J, Taylor DC, Ohlrogge JB (2009) DGAT1 and PDAT1 acyltransferases have overlapping functions in Arabidopsis triacylglycerol biosynthesis and are essential for normal pollen and seed development. Plant Cell **21**: 3885–3901

Zhang YM, Wang CC, Hu HH, Yang L (2011) Cloning and expression of three fatty acid desaturase genes from cold-sensitive lima bean (*Phaseolus lunatus* L.). Biotechnol Lett **33**: 395–401

Zimmermann D, Reuss R, Westhoff M, Geßner P, Bauer W, Bamberg E, Bentrup FW, Zimmermann U (2008) A novel, non-invasive, online-monitoring, versatile and easy plant-based probe for measuring leaf water status. J Exp Bot **59**: 3157–3167

Zimmermann U, Rüger S, Shapira O, Westhoff M, Wegner LH, Reuss R, Gessner P, Zimmermann G, Israeli Y, Zhou A, et al (2010) Effects of environmental parameters and irrigation on the turgor pressure of banana plants measured using the non-invasive, online monitoring leaf patch clamp pressure probe. Plant Biol **12**: 424–436

Zweifel R, Haeni M, Buchmann N, Eugster W (2016) Are trees able to grow in periods of stem shrinkage? New Phytol **211**: 839–849

La agricultura también se ha visto afectada por la era digital y de comunicaciones en la que vivimos. La llamada agricultura digital o *smart farming* está ganando terreno y los agricultores están implementando tecnología para monitorear sus plantaciones y hacer un uso más racional del agua y otros recursos. El cambio climático y el aumento de precios de insumos han generado la necesidad de optimizar la productividad y reducir costes. Esta Tesis Doctoral se enfoca en comprender las respuestas fisiológicas de la planta y del fruto a las condiciones ambientales utilizando las nuevas tecnologías de la Cuarta Revolución Industrial como drones y técnicas de biología molecular. El objetivo es avanzar en el conocimiento de estos procesos y utilizarlos en futuros trabajos para optimizar la producción agrícola.